TECHNISCHE UNIVERSITÄT MÜNCHEN

Lehrstuhl für Humanbiologie

Effect of Neuronal Autoantibodies on Enteric Neurons and Vagal Afferents

Qin Li

Vollständiger Abdruck der von der Fakultät Wissenschaftszentrum Weihenstephan für Ernährung, Landnutzung und Umwelt der Technischen Universität München zur Erlangung des akademischen Grades eines

Doktors der Naturwissenschaften

genehmigten Dissertation.

Vorsitzender:	Univ.-Prof. Dr. J. Hauner
Prüfer der Dissertation:	1. Univ.-Prof. Dr. M. Schemann
	2. Univ.-Prof. Dr. H. Luksch

Die Dissertation wurde am 22.04.2013 bei der Technischen Universität München eingereicht und durch die Fakultät Wissenschaftszentrum Weihenstephan für Ernährung, Landnutzung und Umwelt am 15.07.2013 angenommen

Publications

1. Buhner S*, **Li Q*,** Berger T, Vignali S, Barbara G, De Giorgio R, Stanghellini V, Schemann M. Submucous rather than myenteric neurons are activated by mucosal biopsy supernatants from irritable bowel syndrome patients. *Neurogastroenterol Motil 2012; 24(12): 1134-e572.*

   * Authors Buhner and Li contributed equally to this work.

   http://www.ncbi.nlm.nih.gov/pubmed/22963673

2. Schemann M, Hafsi N, Michel K, Kober OI, Wollmann J**, Li Q,** Zeller F, Langer R, Lee K, Cellek S. The beta3-adrenoceptor agonist GW427353 (solabegron) decreases excitability of human enteric neurons via release of somatostatin. *Gastroenterology 2010; 138: 266-274.*

   http://www.ncbi.nlm.nih.gov/pubmed/19786030

3. Buhner S, **Li Q**, Vignali S, Barbara G, De Giorgio R, Stanghellini V, Cremon C, Zeller F, Langer R, Daniel H, Michel K, Schemann M. Activation of human enteric neurons by supernatants of colonic biopsy specimens from patients with irritable bowel syndrome. *Gastroenterology. 2009; 137(4):1425-34.*

   http://www.ncbi.nlm.nih.gov/pubmed/19596012

Published abstract

1. Buhner S, Hartwig K, **Li Q**, Vignali S, Pehl C, Frieling T, Barbara G, Boeckxstaens G, Demir IE and Schemann M. PAR1 receptors mediate nerve activation by mucosal biopsy supernatants from Irritable Bowel Syndrome (IBS) but not from Ulcerative Colitis (UC) patients. *Neurogastroenterol Motil 2012; 24 Suppl 2: 31-32.*

2. Buhner S, **Li Q**, Braak B, Klooker TK, Vignali S , Schemann M and Boeckxstaens, GE. Excitation of enteric neurons by supernatants of colonic biopsies from irritable bowel syndrome patients (IBS) is linked to visceral sensitivity. *Gastroenterology. 2011; 140 (5), Suppl 1: S521.*

3. Buhner S, **Li Q,** Vignali S, Zeller F, Barbara G, de Giorgio R, Stanghellini V, Michel K, and Schemann M. Activtion of human enteric neurons by supernatants of colonic biopsies from patients with IBS. *Neurogastroenterol Motil 2008; **20** suppl 2: 4.*

4. Buehner S, Li Q, Vignali S, Zeller F , Barbara G, De Giorgio R, Stanghellini V, Michel K and Schemann M. *Mucosal biopsies from IBS patients release mediators that sensitize human enteric nervous system (ENS). Gastroenterology 2008;134 (4), Suppl 1: A146.*

5. Buhner S, **Li Q,** Vignali S, Langer R, Barbara G, de Giorgio R, Stanghellini V, Zeller F, Michel K and Schemann M. Excitory actions of supernatants released from mucosal biopsies of IBS patients mediated by proteases, serotonin and histamine. *Zeitschrift für Gastroenterologie 2008; 1039.*

6. **Li Q**, Buhner S, Vignali S, Weyhern CW, Zeller F, Barbara G, de Giorgio R, Stanghellini V, Michel K and Schemann. A mediator cocktail released from mucosal biopsies of IBS patients excites human and guinea-pig enteric neurons. *Neurogastroenterol Motil 2007; 19 suppl 3:20.*

7. Talamonti L, **Li Q,** Beyak M, Trevisani M, Michel K, Campi B, Barbara G, Geppetti P, Grundy D, Schemann M and De Giorgio R. Impact of Humoral autoimmunity in severe gut dysmotility: actions of anti-Hu on enteric and visceral sensory neurons. *Gastroenterology 2006; 130 (4), Suppl 2: 257.*

Abbreviations

°C	degree celsius
α3-AchR	antibodies against the α3 subunit of the nicotinic acetylcholine receptor
α-DnTX	α-dendrotoxins
µg	microgram
µL	microliter
5-HT	5-hydroxytryptamine (serotonin)
A/D	analog to digital
ACh	acetylcholine
AChRs	acetylcholine receptors
AGID	autoimmune gastrointestinal dysmotility
AH neuron	designation of neurons having slow after-hyperpolarizing potentials
AHP	after-hyperpolarizing potential
ANNA	antineuronal nuclear antibody
ANNA-1	type-1 antineuronal nuclear antibody
ANNA-2	type-2 antineuronal nuclear antibody
anti-Hu	antibody by the first two letters of their index patient's last name
AP	action potential
ATP	adenosine triphosphate
Ca^{2+}	calcium
CNS	central nervous system
COPD	Chronic obstructive pulmonary disease
CSF	cerebrospinal fluid
Di-8-ANEPPS	1-(3-sulfonatopropyl)-4-[β [2-(di-n-octylamino)-6-napthyl]vinyl]pyridinium betaine
DMPP	1,1-dimethyl-4-phenylpiperazinium iodide; nicotinic receptor agonist
DMSO	dimethyl sulfoxide
DRG	dorsal root ganglion
e. g.	for example
ENS	enteric nervous system
EPAN	extrinsic primary afferent
EPSP	excitatory post-synaptic potential

et al.	and others
ΔF/F	change in fluorescence divided by the resting light level
FcγRI	Fc-gamma receptor I
fEPSP	fast excitatory postsynaptic potential
g	gram
GI	gastrointestinal
h	hour
HC	healthy control
ICCs	interstitial cells of Cajal
IgG	immunoglobulin G
IGLE	intraganglionic laminar ending
IGLEs	intraganglionic laminar endings
IMAs	intramuscular arrays
IPAN	intrinsic primary afferent neuron
IPSP	inhibitory post-synaptic potential
K^+	potassium ion
L	liter
LES	Lambert-Eaton syndrome
M	molar
mg	milligram
min	minute
mL	milliliter
MMC	migrating motor complex
MP	myenteric plexus
MSORT	multisite optical recording technique
Mv	millivolt
Na^+	sodium ion
nAchR	nicotinic acethylcholine receptor
NG	nodose ganglion
NK	neurokinin
NO	nitric oxide
NPY	neuropeptide
NTS	nucleus tractus solitarius
PC	patient control

PD	potential difference
pH	negative decadic logarithm of the molar concentration of hydrogen ions
PNS	Paraneoplastic neurological syndrome
RAMEN	rapidly adapting mechanosensitive enteric neurons
S	second
SCLC	small lung cell carcinoma
SD	standard deviation
SEM	standard error of the mean
sEPSPs	slow excitatory postsynaptic potentials
SMP	submucosal plexus
SP	substance P
TTX	tetrodotoxin
V	volt
VIP	vasoactive intestinal peptide
VMR	visceromotor response
Vs.	versus
Y P2X	purine receptor

Declaration

I certify that this thesis does not incorporate without acknowledgment any material previously submitted for a degree or diploma in any university; and that to the best of my knowledge and belief it does not contain any material previously published (except for abstract) or written by another person except where due reference is made in the text.

Qin Li

Contents

Zusammenfassung

Ein kleiner Teil von Patienten mit paraneoplasischem neurologischem Syndrom mit okkultem oder manifestem Tumor entwickeln das Krankheitsbild der paraneoplastischen gastrointestinalen Dysmotilität. Es wird angenommen das bei diesem Krankheitsbild Antigene im Tumorgewebe eine Immunreaktion auslösen die auch mit Antigenen in enterischen oder autonomen Neuronen reagiert. Die Immunreaktion richtet sich damit sowohl gegen den Tumor als auch gegen das enterische Nervensystem. Im Blut dieser Patienten lassen sich häufig Anti-neuronale Antikörper nachweisen. Der häufigste, mit paraneoplastischer gastrointestinaler Dysmotilität assoziierte neuronale Autoantikörper ist der „Autoantikörper gegen Zellkerne neuronaler Zellen Typ 1“ (ANNA-1, auch „anti-Hu“). Ein anderer, typischer Antikörper in diesem Zusammenhang richtet sich gegen ganglionäre nikotinerge Acetylcholinrezeptoren (α3-AChR). Der exakte Mechanismus durch den diese Autoantikörper zur Dysfunktion der enterischen Neurone beitragen ist jedoch noch unklar. Das Ziel der vorliegenden Arbeit war es daher, die akuten Effekte von neuronalen Autoantikörpern auf enterische Neurone und vagale Afferenzen zu charakterisieren. Mit einem schnellen, bildgebenden Verfahren wurden die Auswirkungen der Autoantikörper auf myenterische Neurone im Meerschweinchen-Ileum und in humanen enterischen Neuronen untersucht. Durch extrazelluläre Ableitungen wurde die Wirkung der Autoantikörper auf vagale Afferenzen des Maus-Magens (Fundus) untersucht. Als Proben wurden Seren von Patienten mit paraneoplastischen gastrointestinalen Symptomen die α3-AChR (6 Patienten) oder ANNA-1 (7 Patienten) Autoantikörper enthielten, verwendet. Kontrollseren ohne Autoantikörper kamen von Patienten ohne Symptomatik beziehungsweise Freiwilligen. Sowohl α3-AChR Seren als auch ANNA-1 Seren bewirkten eine schnelle Entladung von Aktionspotentialen in einem erheblichen Prozentsatz der enterischen Neurone im Meerschweinchen und Mensch. Dabei war der Effekt im Allgemeinen in Präparaten des humanen enterischen Nervensystems stärker als in Meerschweinchenpräparaten. Kontrollseren hatten nur vernachlässigbare Effekte. Experimente mit aufgereinigten Antikörpern aus Seren mit besonders hohen ANNA-1-Titer zeigten, dass dieser Effekt hauptsächlich durch Anti-HuD Antikörper und zu einem geringen Teil durch Antikörper der Typen Anti-HuA, Anti-HuB und Anti-HuC (Anti-HuA/B/C) zustande kommt. Es wurden vier Gruppen von Neuronen gefunden: Ein relativ großer Anteil reagierte nur auf Anti-HuD, ein kleinerer Anteil reagierte nur auf Anti-HuA/B/C, eine weitere Gruppe reagierte auf Anti-HuD und anti-HuA/B/C und eine Gruppe die auf keine der Substanzen reagierte. In den Versuchen

mit vagalen Afferenzen zeigte sich, dass rezeptive Felder im Magen-Fundus der Maus durch Anti-HuD erregt wurden aber nicht durch Anti-HuA/B/C. Dabei hatte Anti-HuD einen signifikant stärker erregenden Effekt als Agonisten nikotinerger bzw. purinerger Rezeptoren (DMPP beziehungsweise ATP). Diese Ergebnisse deuten darauf hin, dass die Anti-HuD Wirkung unabhängig von der Aktivierung nikotinerger oder purinerger Rezeptoren ist.

Zusammenfassend zeigt sich, dass Immunglobuline (IgG) aus Patienten mit paraneoplastischen gastrointestinalen Symptomen akut eine Erregung enterischer Neurone und vagaler Afferenzen hervorrufen. Diese Effekte könnten durch eine IgG-induzierte Exzitotoxizität zur Dysmotilität in diesen Patienten beitragen.

Abstract

A small part of paraneoplastic neurological syndrome (PNS) patients with occult or manifest tumor develop paraneoplastic gastrointestinal (GI) dysmotility. In paraneoplastic GI dysmotility, tumor antigens may elicit an immune response that cross-reacts with enteric or autonomic neural tissue leading to an immune attack directed against both the tumor and the enteric nervous system. In the blood of these patients, a humoral immune response involving circulating anti-neuronal antibodies is commonly detected. The most common neuronal autoantibody associated with paraneoplastic GI dysmotility is the type 1 anti-neuronal nuclear antibody (ANNA-1, also called "anti-Hu"). Another commonly reported antibody in these patients is directed against neuronal nicotinic acetylcholine receptors (α3-AChR). However, the exact mechanism of how ANNA-1 and ganglionic nicotinic α3-AChR antibodies cause enteric neuronal dysfunction remains unclear. Therefore, the aim of this study was to characterize the acute effect of neuronal autoantibodies on enteric neurons and vagal afferents. We wanted specifically to gain evidence if anti-HuD antibodies are able to impair the function of enteric neurons and extrinsic afferent pathways. A fast voltage sensitive dye neuroimaging technique was employed to study the effect of the antibodies on myenteric plexus neurons of guinea pig ileum and human enteric neurons. Furthermore, extracellular recordings were used to investigate the effect of these antibodies on vagal afferents in the mouse gastric fundus. Results from this study revealed that sera from patients with paraneoplastic GI syndromes containing α3-AchR (6 patients) or ANNA-1 (7 patients) antibodies but not sera from control individuals reproducibly evoke a fast onset spike discharge in a substantial proportion of guinea pig and human enteric neurons. In general, stronger effects were observed on human enteric neurons than on guinea pig enteric neurons. Most ANNA-1 IgG samples had similar effects on spike frequency and the proportion of activated neurons, whereas control samples had negligible effects. Experiments with purified antibodies from patients with high ANNA-1 titers showed that the excitatory action of anti-ANNA-1 containing sera in enteric neurons is mainly caused by anti-HuD and to a lesser extent by anti-HuA/B/C antibodies. It is noteworthy that we found four types of neurons responding to anti-HuD and anti- HuA/B/C: a high proportion of neuron responded to anti-HuD; a smaller group of neurons responded to anti-HuA/B/C; neurons that responded to both; and neurons that did not respond to any of the substances. In vagal afferents our results show only anti-HuD exerted an excitatory action, but not anti-HuA/B/C. Anti-HuD had a

significantly stronger excitatory action than DMPP and ATP and in addition activated more hot spots than DMPP and ATP. These results suggest that the anti-HuD effect in these receptive fields is independent of nicotinic or purinergic receptor activation. In summary the results indicate for the first time that IgG in serum of patients with autoimmune GI dysmotility elicits activation of both enteric neurons and vagal afferents. This effect may contribute to gut dysmotility via an IgG induced neuronal excitotoxicity. These findings are consistent with IgG of neuronal specificity playing an effector role in autoimmune GI dysmotility.

1. Introduction

1.1 General introduction

The Gastrointestinal (GI) tract digests food and absorbs nutrients while also protecting itself from potential harmful antigenic and pathogenic material (Blackshaw et al., 2007). A number of control systems have evolved to allow the gut to achieve its function and simultaneously protect it from these dangers. The integration of all of these events is exerted by multiple and exceedingly complex regulatory systems, which monitor the events within the GI tract. Neuronal control plays a key role. GI functions are controlled by extrinsic and intrinsic innervation. The extrinsic innervation consists of the sympathetic and the parasympathetic pathways, while the enteric nervous system (ENS) constitutes the intrinsic innervation. Both extrinsic and intrinsic innervation belongs to the autonomic nervous system (Langley, 1921). Because the gut immune system contains 70-80% of the body's immune cells (Furness et al. 1999), more and more attention is drawn to the fact that the digestive tract is recognized as the largest lymphoid organ in the body. The intestinal immune system is an interface between the body and its environment. It is continuously exposed to dietary antigens, infectious agents, toxins, and noxious chemicals. The large antigenic load is insufficiently excluded from access to depper gut layers by physical and chemical barriers at the epithelial interface. Therefore the enteric immune system permanently reacts to his challenges (Wood, 2004). Thus the concept of enteric neuroimmune interactions has become an integral part of physiology and pathophysiology of the gut (Schemann et al. 2005). There are increasing evidences for a bidirectional communication between immune cells in the gut with extrinsic afferents as well as the ENS. They are involved in the control of immune and inflammatory processes throughout the gut (Collins, 1996; Di Nardo et al., 2008). It is therefore not surprising that any damage to nervous control circuits can result in a wide array of gut disorders which compromise patient's quality of life and occasional fatal outcomes. For instance, the inflammatory/immune response in enteric ganglionitis leads to neuronal dysfunction leading to an inflammatory neuropathy caused by paraneoplastic syndrome (Kiers et al., 1991; Posner, et al., 1997; Clement et al., 1999; Lee et al., 2001). The diagnosis of paraneoplastic syndrome is supported by detection of circulating antineuronal autoantibodies against selected molecular targets, including Hu and Yo proteins, neurotransmitter receptors, and ion channels. This feature and the curative effect of immunosuppressive therapies reinforce the concept of a

cause/effect relationship of the immune-mediated insult damaging the enteric innervation (De Giorgio et al., 2004).

The first parts of the introduction will summarise how intrinsic and extrinsic nervous systems regulate gut functions. This will be followed by two chapters that deal with the role of anti-neuronal antibodies and antigens related to paraneoplastic gut dysfunction.

1.2 Innervation of the gut

Since the pioneering observations of Bayliss & Starling at the turn of the century (Bayliss and Starling, 1899, 1900), we have gained significantly more knowledge about the innervation of the GI tract. GI tract functions (motility, sensation, secretion, blood flow and immune resposes) are controlled and coordinated by the autonomic nervous system consisting of extrinsic and ENS elements. The parasympathetic innervation is supplied mainly by the vagus and pelvic nerves, while the sympathetic innervation is supplied by the splanchnic nerves (arising from the thoracolumbar region in the spinal cord) (Langley, 1921). The extrinsic vagal and spinal innervation provide the anatomical connection between the CNS and the gut wall, and consist of efferent (sympathetic and parasympathetic) and even much more afferent (sensory) nerves. Both vagal and spinal extrinsic afferents send axon collaterals to both plexuses of the ENS and provide the basis for spinal and brainstem reflex mechanisms, input to central autonomic circuits that regulate GI physiological function and illness behaviour (Johnson et al., 2006). The intraganglionic laminar endings (IGLEs) and intramuscular arrays (IMAs) which are terminals of vagal and pelvic afferents within the myenteric ganglia and muscle layers (Lynn et al., 2003; Zagorodnyuk et al., 2003) are also important mediators in the communication from the ENS to the extrinsic afferents (Blackshaw et al., 2007). Moreover, the extrinsic nerve endings within the gut wall contribute to the functioning of the ENS (Johnson et al., 2006). The ENS contains ganglia, primary interganglionic fibre tracts, and secondary and tertiary fibres projecting to the effector systems (muscle cells, glands, blood vessels, and immune cells). Neurons in the ganglia of the ENS form an independent nervous system with mechanisms for integration and processing of information similar to those in the brain and spinal cord (Wood, 2007).

1.2.1 Extrinsic afferent innervation

The extrinsic afferents are considered to be of importance to convey information about the state of the GI tract and to modulate intrinsic enteric reflexes. Approximately 50000 vagal

afferents are estimated to supply the GI tract and there may be a similar number of spinal afferents (Blackshaw et al., 2007). The afferent fibres supplying the GI tract greatly outnumber efferent fibres and play an important role in the reflex control of the gut and in carrying sensory information from the viscera to the CNS.

Early studies with light microscope revealed that in the vagus nerve the proportion of afferent fibres is 80-90% (Evans and Murray, 1954). Later studies using electron microscopy and abdominal retrograde tracers have confirmed the predominance of afferents in the vagus. However, it is generally considered that abdominal vagal trunks contain 75-80% afferent nerves (Prechtl and Powley, 1990). The proportion of afferents in the splanchnic nerve is considerably less than in the vagus, constituting only 10-15% of the total fibre population (Neuhuber et al., 1986).

The extrinsic afferent neurons can be anatomically distinguished into three different subtypes:

1) Vagal primary afferent neurons: these innervate the upper GI tract via the parasympathetic vagal nerve and the parasympathetic sacral pelvic nerve, from the stomach to the proximal colon with decreasing density.

2) Spinal primary afferent neurons: they innervate most of the GI tract via the splanchnic and hypogastric nerves. The vagal afferent neurons have their cell bodies in the nodose and jugular ganglia, while the spinal afferent neurons have their cell bodies in dorsal root ganglia (DRG) (Cervero and Sharkey, 1988).

3) Intestinofugal afferents whose cell bodies are located in the myenteric and submucosal ganglia and have intestinofugal projections that runs in the mesenteric nerves to the prevertebral ganglia.

The extrinsic afferents convey a vast amount of information about the physical and chemical condition of the gastrointestinal tract. The adequate stimuli for visceral afferents are those arising from their environment and especially from their own activities and pathologic states. The extrinsic afferents respond to mechanical deformation and are sensitive to intraluminal nutrients, protons and inflammatory mediators (Johnson et al., 2006). There are significant differences in their form and function of transduction in three subtypes (Blackshaw et al., 2007)

1.2.2 Vagal afferent fibres

As mentioned above, the vagus nerves innervate thoracic and abdominal viscera from the proximal oesophagus to the proximal part of the colon. The cell bodies of the vagal afferent fibres are located in the nodose and jugular ganglia and input to the brainstem. The central

processes of vagal afferent neurons enter the medulla and terminate in the nucleus tractus solitarius (NTS). In addition, there is a vagal input into the dorsal motor nucleus of the vagus (Beckstead and Norgren, 1979; Kalia and Sullivan, 1982).

The vagus penetrates the diaphragm, the vagus emerges as dorsal and ventral trunks (or anterior trunks), which are continuous with the right and left cervical vagi respectively. The ventral trunk divides into three branches: the common hepatic, ventral (or accessory) celiac and ventral gastric, whilst the dorsal trunk divides into celiac and gastric branches (Powley et al., 1983; Prechtl et al., 1985). The ventral or anterior gastric branch supplies the ventral side of the stomach and through small fascicles within the circular muscle of the pyloric sphincter it also innervates the proximal duodenum. The dorsal or posterior gastric branch enters the dorsal side of the stomach near the cardia along the left gastric artery (Berthoud and Neuhuber, 2000). The stomach is predominantly innervated by the gastric branches, with additional innervation to the fundus, antrum and pylorus from the hepatic branch of the vagus (Berthoud et al., 1991; Berthoud et al., 1992; Phillips et al., 1998). Vagal afferent fibres contribute the vast majority of fibres present within the vagus nerve outnumbering efferent fibres by a ratio of 9:1 (Sengupta et al., 1994; Johnson et al., 2006).

The majority of vagal afferent fibres are unmyelinated C fibres, which transmit sensory information at low conduction velocity. The rat abdominal vagus (or subdiaphragmatic trunks) contains over 30000 (light microscope) to 50000 (electron microscope) afferent fibres, which input into the brain stem (Grundy and Scratcherd, 1989; Sengupta and Gebhart, 1994). Less than 1% of all fibres are myelinated, and the average size of the unmyelinated fibres is about 0.8 μm, with some axons as thin as 0.1 μm (Andrews, 1986; Berthoud and Neuhuber, 2000).

1.2.3 The vagal afferent terminal: structure and distribution of IGLEs and IMAs

The two main types of vagal afferent endings are termed IGLEs and IMAs (Neuhuber, 1987; Berthoud and Powley, 1992; Berthoud et al., 1997; Phillips et al., 1997; Wang and Powley, 2000). IGLEs were first described 1929 (Lawrentjew, 1929) and shown to be vagal afferents by selective lesions. The function of these endings was characterized fully by Rodrigo in 1975 (Rodrigo et al., 1975). They typically consist of a distinct cluster of terminal puncta which arise from a single afferent fibre. This parent axon commonly ramifies into several individual IGLEs. These encapsulate a myenteric ganglion or the pole of a ganglion. IGLEs have long

been speculated to function as mechanoreceptors within the gut. This hypothesis was confirmed by elegant studies that combined fast anterograde tracing techniques and electrophysiological recordings (Zagorodnyuk et al., 2002).

Wherein the proximal gut, IGLEs have been reported to innervate 100% and 80% of oesophageal and gastric myenteric ganglia respectively. In the ileum and colon only 10-15% of myenteric ganglia seem to be innervated by IGLEs (Berthoud et al., 1997; Neuhuber et al., 1998; Wang et al., 2000; Castelucci et al., 2003). Within individual gut regions, a general rostrocaudal decrease in the density of IGLEs occurs. In circumferential direction, the largest number of IGLEs is found typically near the point of nerve entry, e.g. mesenteric border or lesser curvature of the stomach. The density of IGLEs is highest in the corpus of the stomach (6.3 IGLEs/mm^3). Additional areas of increased IGLE innervation are also reported, before and after the major sphincters of the gut, for example the oesophageal hiatus, the prepyloric area of the stomach and proximal duodenum. In addition to vagal IGLEs, a population of rectal IGLE (rIGLEs) has recently been described, supplied by pelvic afferent fibres (Lynn et al., 2003; Olsson et al., 2004). These rIGLEs resemble vagal IGLEs in many ways, although smaller with less extensive branching and clustering of terminals (Johnson. 2006).

The second type of specialised vagal afferent endings found in gastrointestinal smooth muscle, IMAs, take part in the vagal sensory innervation of the stomach. This second type of ending was first described in detail by Berthoud and Powley in 1992 (Berthoud and Powley, 1992). IMAs typically consist of two or more parallel terminal processes which originate from a single axon.They are interconnected by bridging elements which converge in either circular or longitudinal smooth layers, where they have been found to form appositions with interstitial cells of Cajal (ICCs) (Leonard, 2006). This arrangement of IMAs within the smooth muscle layers has lead to speculation that they function as a further type of vagal mechanosensor within the gut, possibly in association with ICCs. However, data obtained by Zagorodnyuk et al. (Zagorodnyuk et al., 2001) failed to find a correlation between labelled IMAs and areas of increased afferent fibre activity to von Frey hair probing. This indicates that further studies are needed to confirm this hypothesis.

IMAs are predominantly located within the stomach (17.3 IMAs/mm^3) (Wang and Powley, 2000; Berthoud et al., 1997) and the lower esophageal and pyloric sphincters (Berthoud and Powley, 1992; Fox et al., 2000; Phillips et al., 1997; Sengupta et al., 1997). In the intestine IMAs are sparse, with a slight clustering found at the junction of the proximal and midcolon segments (Johnson, 2006).

Vagal afferent input to the central nervous system plays an important part in reflex regulation of gastrointestinal function, in the regulation of feeding behaviour and satiety. Vagal afferents are not generally considered to be involved in conscious visceral sensations. The splanchnic, spinal visceral afferents, very likely mediate pain that arises from the viscera (Mayer and Raybould, 1990). However, vagal gastric and duodenal mechanoreceptors and chemoreceptors are implicated in behavioural changes such as satiety, nausea, and vomiting (Grundy and Reid, 1994). Although there is now evidence that vagal afferent fibres are of importance in the modulation of nociception (Grundy, 1988), experimental data suggest that vagal afferents mediate an antinociceptive message. For example, electrical stimulation of the vagus produces analgesia in classical tests such as the tail-flick reflex (Ren et al., 1991; Ren et al., 1993).

1.2.4 Electrophysiological characteristics of vagal afferent terminals

Mechanical stimuli can directly activate ion channels (Corey and Hudspeth,1983, Sachs,1986). It has recently been shown shown that IGLEs are the mechanotransduction sites of vagal mechanoreceptors in the guinea pig upper gut (Zagorodnyuk and Brookes, 2000; Zagorodnyuk et al., 2001). Recordings from single esophageal vagal fibres by Zagorodnyuk and his colleagues demonstrate that 4-AP and α-dendrotoxins, both blockers of rapidly inactivating I_A like currents, increase basal firing rate and stretch evoked firing, indicating an important role for these channels in regulating the excitability of the gastrointestinal IGLEs (Zagorodnyuk et al., 2002). They found that excitability of mechanically-sensitive vagal afferents was increased dramatically by relatively low dose of 4-AP and by α-DnTX and DnTX K. Their data strongly suggest that voltage-gated Kv1.1, Kv1.2 or Kv1.6 channels are present on these endings. The macroscopic I_A is likely a composite of several currents, with slight differences in activation properties and kinetics. The blockade of this current by α-dendrotoxins suggests the presence of K_v 1.1 and 1.2 and 1.6 subunits (Glazebrook et al., 2002) which in heterologous systems give rise to an I_A like current. In addition, the results showed that excitability of vagal mechanically sensitive endings in the guinea pig oesophagus was increased in Ca^{2+}-free Krebs solution (spontaneous and stretch evoked firing was increased while silent period was decreased) suggesting an involvement of Ca^{2+} dependent K^+ channels (Zagorodnyuk et al., 2002).

1.2.5 Physiological function of vagal afferent terminals

Function as mechanoreceptors

The function of vagal endings correlates well with their anatomy. Different populations of vagal afferent terminations in the gastrointestinal tract indicate different sensory modalities which encode mechanical as well as chemical stimulation. It has been hypothesized that the biophysical arrangements of IGLEs and IMAs allow them to transduce different forms of forces (Powley and Phillips, 2002). IGLEs are in intimate contact with the connective tissue capsule and enteric glial cells surrounding myenteric ganglia and have long been hypothesized to detect mechanical shear forces between the orthogonal muscle layers (Neuhuber, 1987). Evidence for such a mechanosensory function of IGLEs has been elaborated by mapping the receptive field of vagal afferent endings in the oesophagus and stomach and showing morphologically that individual 'hot spots' of mechanosensitivity correspond to single IGLEs (Zagorodnyuk and Brookes, 2000; Zagorodnyuk et al., 2001; McMahon, 2004) which could be activated both by gut distension and by focal mechanical probing with light von Frey hairs.

IMAs, being in parallel to smooth muscle fibres, have been proposed to transduce passive stretch. A recent study has shown in the oesophagus of the guinea pig that several classes of mechanoreceptors can be distinguished functionally from the IGLE-bearing, low threshold in-series tension receptors. It is possible that intramuscular arrays are the transduction sites of this high threshold, wide dynamic range afferents (Yu et al., 2005; Blackshaw et al., 2007).

Function as chemoreceptors

IGLEs may have other functions, such as being transmitter release sites for synaptic interactions with enteric neurons or as chemosensitive sites responding to neurochemicals in enteric ganglia (Blackshaw et al., 2007). IGLEs may also respond to chemical stimuli such as acetylcholine and ATP raising the possibility that these endings also play a key role in detecting release of mediators within the synaptic neuropil of the myenteric ganglia or surrounding tissues (Kirkup et al., 2001). However, evidence that such chemosensory mechanisms contribute to mechanotransduction is lacking (Berthoud et al., 2004). Some specific cells (e.g. mast cells) may release several of these modulating agents, some of which may act directly on the sensory nerve terminal while others may act indirectly, causing release of other agents from other cells in a series of cascades. Other endogenous chemical mediators

can down regulate afferent sensitivity such that an imbalance in pro- and antisensitizing mechanisms may lead to a disordered sensory signal (Berthoud et al., 2004).

Function as nociceptors

The vagal afferents are mainly involved in physiological regulation of the different processes ongoing in the gastrointestinal system; splanchnic afferents mediate mainly nociception from the gut, while pelvic afferents are involved in both physiological regulation and nociception. Although vagal afferents do not themselves evoke pain when activated, evidence from studies of guinea pig vagal afferents indicates that the jugular ganglion contains cell bodies of vagal afferents with very similar properties to small DRG neurons, suggesting they may have a nociceptive role (Yu et al., 2005). However, how this finding translates to other species remains to be determined. There is a great deal of information in the literature about the pharmacology of vagal afferents, both for their central transmission and modulation and for their peripheral sensory function (Blackshaw et al., 2007).

1.3 Enteric nervous system

The ENS is now well recognized by gastroenterologists and gastrointestinal physiologists as the "brain in the gut" (Wood, 1981; Wood, 2002). This is because it can be considered as an autonomic nervous system that controls and coordinates all gut vital functions, including motility, secretion, absorption, blood flow, and aspects of the local immune system, independent of the central nervous system.

1.3.1 Structure of the ENS

The ENS contains about 10^8 neurons in two major ganglionated plexi that are located within the gut wall (Grundy and Schemann. 2005). The myenteric plexus, also known as Auerbach's plexus, is distributed along the entire gastrointestinal tract and is localised between the outer longitudinal and circular muscle layers. A distinct submucous plexus, also called Meissner's plexus, is found only in the small and large intestine where it is localised within the submucosa near the inner surface of the circular muscle layers. Small animals, such as the guinea pig, usually have a single layer of submucosal plexus. In larger mammals, the submucous plexus is subdivided into the inner submucous plexus and outer submucous

plexus. Inner submucous plexus is located close to the muscularis mucosae and outer submucous plexus is located adjacent to the luminal side of circular muscle layer (Furness and Costa 1980; Timmermans et al., 1997) (**Figure 1**). In the human ENS there are as many neurons present as in the spinal cord (10^{10}). The submucous plexus is further subdivided into three separate plexi, namely the outer submucous plexus (Schabadasch or Henle plexus), the inner submucous plexus (Meissner plexus) and an intermediate plexus (Hoyle and Burnstock, 1989, Ibba-Manneschi et al., 1995). In the human small intestine, the intermediate plexus shares similarites in neurochemical content to the inner submucous plexus, whereas in the human colon the intermediate plexus more closely resembles the outer submucosal plexus (Crowe et al., 1992).

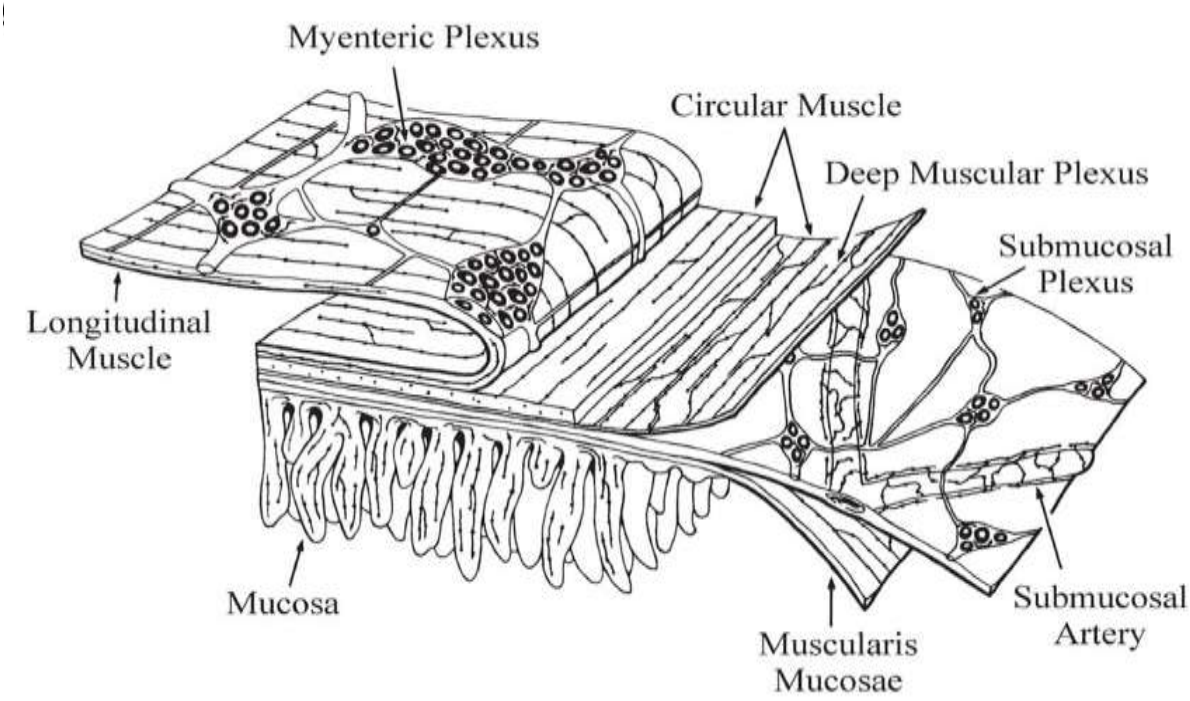

Figure 1: The ENS consists of two major ganglionated plexi layers: the myenteric and the submucous plexus and non-ganglionated plexi of nerve fibres innervating muscle layers, blood vessels, glands and epithelium. In the human ENS, the submucous plexus can be subdivided into three distinguishable layers (see text). Picture adopted by Sebastian Hoff from (Furness & Costa 1980).

The two plexi are connected to each other by numerous fibre bundles that run almost perpendicular to the circular muscle layer. Reflexes can involve one or both plexi, although during normal motility their activities are synchronized (Wood, 2006). The two ganglionated neural networks contain complete reflex arcs (Furness et al., 1998; Costa et al., 2000; Lomax et al., 2000; Smith et al., 2005). The myenteric neurons are largely involved in motility of the gut, as most of the motor neurons that innervate circular and longitudinal muscles reside in this plexus (Wilson et al. 1987). The submucous neurons are predominantly involved in the

regulation of transmucosal movement of water and electrolytes, and local blood flow (Timmermans et al., 2001).

1.3.2 Classification of neurons in the ENS

Neuronal classification

Most of the characterizations of the ENS originate from studies in guinea pig ileum. Enteric neurons can be classified by their morphology and electrophysiologic properties (Grundy and Schemann. 2005).

Morphological classification

To characterize the enteric neurons based on their different lengths and shapes of the dendrites by Alexander Dogiel remains the most widely used classification (Dogiel, 1899). They are divided into three main groups: Dogiel Type I, Type II and Type III. Dogiel type I neurons are characterized by flattened, slightly elongated cells with 4 to 20 dendrites and a unique long axon (uniaxonal), with the initial part often giving rise to axonal spines. Neurons with this type of morphology can belong to different functional classes. They project to the circular muscle (circular muscle motor neurons), to the longitudinal muscle (longitudinal muscle motor neurons), and to other myenteric ganglia (interneurons). Dogiel type II neurons have large round or oval cell bodies with 3 to 10 dendrites and multiple long axon processes which project preferentially in the circumferentiall direction (Furness JB et al., 1990, Hendriks et al., 1990; Clerc et al., 1997). The axons give rise to large numbers of varicose nerve endings in myenteric ganglia. Dogiel type II neurons are located both in the myenteric and submucosal ganglia. Terminals of Dogiel type II project into mucosal regions, and are excited by mechanical and chemical stimulation of the mucosa. About 80-90% of Dogiel type II neurons are immunoreactive for the calcium binding protein calbindin (Furness et al., 1990). Dogiel type III neurons are intermediate between type I and type II, with 2 to 10 short dendritic processes that project over a short distance. For their electrophysiologic properties enteric neurons can be divided into two groups based on intracellular recordings (Hirst et al. 1974).

AH neurons have slow excitatory postsynaptic potentials (sEPSP), characterized by a phasic spike discharge with a late prolonged afterhyperpolarization (AHP) current that can last between 2 to about 30 s following a single action potential discharge. The action potential of AH neurons are not only dependent on voltage-activated sodium channels but also calcium channels. Increasing intracellular calcium concentration activates calcium-dependent

potassium-channels, ultimately resulting in repolarization and prolonged afterhyperpolarization in those neurons. The action potential as well as the afterhyperpolarization of AH neurons remain unaffected by tetrodotoxin. These neurons are mostly sensory neurons or interneurons with Dogiel type II morphology (Hirst et al. 1974; Furness 2006).

S-neurons have electrophysiological characteristics consisting of action potentials of short duration followed by only a brief afterhyperpolarization (< 100ms). The action potential is generated by tetrodotoxin-sensitive sodium channels. They are mediated by opening of rapid sodium channels. Electrical stimulation of these neurons leads to fast excitatory postsynaptic potentials (fEPSP) that are blocked by hexamethonium. The transmission thus involves acetylcholine binding to nicotinic acetylcholine receptors. These neurons are considered to function as excitatory and inhibitory motor neurons or interneurons with Dogiel type I morphology (Hirst et al. 1974; Furness, 2006).

Functional classification

According to the main functional and neurochemical properties of the enteric neurons they are classified into 17 different neuronal populations in the guinea pig. Of these14 are present in the small intestine (Furness 2000). These neurons can be grouped in three main categories: sensory neurons, interneurons and motor neurons. Only less than 1% of the neurons are classified as intestinofugal neurons.

Sensory neurons

Two broad classes of primary afferent neurons are associated with the gut, the intrinsic primary afferent neurons (IPANs) and the extrinsic primary afferent neurons (EPANs). IPANs are located within the gut wall and are likely to initiate local reflexes (Furness JB et al., 2004). They receive information on luminal contents from entero-endocrine cells, but may also directly function as sensory neurons. They can detect and transmit information about character and intensity of a stimulus. The transmission takes place by cholinergic and non cholinergic synapses (Furness et al. 1984). IPANs have the properties of Dogiel type II neurons. Electrophysiologically they are AH neurons.

Interneurons

There are three descending interneurons and one ascending interneuron in the guinea pig small intestine (Bornstein et al. 2004). Functionally, these neurons are involved in the

conduction of the sensory signal from the afferents to the motor neurons. The ascending interneurons are excitatory and contain acetylcholine, substance P and tachykinins. They are arranged in functional chains that are linked by cholinergic nicotinic synapses (Brookes et al., 1997). The descending pathways are inhibitory and include neurons that contain acetylcholine, somatostatin, 5-HT, VIP and NO. They connect via cholinergic and non-cholinergic pathways. The descending interneurons are involved in local motility reflexes, migrating myoelectric complexes in the small intestine and secretomotor reflexes and not directly in motility reflexes. Most of the interneurons have Dogiel type I morphology. Electrophysiologically interneurons are S neurons.

Motor neurons

Motor neurons of the myenteric plexus are subdivided in five types including excitatory and inhibitory muscle motor neurons, secretomotor/vasodilator neurons, secretomotor neurons that are not vasodilator and neurons innervating enteroendocrine cells. Both excitatory and inhibitory motor neurons receive information from interneurons and forward it to the circular and to the longitudinal muscles. The excitatory motor neurons project orally about 6-12 mm to the circular muscle and their primary transmitters are acetylcholine and tachykinins. The inhibitory motor neurons project in the anal direction for distances of about 3-25 mm and their main neurotransmitter are ATP, NO, VIP and PACAP. Activation of excitatory motor neurons elicits a depolarization in circular smooth muscle and results in contraction, whereas activation of the inhibitory motor neurons elicits a hyperpolarization leading to relaxation of the smooth muscle (Bornstein et al., 2004). Motor neurons are Dogiel type I morphology. Electrophysiologically motor neurons are S neurons. They generate both fast and slow EPSPs and their cell bodies lie in the myenteric plexus.

Secretomotor and vasomotor neurons: The submucous plexus contains secretomotor and vasomotor neurons. They project to the mucosa where they induce secretion, or, in the case of vasomotor neurons, to the small arterioles where they induce vasodilatation.

Multifunctional enteric neurons

The reflex pathway in enteric neurons includes stimulation of sensory neurons, transmission through interneurons, and activation of motor neurons that finally induces responses of the effectors. A new concept considers the existence of “multifunctional enteric neurons” and is based on findings that a substantial proportion of enteric neurons are multifunctional or multitasking as opposed to the classical view that a single function can be assigned to a

particular neuronal population (Schemann and Mazzuoli, 2010). Mazzuoli et al. recently showed spike discharge evoked by deformation in myenteric neurons of the guinea pig ileum. The data suggest that interneurons and even motorneurons are mechanosensitive. These neurons are referred to as rapidly adapting mechanosensitive enteric neurons (RAMEN). This term is based on their response with spike discharge to dynamic changes during deformation and their response pattern. These neurons may behave like rapidly adapting mechanosensors (Mazzuoli and Schemann 2009). RAMEN differ from IPANs in various aspects. RAMEN have no unique morphology or neurochemical code and belong to functionally different classes. RAMEN show multifunctionality with probably sensory, integrative and motor functions. Retrograde labelling identified them as interneurons and also as motorneurons. The rapid adaptation in RAMEN may be very important in the gut where neurons have to rapidly integrate a variety of different stimuli in order to adjust their output and to appropriately modulate muscle activity.

1.3.3 Types of neuronal transmission in ENS

Fundamental mechanisms for chemically mediated synaptic transmission in the ENS are the same as elsewhere in the nervous system. Synaptic transmitters from axonal terminals or transaxonal varicosities are released by action potential triggering voltage activated Ca^{2+} channels to open. Once released, enteric neurotransmitters bind to their specific postsynaptic receptors to evoke ionotropic or metabotropic synaptic events (Leonard R. Johnson, 2006). There are four main types of neuronal transmissions that occur between neuronal synapses in the ENS: excitatory postsynaptic potentials (EPSPs), inhibitory postsynaptic potentials (IPSPs), and presynaptic inhibition and facilitation. The EPSPs include fast excitatory postsynaptic potentials (fEPSPs) with durations in the millisecond range and slow excitatory postsynaptic potentials (sEPSPs) last for several seconds, minutes, or longer. The fEPSPs occur in AH and S neurons in both myenteric and submucosal plexi. They appear to be the only mechanism of transmission between vagal efferent and enteric neurons. The dominant part of fast transmission in the ENS is cholinergic, involving nicotinic cholinergic receptors (Galligan and North, 2004). ATP acting at purinergic P2X receptors and 5-HT (serotonin) acting through 5-HT3 receptors has also been shown to be involved (Galligan, 2002). The sEPSPs are primarily due to reduction in resting K^+ conductance. Slow IPSPs are more prominent in submucosal neurons than in myenteric neurons (Hirst and McKirdy, 1975). Slow IPSPs are primarily due to increased K^+ conductance. In addition, neurotransmitters can reduce transmitter release at excitatory synapses, a process called presynaptic inhibition.

Action of acetylcholine is mediated by presynaptic muscarinic receptors and decreases the release of transmitters. This mechanism plays an important role for autoinhibitory function in negative feedback regulation of the amount of local transmitter release. Norepinephrine and opioids may also bind presynaptically to reduce the release of acetylcholine (Johnson, 2006).

1.3.4 Immuno-neural interactions

The immune system in the gut with mast cells, resident macrophages, and white blood cells, can be activated at short notice and forms another powerful control system (Johnson, 2006). The enteric immune system provides security at one of the most contaminated borders between the interior of the body and his environment. It deals continuously with dietary antigens, parasites, bacteria, viruses, and toxins as they appear in the warm-dark-moist-anaerobic environment of the intestinal lumen. The system is continuously challenged because physical and chemical barriers at the epithelial interface never exclude the large antigenic load in its entirety. Electrophysiological studies in enteric neurons confirm that inflammatory mediators released in paracrine fashion alter electrical and synaptic behavior of enteric neurons (Wood, 2007).

Chronic intestinal pseudo-obstruction and achalasia are disease of unknown cause. Proposed causes of these diseases include autoimmune disorders. There are anti-neuronal antibodies present in the serum of some patients with autoimmune diseases. The level of circulating anti-enteric antibodies, however, was not found to correlate with symptom severity and their presence may be related to tissue injury and may therefore represent an epiphenomenon rather than cause an effect. In this respect, Bruley des Varannes et al. found that the application of serum from achalasia patients to biopsy specimens of human fundus maintained in culture for up to 72 h resulted in a reduction of the number of NOS neurons and a concomitant increase in choline acetyltransferase neurons without affecting the total number of myenteric neurons (Bruley des Varannes, 2006). The functional consequence of these changes was demonstrated by the decrease of nerve evoked, nitric oxide-mediated, inhibitory muscle response following exposure to the achalasia serum. Factors in the sera of these patients responsible for the phenotypic changes in enteric neurons have not been identified but could include neuronal antibodies, neurotrophins and a variety of inflammatory mediators including cytokines (Grundy and Schemann, 2006).

1.4 Paraneoplastic syndromes

Paraneoplastic syndromes result from damage or dysfunction of organs that are not invaded by a neoplasm or its metastases, also called remote effects of cancer (Honnorat, 2007). By definition, these disorders are not caused by tumor cell infiltration, infection, ischemia, metabolic and nutritional deficits, surgery or other forms of tumor treatment. Symptoms may be secondary to substances secreted by the tumor or may be a result of antibodies directed against tumors that cross-react with other tissue. Symptoms may occur in any organ or physiologic system. Despite the unknown pathogenesis of paraneoplastic syndromes antibodies and T-cell responses are believed to be important for many of these disorders (Vernino, 2006). Paraneoplastic syndromes occur in 20% of cancer patients, but these syndromes are often unrecognized. The most common cancers associated with paraneoplastic syndromes are those that arise from the lung; others include renal carcinoma, hepatocellular carcinoma, leukemias, lymphomas, breast and ovarian tumors, neural cancers, gastric and pancreatic tumors (Posner and Dalmau, 1997; Darnell, Posner, 2006).

1.4.1 Types of Paraneoplastic Syndromes

The following types of paraneoplastic syndromes have been defined: Endocrine, mucocutaneous, hematological and neurological paraneoplastic syndromes.

Most of the paraneoplastic endocrine syndromes are associated with the production of peptide hormones, which in some instances have autocrine stimulatory effects (DeLellis and Xia, 2003).

Patients with paraneoplastic hematological syndromes may develop erythrocytosis, anemia, neutrophilia, neutropenia, eosinophilia, thrombocytosis, thrombocytopenia, venous thromboembolism and disseminated intravascular coagulation. These abnormalities are caused by the production of biologically active growth factors, hormones or as yet unidentified "humors" by the tumor (Staszewski, 1997).

Paraneoplastic mucocutaneous syndromes are a group of dermatoses exhibiting a variable morphologic and pathologic picture. They can occur in association with solid tumors or hematologic malignancies. Itching is the most common cutaneous symptom experienced by patients with cancer (eg, leukemia, lymphomas) and may result from hypereosinophilia (Steele and George, 2001).

Paraneoplastic neurological syndrome (PNS) is a particularly devastating form of paraneoplastic syndromes (Steele and George, 2001). These paraneoplastic disorders affect the central or peripheral nervous system; some are degenerative (Darnell, Posner, 2006). As a result of these immune responses, discrete or multifocal areas of the nervous system degenerate, causing diverse symptoms and deficits. The nervous system is one of the most commonly affected areas.

1.4.2 Historical considerations

Probably the first unequivocal paraneoplastic syndrome was described in 1865 by Armand Trousseau (Trousseau, 1865; Trousseau, 1873). The most common clinical manifestation of a paraneoplastic syndrome, a sub-acute progressive sensory neuronopathy, was reported by Weber and Hill in 1933. They noted a complete degeneration of the posterior columns on examination of the spinal cord from a patient with "chronic polyneuritis" that also suffered from an oat cell carcinoma of the lung (Weber and Hill, 1933). In 1965 the first paraneoplastic antineuronal antibody was reported by Wilkinson and Zeromski (Wilkinson and Zeromski 1965). Graus et al. in 1985 described the anti-Hu immunoglublin G antibody in immunohistochemical preparations and yielded bands in the 35-40 kD region on Western blot analysis of proteins from cerebrocortical neurons, serum and cerebrospinal fluid (CSF) of patients with subacute sensory polyneuropathy accompanying small lung cell carcinoma (SCLC) for the first time (Graus, 1985). They designated the antibody by the first two letters of their index patient's last name, and it was named as anti-Hu antibody (Graus, 1985). During the 1980ies several groups started to work on this topic and a number of antineuronal antibodies have been described since then. The number of immunological responses detected in association with paraneoplastic syndromes of the nervous system has steadily increased. These responses were supported by the presence of antineuronal antibodies in serum and CSF and/or infiltrates of T-cells in the tumor and nervous system (Dalmau et al., 1999). Later, cytotoxic T cells have been shown to transform in response to specific paraneoplastic antigens, and these cells are capable of inducing tumor cell cytotoxicity (Albert et al., 2000).

1.4.3 Paraneoplastic gastrointestinal dysmotility

A small proportion of patients with occult or established neoplasms develop a gastrointestinal motility disorder, named as paraneoplastic GI dysmotility. Although rare, it often affects the entire GI tract. Paraneoplastic GI dysmotility may also affect isolated segments resulting in

discrete syndromes (DiBaise, 2011). In patients with paraneoplastic GI dysmotility, a humoral immune response involving circulating antineuronal antibodies is commonly seen. A variety of specific serum antibodies directed against antigens expressed by both the tumor and the enteric neuron as the „innocent' bystander (onconeural antibodies) has been reported in association with paraneoplastic GI dysmotility. This helps to define different subtypes and, potentially, leads to an earlier diagnosis (Kashyap and Farrugia, 2008). The antigens for these antibodies may be localized at the nucleus, plasma membrane or the cytoplasm. The exact mechanism by which these antibodies are generated is unknown (Kashyapand and Farrugia, 2008).

Clinical symptoms of paraneoplastic gastrointestinal dysmotility

Esophageal dysmotility (pseudoachalasia), gastroparesis, and intestinal pseudo-obstruction may be observed as symptoms of paraneoplastic GI dysmotility (Kashyap and Farrugia, 2008). Patients with paraneoplastic GI dysmotility may have a dominant symptom suggesting involvement of an isolated segment of the GI tract. However, in most cases the entire gut is involved and there is a wide variety of symptoms present (DiBaise, 2011). Paraneoplastic GI dysmotility is often rapidly progressive, leaving the affected patients debilitated in a matter of months. Indeed, a subacute (less than 6 months) progressive clinical course and an associated severe disability are highly suggestive for a paraneoplastic etiology of the GI dysmotility (Dhamija et al., 2008). In up to 80% of patients these symptoms may precede the diagnosis of the underlying tumor by weeks to years (usually 6 months). Occasionally, the tumor may only be diagnosed at autopsy. Indeed, in one of the larger case series, the GI dysmotility was observed to precede the diagnosis of SCLC by a mean of 8.7 months (Lee et al., 2001).

Neuropathology of paraneoplastic gastrointestinal dysmotility

In patients who have had a full thickness biopsy, all had an inflammatory lymphocytic and plasma cell infiltrate of the myenteric plexus and a decrease in the number of ganglion cells, replacement of neurons by Schwann cells and collagen. Smooth muscle cells are typically unaffected (Krishnamurthy and Schuffler, 1987; Smith et al., 1997; De Giorgio R et al., 2000a; De Giorgio R et al., 2000b; De Giorgio et al., 2004). Chronic intestinal pseudo-obstruction can involve the extrinsic nerves of the gut, the myenteric plexus and the intestinal pacemaker cells of Cajal (Kashyap et al., 2005; Lorusso et al., 2007). Histological examination of the bowel wall shows abnormalities of the number or relative proportion of argyrophilic neurons, and neuronal fibrosis (Freeman et al., 2005).

Recently, a loss of interstitial cells of Cajal was demonstrated in a patient with paraneoplastic dysmotility, suggesting that enteric neurons are not the only enteric target of paraneoplastic autoimmunity (Pardi et al., 2002).

Pathogenetic hypothesis of paraneoplastic gastrointestinal dysmotility

Both humoral and cellular immune mechanisms are involved. The current concept is that most, if not all, paraneoplastic neurological syndromes that affect the nervous system are autoimmune-mediated (Posner and Dalmau, 1997). The hypothesis is that antigens normally expressed only in the nervous system are aberrantly expressed in a tumor. Apoptosis of tumor cells may release antigens which then stimulate antibody formation (Dalmau et al., 1999). The immune response not only represses growth of the tumors, it also attacks those parts of the nervous system that express the „onconeural' antigen. The result is that the tumor remains small but patients suffer severe neurologic dysfunction (Roberts and Darnell, 2004). Immune damage of the nervous cells may then result in symptoms related to loss of normal function. Paraneoplastic syndromes may affect any part of the central and peripheral nervous systems (Honnorat and Antoine, 2007).

There is similar pathogenetic hypothesis in paraneoplastic GI dysmotility and paraneoplastic neurological syndromes. In paraneoplastic GI dysmotility, tumor antigens may elicit an immune response that cross-reacts with enteric or autonomic neural tissue leading to an immune attack directed against both the tumor and the respective nervous system (DiBaise, 2011; Maverakis et al., 2012). Consistent with this hypothesis is the finding demonstrating that onconeural antibodies selectively bind to enteric neurons in the myenteric plexus (Lennon et al., 1991; Condom et al., 1993; De Giorgio et al., 2003). The pathogenetic hypothesis in paraneoplastic GI dysmotility is also supported by a study in which mice in which IgG prepared from serum containing ganglionic-type acetylcholine receptors (NAChRs) was systematically injected. They developed slowed GI transit, urinary retention, and other si of dysautonomia (Vernino, 2004).

Cellular immune mechanism has been suggested to play a role in the pathogenesis of PNS (Albert et al., 1998; Albert et al., 2000; Plonquet et al., 2003). However, it has not been consistently demonstrated for the following reasons: (1) Presence of extensive infiltrates of T cells in the nervous system. (2) T cell proliferation in the tumor. (3) Most tumors express major histocompatibility complex proteins, which indicate the need for antigen presentation to T cells, whereas MHC class 1 proteins are rarely expressed in SCLC that are not associated with paraneoplastic syndromes. (4) Passive transfer experiments do not provide evidence in

favor of antibody-mediated disease alone. Furthermore, the histologic nature of the underlying malignancy does not always dictate a certain autoantibody formation or specific dysmotility syndrome (Sutton et al., 2004, Honnorat and Antoine, 2007; DiBaise, 2011; Kashyap and Farrugia, 2008).

Despite these histologic findings and the presence of autoantibodies, the exact role of antineuronal antibodies in the pathogenesis of the disease is unknown (Senties-Madrid and Vega-Boada, 2001; DiBaise, 2011).

1.5 Antineuronal autoantibodies

Types of circulating antineuronal antibodies can be differentiated by immunohistochemistry and western blot. Circulating antineuronal antibodies have been described in conjunction with certain tumors and paraneoplastic neurological syndromes. It has been shown that these patients have developed an immune response against the Hu antigens, a family of neuronal RNA-binding proteins (Graus, 1985). Since then, a continuously growing number of more or less characterized paraneoplastic antibodies have been defined. For example, anti-Hu antibody is also called antineuronal nuclear antibody (ANNA). ANNA is classified into ANNA-1 (type-1 antineuronal nuclear antihody, anti-Hu) and ANNA-2 (type-2 antineuronal nuclear antibody, anti-Ri). Detection of paraneoplastic antibodies is clinically important because it diagnoses an often serious neurological syndrome as paraneoplastic and directs the search for an underlying neoplasm. Involvement of diferent onconeural antibodies in paraneoplastic GI dysmotility is summarised below (**Table 1**).

Table 1: Onconeural antibodies associated with paraneoplastic GI dysmotility.

Antibodies	**Tumor Types**
ANNA-1	SCLC and thymoma
ANNA-2	SCLC and breast
Calcium Channel Antibodies	SCLC, non-SCLC, other carcinomas
AChR	SCLC, non-SCLC, other carcinomas
Striational antibody	SCLC, non-SCLC, other carcinomas
voltage-gated potassium channel	SCLC, non-SCLC, other carcinomas

Abbreviations: ANNA, anti–neuronal nuclear antibody; AChR, Nicotinic Acetylcholine Receptors.

1.5.1 ANNA-1 (anti-Hu)

The first and most common autoantibody recognized to be associated with paraneoplastic GI dysmotility is the ANNA-1 also known as anti-Hu antibody (Kashyap and Farrugia, 2008; DiBaise, 2011). The routine laboratory detection of Hu antibodies is generally performed by an immunohistochemical technique (e.g. indirect immunofluorescence) followed by confirmation with Western blot using purified recombinant HuD protein as substrate (Moll and Vecht, 1995). High titers of Hu antibodies are invariably associated with a paraneoplastic neurological syndrome and in more than 80% of adult patients the underlying tumor is SCLC (Kiers et al., 1991; Pittock et al., 2004). Other tumors that may express ANNA-1 include breast, prostate, ovarian carcinomas, and lymphomas (Lucchinetti et al., 1998). At the time of neurological presentation, approximately 70% of patients have no diagnosed cancer (Dalmau et al., 1992; Graus et al., 2001; Sillevis Smitt et al., 2002). After detection of ANNA-1, a careful search for an underlying SCLC should be performed. Approximately 30% of patients with ANNA-1 autoimmunity have symptoms of GI dysmotility. The presence of ANNA-1 in the serum of SCLC patients has been shown to correlate with limited stage disease, response to chemotherapy, and improved patient survival. This further supports an autoimmune-mediated disease (Kashyap and Farrugia, 2008). How Hu-antibody participated in SCLC related paraneoplastic neurological syndromes remains unknown.

A preliminary study in guinea pig ileum has suggested that ANNA-1 impair the ascending excitatory reflex and therefore peristalsis in vitro preparations. Enteric neuronal degeneration has also been reported in patients with paraneoplastic GI dysmotility as a possible pathogenetic mechanism (Caras et al., 1995). PNS sera have a cytotoxic effect on cultured myenteric plexus (Schäfer et al., 2000). These cells are a convenient system for the investigation of neurotoxic effects. The observed effect is IgG mediated, complement-independent and was specific for paraneoplasia sera. anti-HuD-positive sera from patients with a paraneoplastic GI dysmotility disorder as well as commercial anti-HuD antibodies have been shown to induce apoptosis in a human neuroblastoma cell line (SH-Sy5Y) as well as guinea pig cultured myenteric neurons (De Giorgio et al., 2003). However, the mechanistics behind the neurotoxic actions is poorly understood.

1.5.2 Hu antigen

The Hu antigen was first identified as the target of autoantibodies found in patients with paraneoplastic encephalomyelitis (Dalmau et al., 1990). Hu antigens are 35-40 kDa proteins which belong to a family of conserved RNA binding proteins. The Hu-proteins are highly homologous to a drosophila protein (Elav), which is critical for nervous system development of the fly (Campos et al., 1985; Szabo et al., 1991). The exact function of the Hu proteins is unknown, but their homology to Elav and their early expression during embryogenesis of the mammalian nervous system suggest that they are likewise crucial for development and maintenance of the neuronal phenotype. There are four mammalian ELAV/Hu proteins, HuA also known as HuR, HuB also known as Hel-N1, HuC, and HuD. HuD was the first of the Hu proteins to be identified as the Hu antigen in patients with paraneoplastic encephalomyelitis and sensory neuropathy (Szabo et al., 1991). ANNA-1 recognizes the nuclear binding protein Hu. The Hu-proteins are mainly expressed in the nucleus, but are also present in the plasma membrane or cytoplasm of neurons in the central, peripheral, and enteric nervous systems, with the exception of HuR, which is ubiquitously expressed in extraneuronal tissues (Wakamatsu and Weston, 1997). Hu proteins are most commonly expressed in SCLC, but may also be expressed in multiple other tumor types (DiBaise, 2011).

1.5.3 Antibodies against acetylcholine receptors

Some antibodies associated with both idiopathic and paraneoplastic forms of GI dysmotility are directed against neuronal nicotinic acetylcholine receptors (nAChR) (Kashyap and Farrugia, 2008; DiBaise, 2011). Antibodies against nAChR present on skeletal muscles endplate cause myasthenia gravis (Griesmann et al., 1997). The ganglionic (consisting of α3-subunits) neuronal nAChR mediates fast synaptic transmission in sympathetic, parasympathetic and as well as in the ENS (Vernino et al., 1998: Vernino et al., 2009). AChR antibodies targeting this protein have a potential to impair cholinergic synaptic transmission leading to autonomic failure (Vernino, 2009).

Nicotinic AChR are a family of ligand-gated cation channels found throughout the central and peripheral nervous system. Neuronal nicotinic AChR are formed from a variety of subunits. These neuronal nAChR have many functions in the nervous system. The nAChRs on autonomic neurons are typically composed of two α3 subunits in combination with three other nAChR subunits. Although autonomic ganglia neurons can express numerous neuronal nAChR subunits, including α3, α4, α5, α7, β2, and β4, the properties of the nAChR at mammalian ganglionic synapses are most similar to nAChR formed by α3 and β4 subunits (Skok et al., 1999; Vernino, 2009).

The clinical and experimental findings indicate that autoimmune autonomic ganglionopathy is an antibody-mediated neurological disorder. Ganglionic nAChR antibodies are found in many patients with autoimmune autonomic ganglionopathy. nAChR antibodies are also found in some patients with other paraneoplastic neurological disorders related to thymoma and small-cell lung cancer (Vernino and Lennon, 2004). Neuronal AChR antibodies are most likely directly pathogenic effectors of autonomic dysfunction. This is indicated by several evidences. Firstly, serum AChR antibody levels correspond to the severity of the autonomic dysfunction and decrease with clinical improvement (Vernino et al., 2000). Secondly, plasmapheresis to remove autoantibodies can produce a dramatic improvement in autonomic function in some cases (Schroeder et al., 2005; Gibbons et al., 2008). Thirdly, when neuroblastoma cells are exposed to ganglionic AChR IgG, the amplitudes of neuronal AChR membrane currents are progressively reduced (Wang et al., 2007).

The aim of this study was to characterize the acute effect of neuronal autoantibodies on enteric neurons and vagal afferents. Serum IgG prepared from patients with ANNA-1 or ganglionic nicotinic α3-AChR autoantibodies were tested in animal and human enteric neurons. As animal model myenteric neurons from longitudinal muscle myenteric plexus preparations from the ileum of guinea pigs was used. The human submucous plexus was chosen as a read out, because it is not possible to reliably record from human myenteric plexus neurons. Serum prepared from healthy subjects or neurologic patients without GI symptoms served as controls.

The purpose of the present study was to identify the mechanism through which ANNA-1 may contribute to enteric neuronal dysfunction. Previous study indicated that anti-HuD positive sera from patients with a paraneoplastic GI dysmotility disorder as well as commercial anti-HuD antibodies induce apoptosis in a human neuroblastoma cell line (SH-Sy5Y) as well as guinea pig cultured myenteric neurons (De Giorgio et al., 2003). Thus, we wanted specifically to gain evidence if anti-HuD antibodies are able to impair the function of enteric and extrinsic mechanosensory neurons. A fast voltage sensitive dye neuroimaging technique was employed to study the effect of anti-HuD or anti-HuA/B/C antibodies on myenteric plexus neurons of guinea pig ileum. Furthermore, extracellular recordings from vagal afferents were used to investigate the effect of these antibodies on vagal afferents in C57B16 mouse gastric fundus. The findings are of great clinical relevance as they provide a mechanistic basis for the exploration of pathogenesis of PNS as well as important evidences for the diagnosis, treatment and prognosis of primary tumors.

2. Materials and Methods

Four experimental methods were employed to investigate the influence of the serum IgG samples on enteric neurons and vagal mechanosensory afferents.

Firstly, serum IgG samples with high concentrations or high titers of antibodies (α3-AchR, ANNA-1 also named anti-Hu or antineuronal nuclear antibodies type 1) were collected. Sera from two patients were affinity purified to isolate the anti-HuD antibody fraction and a second fraction, containing presumably a mixture of anti-HuA, anti-HuB and anti-HuC antibodies. This second fraction was therefore named anti-HuA/B/C. The serum IgG sample from patients without GI symptoms and the serum IgG sample from healthy volunteers served as patient control (PC) and healthy control (HC).

Secondly, Immunohistochemistry was used to study differences in the binding to neuronal structures between the serum IgG samples or the antibodies in guinea pig myenteric plexus longitudinal muscle preparations.

Thirdly, the effect of the serum IgG samples, purified anti-HuD antibody, the anti-HuA/B/C antibodies, HuD antigen and the healthy blood donor sera on guinea pig myenteric neurons and human submucous neurons was examined with neuroimaging techniques.

Fourthly, we examined the response of gastric mechanosensitive vagal afferent fibres to anti-HuD antibodies and the anti-HuA/B/C antibodies using extracellular suction electrode measurements in stomach preparations of C57Bl6 mice.

2. 1 Patient material

2.1.1 Serum IgG samples

The IgG samples were obtained by purifying patient serum samples using protein G. Collection and purification was done at the Mayo Clinic (Lennon's Laboratory, Mayo Clinic, Minnesota, USA). The samples were chosen because they contained high concentrations of antibodies against the α3-AchR or they had high titers of ANNA-1 autoantibodies. The IgG samples from patients without GI symptoms (PC) and samples from healthy volunteers (HC) contained none of the antibodies tested. All samples were also tested for the following antibodies: VGKC (Voltage gated potassium channels), N-, P/Q-Calcium Channels, α1-AchR, CRMP-5 (Collapsin response mediator protein 5), GAD65 (glutamate decarboxylase 65kD), PCA-1 (type 1 anti-Purkinje cell antibody), striational muscle. Concentrations of these antibodies were zero or very low in all samples (**Table 2**).

Table 2: Purified serum IgG samples, purified antibody and completely serum.

Samples	Samples name	Samples number	Sex	Age	Total IgG mg/ml	Antibody concentration	Clinical information	Source
Purified IgG	**α3-AchR**	4	F	46	9.92	5.61(nmol/L)	Pandysautonomia	V. Lennon Laboratory, Mayo Clinic, Minnesota, USA
		5	M	46	7.73	2.99(nmol/L)	Presumed pandysautonomia	
		8	F	31	6.34	1.42(nmol/L)	Pandysautonomia + pseudoobstruction	
		11	F	44	10.60	5.36(nmol/L)	Pandysautonomia	
		16	F	70	0.83	1.35(nmol/L)	Subacute pandysautonomia	
		19	F	60	8.36	0.74(nmol/L)	Smoker. Hypothyroid. Chr gen dysautonomia	
	ANNA-1	2	M	72	2.12	15,360(titer)	Pseudoobstruction	
		3	M	61	6.27	61,440(titer)	Smoker. Pseudoobstruction SCLC	
		9	F	76	1.28	15,360(titer)	Smoker. Graves disease. Pseudoobstruction	
		10	F	67	1.97	61,440(titer)	Subacute pseudoobstruction SCLC	
		14	M	76	1.80	122,880(titer)	AGID +SCLC	
		17	M	76	5.14	7680(titer)	Smoker. COPD. AGID. malaise, anorexia	
		20	F	44	11.24	30720(titer)	Smoker. sensory neronopathy	
	Patient control	1	-	-	6.27	-	Normal	
		6	-	-	4.30	-	Never smoked. LES.	

	(PC)	7	-	-	4.87	-	Normal	
		12	F	-	3.45	-	Normal	
		13	-	-	8.12	-	Normal	
		15	-	-	5.62	-	Normal	
		18	-	-	7.96	-	Normal	
	Healthy control **(HC)**	21	-	-	3.99	-	Normal	
		22	-	-	2.55	-	Normal	
		23	-	-	3.01	-	Normal	
		24	-	-	3.58	-	Normal	
		25	-	-	3.94	-	Normal	
Purified antibody	Anti-HuD and anti-HuABC	26_EI	-	-	-	-		Euroimmun AG, Lübeck, Germany
		27_PR	-	-	-	-		
Serum	Patient serum	27_serum	-	-	-	-		Supplied by Roberto De Giorgio
	Blood donor	Blood donor serum	-	-	-	-		
Antigen	HuD antigen	HuD antigen	-	-	2mg/mL	-		Supplied by Josep Dalmau

2.1.2 Anti-HuD and anti-HuA/B/C fractions were isolated by affinity chromatography

Extraction of the anti-HuD fraction and anti-HuA/B/C fraction by affinity chromatography was done with the sera of two patients named as 26_EI and 27_PR (from a patient with anti-Hu symptom) (by Euroimmun Medizinische Labordiagnostika AG, Lübeck, Germany). These two patients suffered from small cell lung carcinoma with severe gut dysfunction. The anti-Hu antibodies were detectable in their sera. The 27_PR patient (female) had severe dysmotility (chronic intestinal pseudo-obstruction in total parenteral nutrition).

Preparation of recombinant HuD

The purification procedure of anti-HuD was performed as follows (information provided by Euroimmun): Human HuD (Acc. NM-021952) was expressed in *E. coli* BL21 as previously described with some modifications (Chung et al. 1996). Full length cDNA coding for HuD was ligated into pET24d (Novagen, Germany) in frame with the coding sequence for a C-terminal histidyl octamer to allow metal chelate chromatography purification. Expression was obtained using the pET system standard conditions. Recombinant HuD-His was purified from inclusion bodies by differential centrifugation, extraction in 5 mM tris-HCl pH 8, 300 mM NaCl, 8 M urea, and subsequently metal chelate chromatography on NiNTA sepharose (Qiagen). The protein was eluted in 50 mM sodium acetate pH 4.5, 8 M urea.

Coupling of recombinant HuD to NHS activated sepharose

Purified, denatured HuD-His was mixed with four volumes of refolding buffer (200 mM ethanolamine pH 10, 500 mM NaCl with 50% (w/v) glycerol) and dialysed against coupling buffer (200 mM $NaHCO_3$, pH 8.3, 500 mM NaCl). Insoluble material was removed by filtration with a 0.2 µm filter. A 1ml HiTrap NHS column (GE Healthcare) was washed with ice-cold HCl (1 mM) and coupling buffer and then loaded with 1.5 mg soluble HuD-His in 1ml coupling buffer for 30 min at room temperature. After 3 washes with high pH buffer (500 mM ethanolamine pH 8.3, 500 mM NaCl) and low pH buffer (500 mM sodium acetate pH 4, 500 mM NaCl), respectively, the column was finally washed with PBS.

Purification of anti-HuD

Serum with high anti-HuD titers (200 µL) was mixed with PBS (800 µL), filter sterilized and passed onto the HuD-column. The flow through was collected. After having washed the column with PBS (10 mL) anti-HuD was eluted with 200 mM glycine pH 2.5. Eluate fractions were neutralised with one volume of 7.5% (w/v) Na_2CO_3) and then dialysed five times against 10 volumes PBS.

2.2 Immunohistochemistry

The immunohistochemistry was performed as follows. Freshly dissected guinea pig tissue was fixed overnight at 4°C in a solution containing 4% paraformaldehyde and 0.2% picric acid in 0.1 mol/L phosphate buffer and followed by several washes (3 × 10 min) with 0.1 mol/L phosphate buffer. The tissue specimens were stored at 4°C in 0.1 mol/L phosphate buffer saline (PBS) solution containing 0.1% NaN_3 until further processing. Pre-incubation was done in PBS/NaN_3 containing Triton X-100 (TX100; 0.5%) and normal horse serum (4%) for 1 h at room temperature. The tissue was then incubated in a solution containing primary antibodies (the patient serum samples, the α3-AchR, ANNA-1, PC, anti-HuD and anti-HuA/B/C at 1:1000-1:5000 dilution in PBS/NaN_3/HS/TX100 and normal horse serum (4%) for 12-16 h at room temperature. After washing (3 × 10 min) with PBS buffer, samples were exposed to the secondary antibodies (Cy3^{TM}-conjugated affinipure donkey anti-IgG at 1:500 dilution (Dianova, Hamburg, Germany). After a final wash (3 × 10 min with PBS buffer), the preparations were mounted on slides in citifluor AF1 (Citifluor AF1 Ltd, London, United Kingdom). For the inspection of the tissue an Olympus microscope (BX61 WI; Olympus, Hamburg, Germany) with appropriate filter blocks was used. The microscope was equipped with a SIS Fview II CCD camera and analySIS 3.1 software (Soft Imaging System GmbH, Münster, Germany) for image acquisition, processing and editing.

2.3 Neuroimaging studies

2.3.1 Animals

Bowel specimen were obtained from adult male guinea pigs (Dunkin-Hartley; Charles River, Kisslegg, Germany; total N = 56) weighing between 250 g and 550 g,which were allowed free access to food and water *ad libitum* before the experiments. All procedures used in this study were approved by the ethic committee of the Technische Universität München.

2.3.2 Human tissue specimen

Human tissue specimen from surgery of small and large bowel were obtained from 45 patients (23 females, 22 males; age: 63.5±11.7 years [mean±SD]) undergoing surgery at the Medical Clinic in Freising or the Department of Surgery, Technische Universität München, Germany. Samples were taken from macroscopically unaffected areas as determined by visual inspection of the pathologists. Diagnoses that led to surgery were carcinoma of the large bowel (26), diverticulitis (5), ovarian carcinoma (2), gastric carcinoma (2), sigmastenose (1), polyposis (1), fistulation (1), restgastrectomie (1), pancreas carcinoma (2), hemicolectomy (1), sepsis (1) and others (3). Experiments were performed on 28 colon, 6 jejunum, 4 rectum, 5 ileum, and 2 duodenum specimens. All procedures were approved by the ethics committee of the Technische Universität München (project approval 1748/07 and 2595/09). After removal, the surgical specimens were placed in ice-cold oxygenated sterile Krebs solution and were immediately transported to the laboratory for further processing.

2.3.3 Tissue preparation

The experiments were performed on isolated segments of the guinea pig ileum and human tissue samples. The guinea pig was killed by cervical dislocation and exsanguination. A segment of ileum was removed quickly and placed in ice-cold Krebs solution (for composition see below) aerated (95% O_2, 5% CO_2; pH=7.4). The segment was opened along the mesenteric border, washed several times and pinned out flat (mucosal surface up) in a petri dish lined with Sylgard (Sylgard 184, Dow Corning, Midland, USA). The segment was constantly perfused with oxygenated ice-cold Krebs solution containing the L-type calcium channel blocker nifedipine (1-3 μmol/L) to reduce muscle movements. The mucosal, submucosal, and circular muscle layers were carefully dissected under a dissection microscope in order to obtain the myenteric plexus preparations with longitudinal muscle.

The procedures for the human tissue samples were as followed. After washing, human bowel segments were also cut along the mesenteric border and pinned flat in a dissection dish which was continually perfused with ice-cold oxygenated Krebs solution. The mucosa and muscle layers were carefully removed under a dissection microscope to obtain a preparation of the inner submucous plexus.

The final preparations of both species were pinned under light stretch over a window on a Sylgard ring with a size of 10 × 20 mm which was then transferred into a recording chamber (approximately 7ml volume) with a 42 mm diameter glass bottom (130 – 170 μm thickness;

Sauer, Reutlingen, Germany). The preparations were perfused continuously with 37°C warm Krebs solution (pH=7.4) gassed with carbogen (5% CO_2 and 95% O_2; Linde Gas, Unterschleissheim, Germany) at a flow rate of 18 ml/min. The solution contained nifedipine (1–3 µmol/L) to block spontaneous contractions in guinea pig preparations.

2.3.4 Voltage sensitive dye labeling

The tissue chamber was mounted onto an epifluorescence Olympus IX 50 microscope (Olympus, Hamburg, Germany) equipped with a 150W xenon arc lamp (Osram, Munich, Germany) which was connected to a stabilized power supply (OptiQuip, Highlands Mills, NY, USA). Individual ganglia were visualized at 10× magnification using Hoffmann modulation contrast optics. The fluorescent voltage sensitive dye 1-(3-sulfonatopropyl)-4-[β [2-(di-n-octylamino)-6-hapthyl]vinyl] pyridinium betaine (Di-8-ANEPPS; Molecular Probes, Eugene, OR, USA) was used in all experiments. Individual ganglia were stained with Di-8-ANEPPS dye by local pressure application through a microejection pipette loaded with a 20 µmol/L Di-8-ANEPPS solution. A 15 mmol/L stock solution of Di-8-ANEPPS containing DMSO (final DMSO concentration 0.135% in the spritz pipette; Sigma, Deisenhofen, Germany) and pluronic F-127 (final concentration in the spritz pipette 0.0135%; Molecular Probes) was dissolved in Krebs solution to a final concentration of 20 µmol/L. The glass pipette was placed in close contact to the ganglia and pressure ejection (2 psi) pulses of 200-800 ms were used to apply the dye. The dye was allowed to incorporate into the outer cell membrane of the neurons for 5-10 min in the dark before starting the experiment. During the incubation period it was possible to follow and to assess the progress of the labeling by briefly illuminating the ganglion.

2.3.5 Neuroimaging with multisite optical recording technique

The multisite optical recording technique (MSORT) is a fast imaging technique that allows monitoring membrane potential changes at single cell level. It has previously been described in detail (Michel et al., 2005; Schemann et al., 2005; Schicho et al., 2006; Buhner et al., 2009; Vignali et al., 2010; Mueller et al., 2011). Neunlist et al. found that staining the neurons with Di-8-ANEPPS did not change their electrical or synaptic properties by comparing intracellular with simultaneous optical recordings (Neunlist et al., 1999b). In the present study, recordings from Di-8-ANEPPS stained neurons were made with a 40× oil immersion objective (UAPO/340 Olympus, Hamburg, Germany) by using a filter cube equipped with a 545±15 nm excitation filter, a 565 nm dichroic mirror and a 580 nm barrier filter (AHF Analysentechnik,

Tübingen, Germany). The fluorescent images of the ganglia were acquired and processed by the Neuroplex system that consists of a photodiode array, an amplification system and software for acquisition, processing and storage of the data. The fluorescent images were projected onto a tightly packed fibre optic bundle (464 optical fibres) leading to individual photodiodes (see **Figure 2**, RedShirt Imaging, Decatur, GA, USA). Frames were acquired at a frequency of 1 kHz and signals were filtered with a band pass of 3-300 Hz. Controlled illumination of the preparation was achieved by a software-operated shutter (Uniblitz D122; Vincent Associates, New York, NY). In the experiments, illumination periods of 0.68 s for a single pulse stimulation of a nerve strand and 1.8-2.5 s for drug and sera application were used to record neurons membrane potential changes. The multisite optical recording technique set-up allows measurement of fluorescence intensity and relative changes in fluorescence ($\Delta F/F$) which is linearly related to changes in the membrane potential (Neunlist et al., 1999). To ensure proper staining and viability of the neurons it was possible to stimulate interganglionic fibre tracts with a 25 µm teflon-coated platinum electrode connected to a pulse generator (Master 8, Science Products, Hofheim, Germany) and a constant current stimulus isolating unit (A360; World Precision Instruments, Berlin, Germany). Electrical pulses had durations of 400 µs and amplitudes varying between 10 and 70 µA. The reference electrode was placed in the chamber which was superfused with Krebs solution. Video images of the preparation were taken by video camera (Cohu 4910, Cohu Inc., San Diego, CA, USA) to identify the location of the neurons in the ganglia. It is important to emphasize that the photodiode system used for this study is an AC-coupled system with a time constant of 500 ms. Thus, slowly developing, small amplitude changes in membrane potential are not detected. Therefore, all neuronal activity is reflected by action potential discharge. The underlying slow depolarization of the membrane potential is not seen in any of these traces.

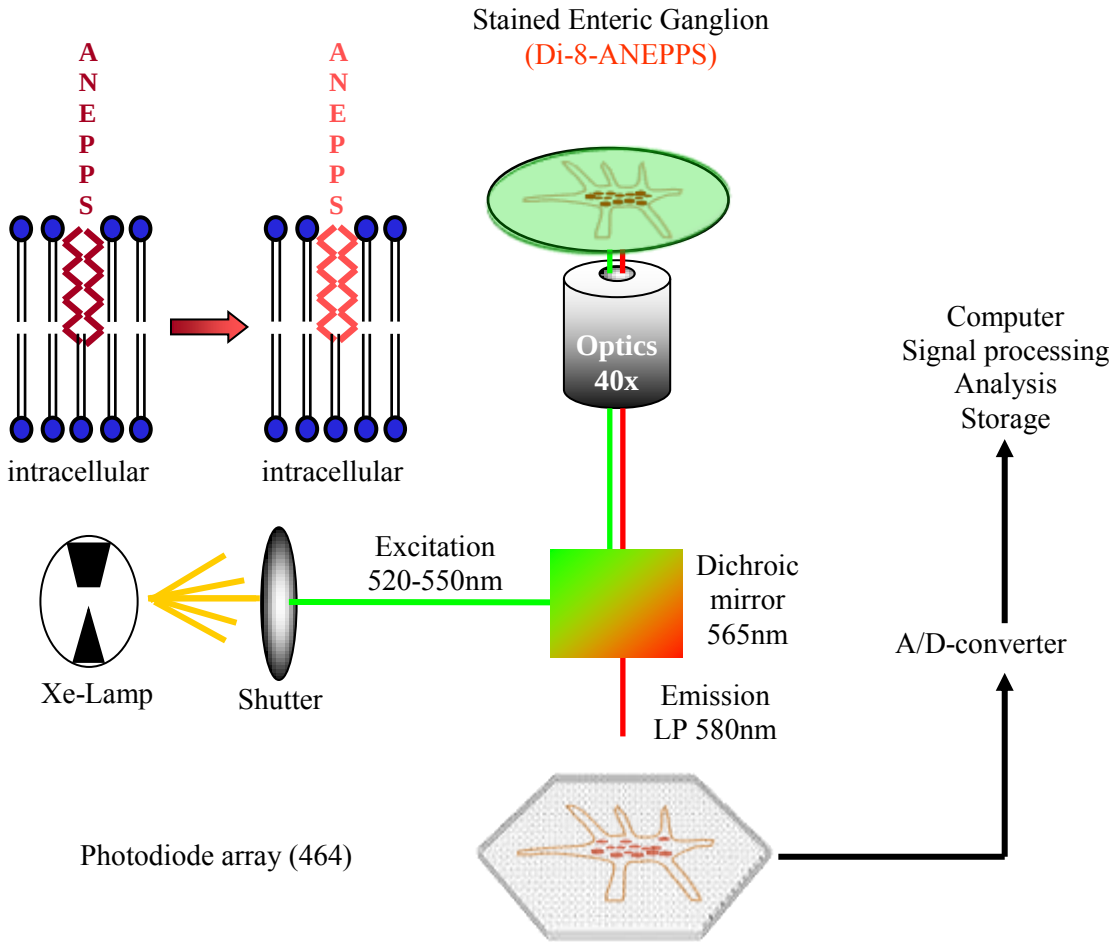

Figure 2: Principles of multisite optical recording technique (MSORT). 1-(3-sulfonatopropyl)-4-[3[2-(di-n-octylamino)-6-hapthyl]vinyl]pyridinium betaine (Di-8-ANEPPS)-stained tissue is excited with a xenon arc lamp (lamp house model 770 with 1600 series power supply, Opti-Quip, Highland Mills, NY). The fluorescence changes are detected with a 468-photodiodes array. Optical signals are processed with a computer; frame rate is 1 kHz with the photodiode-system, enabling the detection of action potentials. With a 40× objective (UAPO/340, NA=1.4, Olympus, Hamburg, Germany), we detected fractional changes (ΔF/F=% change in fluorescence divided by the resting light level) in the range of 0.05-4%. With the 40× objective, the photodiode system has a spatial resolution of ~280 μm^2 per diode. The system allows resolution at a cellular range. (Adapted from Schemann et al., 2002)

2.3.6 Solutions and drug application

Krebs solution for tissue dissection and neuroimaging contained (in mmol/L): 117 NaCl, 4.7 KCl, 1.2 $MgCl_2$ 6 H_2O, 1.2 NaH_2PO_4, 25 (20 for neuroimaging) $NaHCO_3$, 2.5 $CaCl_2$ 2 H_2O, and 11 glucose. The purified serum IgG (α3-AchR 0.7 - 5.4 nmol/L, ANNA-1 7,600 - 123,000 titer, the PC and HC) samples were collected at the Mayo Clinic (Lennons

Laboratory, Mayo Clinic, Minnesota, USA). The purified patient serum containing anti-HuD or anti-HuA/B/C antibodies (26_EI and 27_PR antibodies, made by Euroimmun Medizinische Labordiagnostika AG, Lübeck, Germany) and complete patient serum (named as 27_PR serum, from Laboratory De Giorgio, Bologna, Italy) came from two patients with high anti-Hu titer. The control sera were provided by healthy blood donors (De Giorgios Laboratory, Bologna, Italy). Additional purified Hu-D antigen (2 mg/mL, kindly supplied by Josep Dalmau) was used (**Table 2**).

All sera were freshly prepared immediately prior to experiments from aliquots that were stored at -80°C or 4°C, and applied to single ganglia by pressure ejection (1-2 psi, 200-400 ms duration) from microejection pipettes that were placed close to the ganglion (approximate distance: 100-200 μm) using a micromanipulator. The sera in the pipette were diluted (1:1) with Krebs solution. In some experiments hexamethonium (200 μM; Sigma-Aldrich) was perfused for 20 min to block action of acetylcholine at nicotinic receptors.

2.3.7 Data analysis and statistics

Data were processed using Neuroplex 7.02 software (RedShirtImaging, Decatur, GA). The voltage sensitive dye incorporates into the outer membrane revealing the outline of individual cell bodies. The total number of neurons for each ganglion was determined by visual inspection of images from the Di-8-ANEPPS stained ganglion, as previously described (Michel et al., 2005; Schicho et al., 2006; Breuning et al., 2007; Schemann et al., 2010). To prevent the effect of dye bleaching these images were taken from the respective ganglion after the neuroimaging recoding using a high resolution video camera. During the analysis of optical signals, traces of all photodiodes can be superimposed upon the corresponding image of the ganglion. The percentage of neurons or photodiodes responding to the application of serum samples or chemicals was calculated individually for each ganglion. For analyzing the response activity and frequency of action potentials, basal firing activity was subtracted from the activity that was evoked by the application of the samples to evaluate the excitation induced by the samples. Data are presented as the arithmetic mean±SD from response to purified serum IgG samples, anti-HuD, anti-HuA/B/C antibodies, control serum, blood donor or basal firing activity. Significant differences between group means were determined using paired t-test or unpaired t-test or one-way analysis of variance test (ANOVA) followed by a post hoc Dunnett's, Dunn's or the student-Newman-Keuls method multiple comparison test with SigmaStat Software (Sigmastat 12.1, Systat Software Inc., Erkrath, Germany). Non-

normally distributed data were expressed as their median together with the 25th and 75th percentiles. *P* values less than 0.05 were considered statistically significant.

2.4 Extracellular recordings from vagal afferents

2.4.1 Animals

These experiments were performed at the University of Sheffield (Department of Biomedical Science, Laboratory of Professor Grundy) according to the UK Animals Scientific Procedures Act (1986). Experiments were performed in tissues of 14 C57Bl6 mice of either sex (8-12 weeks old, 20-30 g) that were bred by a rodent breeding unit and maintained on a standard *ad libitum* diet.

2.4.2 Tissue preparation

The mice were stunned humanely by a blow to the head and killed by cervical dislocation. A midline laparotomy was performed, and the stomachs and distal esophagus were rapidly removed from C57Bl6 mice. The excised stomach and distal esophagus were immediately placed into oxygenated (95% O_2 and 5% CO_2, pH=7.4) Krebs solution (for composition see below) at room temperature. The stomach was then separated into two parts by an incision from the proximal corpus.The contents of the fundus and distal esophagus were thoroughly flushed with Krebs solution. Under the microscope, the fundus of stomach and distal esophagus were carefully opened along the lesser curvature into a flat sheet, and pinned mucosa up in a dissection dish (approximate volume of 10 mL). The mucosa was removed by sharp dissection. The fundus and distal esophagus preparation was cut down to final dimensions of approximately 12 mm width × 15-18 mm length and pinned serosal side up. The fine branches of the vagus nerve (originating from the dorsal subdiaphragmic vagus nerve), which innervated the fundus, was carefully dissected free of connective tissue for a length of 4-6 mm. Tissue preparations were constantly perfused at 5 mL/min with oxygenated Krebs solution (37°C) which contained nicardipine (1 μM) to reduce muscle movement.

2.4.3 Afferent recordings

The extracellular suction electrode technique that was used for the following experiments has been described previously in detail (Rong et al., 2002; Rong et al., 2004). Briefly, the gastric vagal multifibre afferent discharge was recorded using the extracellular suction electrode (tip diameter 50-100 µm), which was attached to branches of the vagus nerve innervating the fundus. Suction recording extended preparation viability and allowed single-unit discrimination because of an enhanced signal to noise ratio. The electrode was connected to a Neurolog headstage (NL100, Digitimer, Welwyn Garden City, UK) and the signal was amplified (NL104, Digitimer) and filtered with a band pass 200-3000 Hz (NL 125, Digitimer). The nerve signal was acquired at 20 kHz sampling rate by a computer through a Micro 1401 interface (CED, Cambridge Electronic Design, UK) and Spike2 software (version 5.03, CED). In addition to the raw nerve signals, afferent nerve activity was recorded as a rate histogram with spike discriminating software. See **Figure 3** for schematic of the nerve recording set-up. The preparation was allowed to equilibrate for at least 30 min before experiments started.

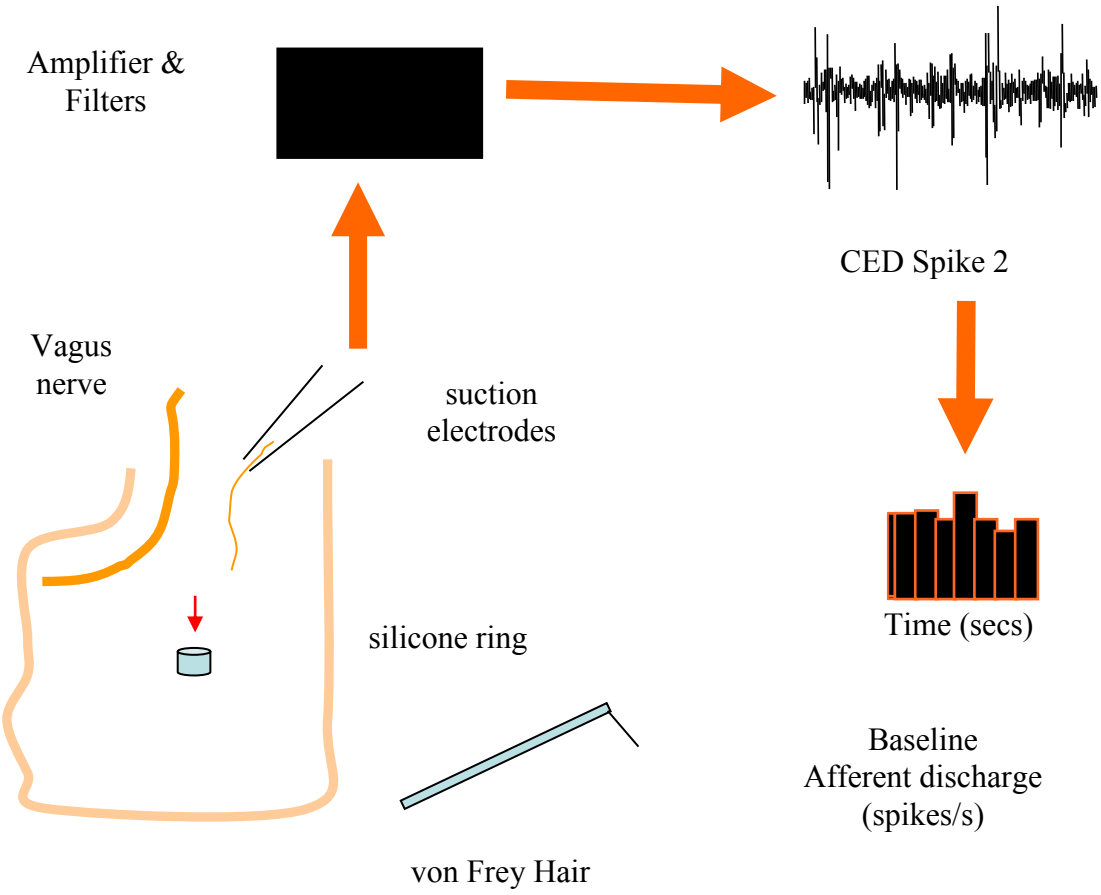

Figure 3: Gastric vagal afferent fibres recoding. The branches of the vagus nerve innervating the fundus were dissected and attached to an extracellular suction electrode. The action potentials recorded from those afferent fibres are amplified, filtered, and recorded using computer software. The afferent fibres activity was counted and plotted into a frequency histogram in spikes per second.

2.4.4 Mechanosensitive receptive field (hot spots) identification

Mechanosensitive receptive fields were located by probing with hand-held von Frey hairs (tip diameters <50 μm) which exerted a force of 1-2 mN over the width and length of the serosal surface of the preparation spot by spot. At the sensitive sites or „hot spots', von Frey hairs evoked a burst of firing that stopped abruptly on removal of the stimulus (**Figure 4**). When an active site was identified, its position was marked using fine carbon particles attached to the tip of the hair onto the serosal surface of the preparation.

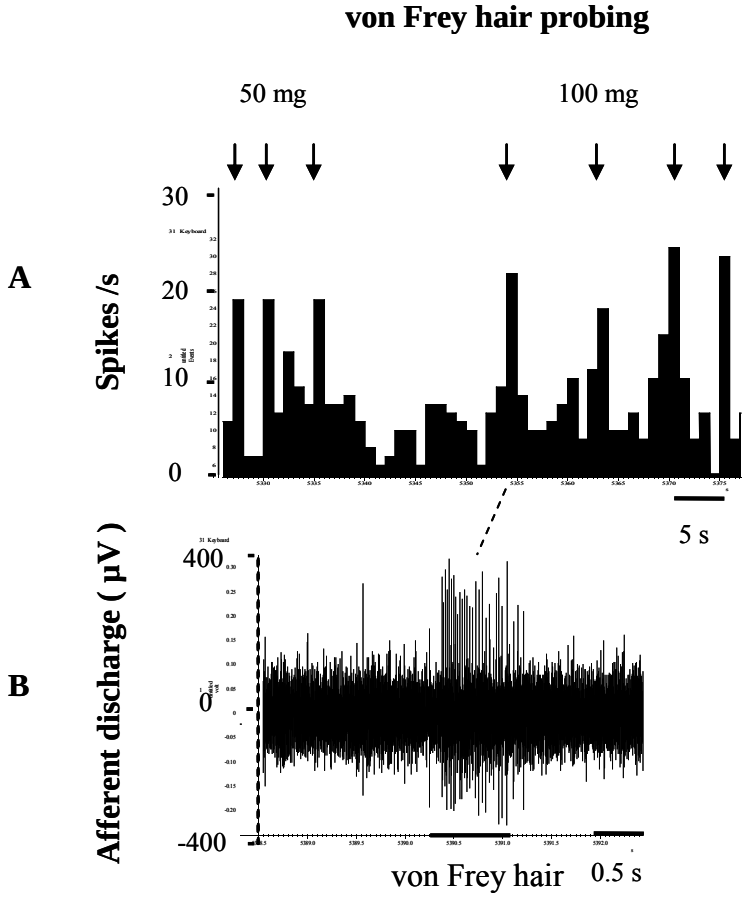

Figure 4: In the fundus of a mouse stomach preparation, mechanoreceptive „hot spots' responded to stimulation with a von Frey hair. The „hot spots' were marked on the tissue for later stimulation with serum samples. (A**)**. Spike histogram of a typical recording with repeated stimulation with two different von Frey hairs (arrows, 50 mg and 100 mg). Each stimulation evokes a burst of action potentials. (B**)**. Raw recording of the effects of probing a „hot spot" with the 100 mg von Frey hair.

2.4.5 Solutions and drug application

Krebs solution for tissue preparation and afferent recording experiments contained (composition in mmol/L): 117 NaC1, 4.7 KC1, 25 $NaHCO_3$, 2.5 $CaC1_2$, 1.2 $MgSO_4$, 1.2

NaH_2PO_4, and 11 glucose. The calcium-free Krebs solution for studying the role of extracellular calcium in the response to anti-Hu contained no calcium but $MgCl_2$ at a concentration of 3.6 mmol/L. 1,1-dimethyl-4-phenylpiperazinium iodide (DMPP), adenosine 5'-triphosphate (ATP) and nicardipine (all from Sigma-Aldrich). „Hot spots' were isolated from the bathing solution by means of a silicone ring (approximately 100 µL volume) placed over the receptive field. Drugs or serum could be thus delivered in a small volume to an identified receptive field. Most units were first tested for sensitivity to DMPP (nicotinic receptor agonist, 100 µmol/L) and/or adenosine 5'- triphosphate (ATP, 100 µmol/L), and then anti-HuD and anti-HuA/B/C samples (from patient 1) were applied to the same „hot spot'. anti-HuD and anti-HuA/B/C samples were stored at 4℃ in aliquots and were diluted (1:10) with Krebs solution just before the experiments.

2.4.6 Data analysis and statistics

Afferent neurograms were analyzed using Spike2 software in order to calculate the firing rate exceeding a preset threshold in sequential time bins. The gastric vagal afferent activity was expressed in spikes per s over a period of the response. Baseline afferent fibre activity was defined as the mean discharge per s during the 1 min period prior the application of drugs or serum. The baseline afferent activity was subtracted in order to evaluate the peak increases in discharge under the various experimental conditions. For the persistence time course of drugs or serum studies these parameters were assessed at various time points from 3 s to 20 min after application of drugs or serum. At each time point the mean discharge rate was determined over a 3 s period. The latency was measured from drug delivery to firing rate increase 20% above baseline afferent fibre activity or when the peak response was reached. Statistical analysis was performed using Graphpad Prism version 4.01 (Graphpad Software, San Diego, USA) and Sigma plot 9.0 (Systat Software Inc, Erkrath, Germany). Where appropriate, normally distributed data were analyzed by using the unpaired Student's t-test and data are expressed as means±SEM. Non-normally distributed data were analyzed by the Kruskal-Wallis one-way analysis of variance on ranks. The multiple comparisons were performed with the Dunn's method. The data are expressed as the median with the 25th and 75th percentiles. A P value of less than 0.05 is considered as statistically significant.

3. Results

3.1 Immunohistochemistry

3.1.1 The immunostaining of the serum IgG samples in the guinea pig

We used immunohistochemistry to detect IgG labelling in the ENS after serum incubation. The α3-AchR, ANNA-1 and patient control samples were used as primary antibodies in myenteric plexus preparations of the guinea pig. The immunohistochemistry results showed that many neurons in the myenteric plexus of guinea pig were labeled by the α3-AchR (1:500) and by the ANNA-1 samples (1:500) while most control samples (1:500) did not stain any structure except one sample that showed weak staining. Two out of six α3-AchR samples and all ANNA-1 samples produced similar stainings (**Figure 5**, **Figure 6**, **Figure 7**and **Table 3**).

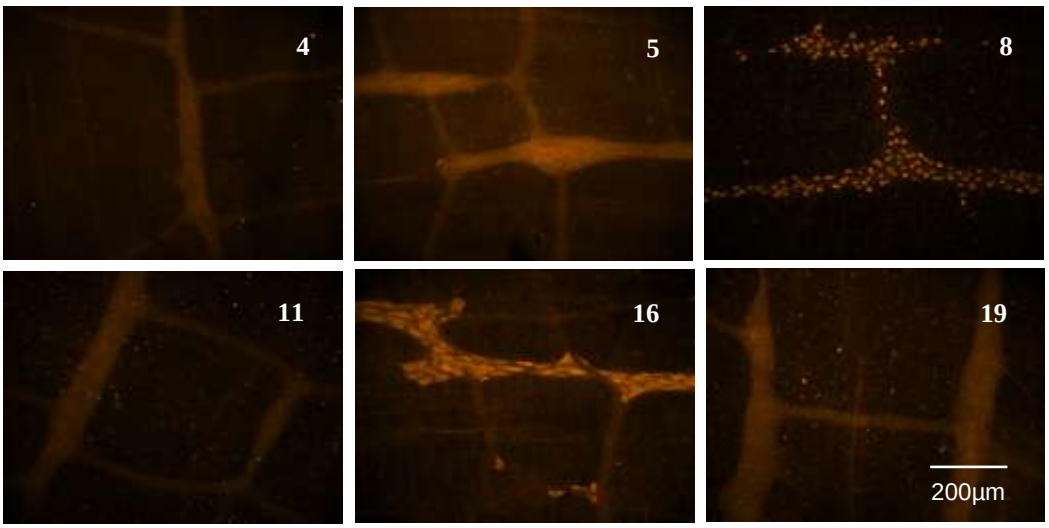

Figure 5: The immunostaining of the α3-AchR (1:500) samples in the guinea pig ileum myenteric plexus neurons. The numbers in white on the top right on each picture are the patient numbers. α3-AchR samples (patient number 8 and 16) stained many neurons .

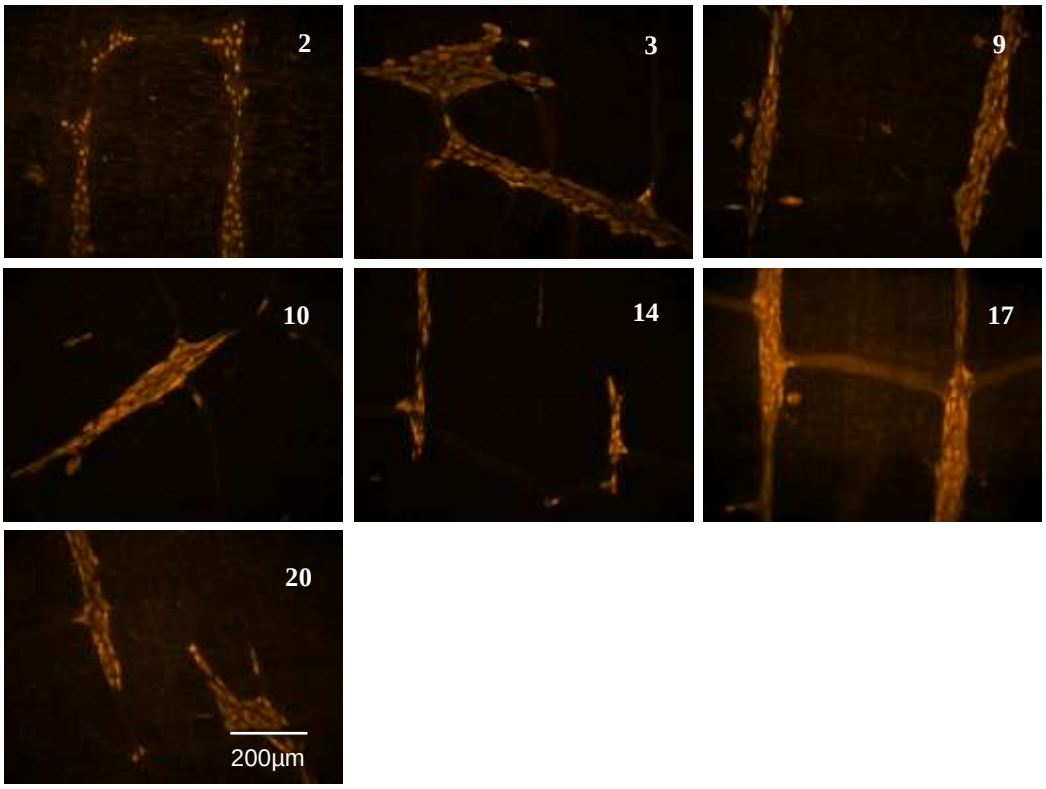

Figure 6: The immunostaining of the ANNA-1 (1:500) samples in the guinea pig ileum myenteric plexus neurons. All ANNA-1 samples stained neurons.

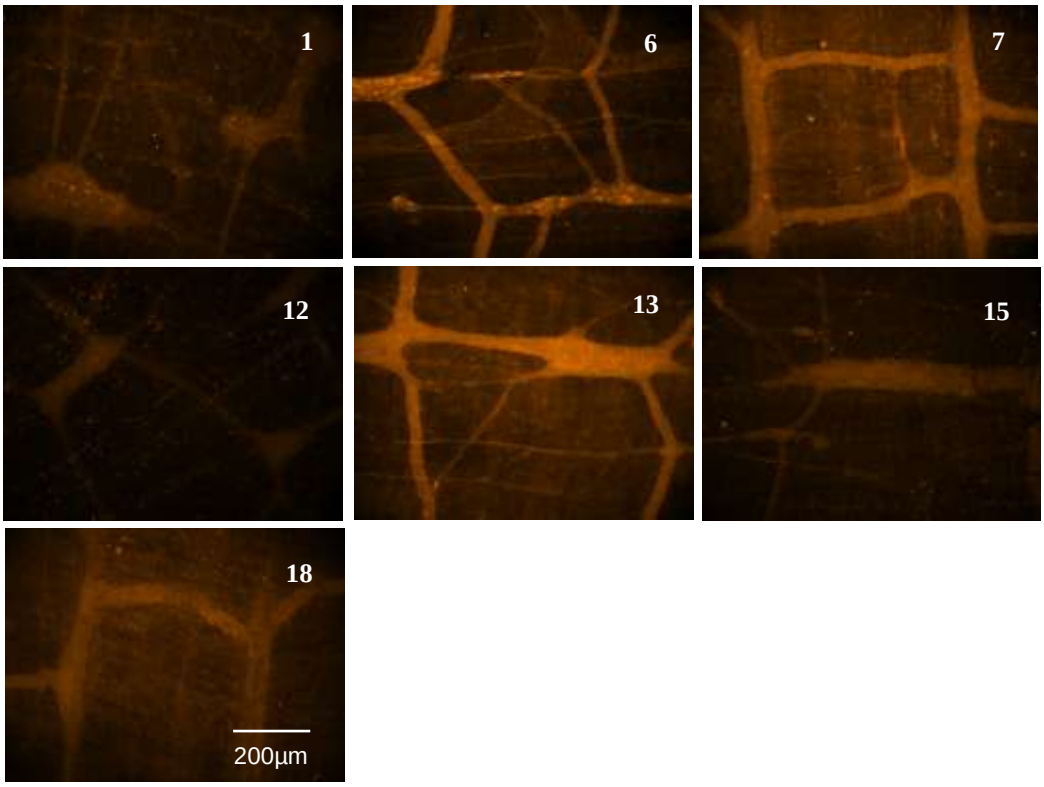

Figure 7: The patient control samples (1:500) stained no structures in the guinea pig ileum myenteric plexus, except for the sample of patient 6 which produced a weak staining (patient number is shown in top right of each picture).

Table 3: Number of serum IgG samples revealing positive or no staining in the guinea-pig myenteric plexus.

	α3-AchR	ANNA-1	Patient control
Positive staining:	2	7	1
No staining	4	0	6

3.1.2 The immunostaining of the anti-HuD antibody and the anti-HuA/B/C antibodies in the guinea pig

The purification of the serum samples from patient 26_EI yielded two fractions: one fraction contained the affinity purified anti-HuD antibodies while the other fraction very likely contained other Hu-antibodies (anti-HuA/B/C). To test the immunereactivity of both fractions we also used them as primary antibodies in guinea pig myenteric plexus preparations. The results showed that all neurons in the guinea-pig myenteric plexus were labeled by the anti-HuD antibody (**Figure 8**A). The anti-HuA/B/C antibodies labeled not only neurons but also nerve fibres (**Figure 8**B).

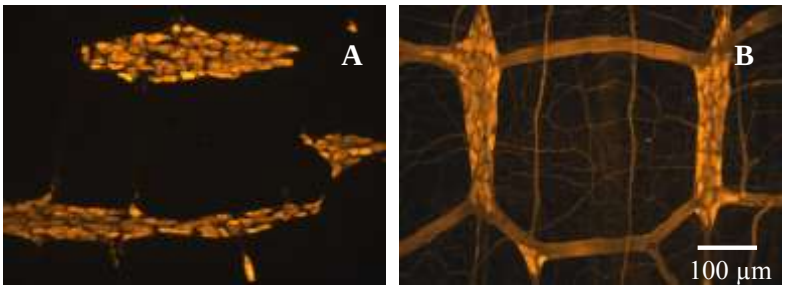

Figure 8: The immunostaining of the anti-HuD antibody and the anti-HuA/B/C antibodies in the guinea pig myenteric plexus neurons. The anti-HuD antibody (1:5000) specifically labeled all myenteric neuronal bodies (A) while the antibodies in the anti-HuA/B/C antibodies (1:5000) samples also labeled neuronal fibres (B).

3.2 Neuroimaging studies

Neuroimaging studies were performed in a total 56 adult male guinea pigs containing 6,244 neurons from 198 myenteric ganglia (the mean number of neurons per ganglion was 31.9±7.4)

and in 45 human patients. The maximum recording periods after serum application was based on previous findings that showed no significant bleaching or phototoxicity during exposure times up to 5 s. However, we found that recording periods of 2.513 s in guinea pig or 1.885 s in human preparations yielded reproducible and representative responses in most preparations. We were also able to evaluate basal firing activity between the recordings (blank) by using shorter recording periods of 1.256 s.

To improve readability, guinea pig or human tissues preparations, ganglia and numbers of neurons are given in sequence without further specification, e.g. a result based on experiments in 3 guinea pigs 17 ganglia and 643 neurons is presented as (3/17/643). In the same way, for data from box plot the median and interquartile ranges (25th and 75th percentile) are shown in sequence, e.g. the median is 2.6 Hz, 25th and 75th percentile is 1.0 Hz and 5.7 Hz is presented as (2.6[1.0/5.7] Hz).

3.2.1 α3-AChR and ANNA-1 IgG samples evoke enteric neuron excitation in guinea pig and in human

The purpose of this part of the study was to identify the effect of serum IgG samples that were affinity purified from paraneoplastic syndrome patients on guinea pig and human enteric neurons in order to investigate possible mechanism(s) how serum IgG samples may contribute to gut dysfunction. Sera IgG samples from patients without neurologic autoimmunity disorder and healthy volunteers served as control.

3.2.1.1 Guinea pig myenteric neurons responded to serum IgG

We studied effects of serum IgG samples from four groups (α3-AchR, ANNA-1, PC and HC) on guinea pig myenteric neurons. Neuroimaging experiments were performed in 37 guinea pigs. A total of 103 myenteric ganglia containing 2,816 neurons were analyzed. Application of the serum IgG samples via the local pipette directly onto myenteric ganglia revealed an excitatory response in a subpopulation of neurons. Action potential discharge occurred shortly after pressure application of serum IgG samples and usually lasted throughout the recording period of several seconds. The excitatory response consisted of an immediate action potential discharge or an increase in spike discharge in spontaneously active neurons, i.e. neurons that already fired action potentials prior to IgG application (**Figure 9** and **Table 13**).

Samples from PC and HC had no or very weak excitatory effects in low numbers of neurons. As there were no significant differences between both groups in the percentage of excited neurons, action potential frequency or neuroindex, the results for both groups were pooled.

If analysed as a group a significantly larger proportion of neurons responded to application of α3-AchR and ANNA-1 samples compared to the pooled PC and HC samples (7.1[4.2/13.6]% and 11.0[5.4/20.0]% versus 1.2[0.0/2.9]%, P <0.05, **Figure 10**A). In those responding neurons the α3-AchR and ANNA-1 samples evoked a significantly higher spike discharge (2.3±1.2 Hz and 2.3±0.7Hz versus 0.7±0.8 Hz, P <0.05, **Figure 10**B) than samples from PC and HC. The neuroindex which is the product of action potential frequency and proportion of responding neurons was also significantly different from the control samples (18.3[12.7/36.8]% × Hz and 33.0[16.2/42.7]% × Hz versus 1.2[0.0/2.9]% × Hz, P <0.05, **Figure 10**C).

Analysis of the individual serum IgG samples revealed that none of the control sera caused a significant activation of neurons. Although 5 out of 6 α3-AchR samples (except sample 11) and all ANNA-1 samples had excitatory effects on myenteric neurons, this did not reach statistical significance for all samples. The α3-AchR sample 8 and ANNA-1 sample 9 activated a significantly larger number of neurons (27.7[11.4/46.9]% and 14.0[5.4/32.9]%) compared to control samples (0.0[0.0/0.0]%, P <0.05, **Figure 11A**). The α3-AchR sample 4, 5 16 and ANNA-1 sample 10, 14, 20 evoked a significantly higher rate of action potential discharge (2.4[1.9/3.0] Hz, 3.0[2.4/3.9] Hz, 2.2[1.3/5.2] Hz, respectively and 2.2[1.3/3.0] Hz, 2.6[1.9/3.9] Hz, 2.6[1.9/3.9] Hz, respectively) compared to control samples (1.3[0.9/1.7]%, P <0.05, **Figure 11B**). The neuroindex for the sample 8 was significantly higher than for control sample (70.9[21.6/98.2]% × Hz versus 0.0[0.0/0.0]% × Hz, P <0.05, **Figure 11C**).

Statistical comparison between α3-AchR and ANNA-1 samples showed no significant differences (**Table 4**).

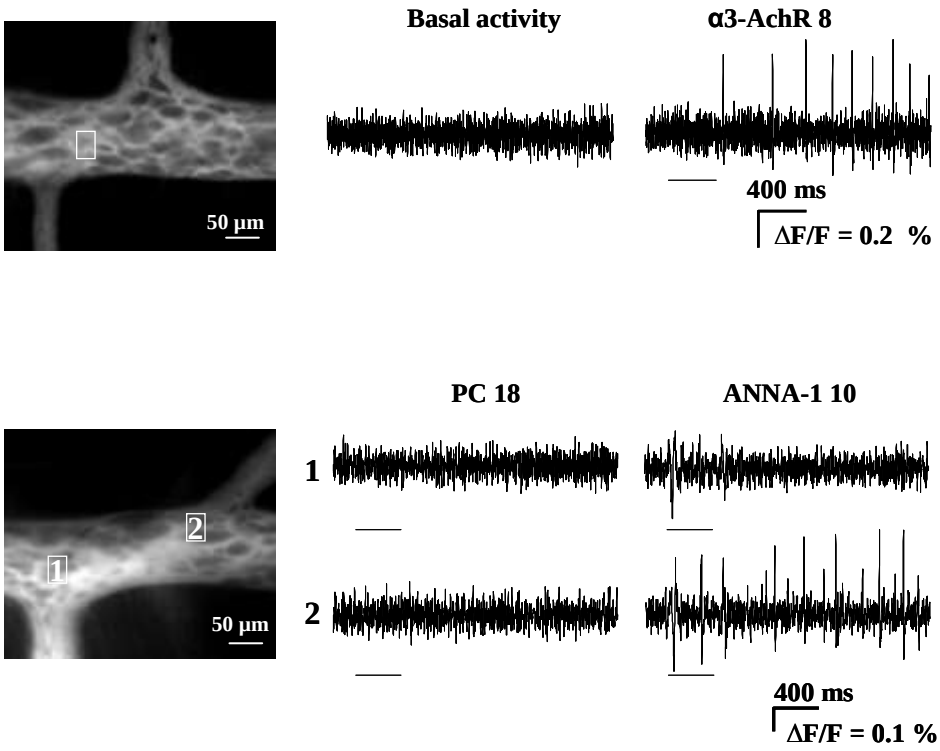

Figure 9: The serum IgG samples α3-AchR and ANNA-1 evoked a discharge of action potentials in neurons of guinea pig myenteric plexus. The pictures on the left show the Di-8-ANEPPS labeled myenteric ganglia. Outline of dye labeled individual neurons can be visualized as the dye is staining the neuronal membranes. Signals from the neurons (marked by white rectangles and numbers) are shown in the traces on the right. The top left trace shows that there is no spontaneous activity occurring during basal activity. The top right trace shows the response (discharge of action potentials) to the application of the serum IgG samples α3-AchR. The middle left and bottom left traces show signals from neuron 1 and neuron 2. They both did not respond to the application of the control serum PC 18. In contrast, ANNA-1 evoked a discharge of action potentials in neuron 2. Each peak corresponds to one action potential. The bars below the traces indicate the 400 ms application.

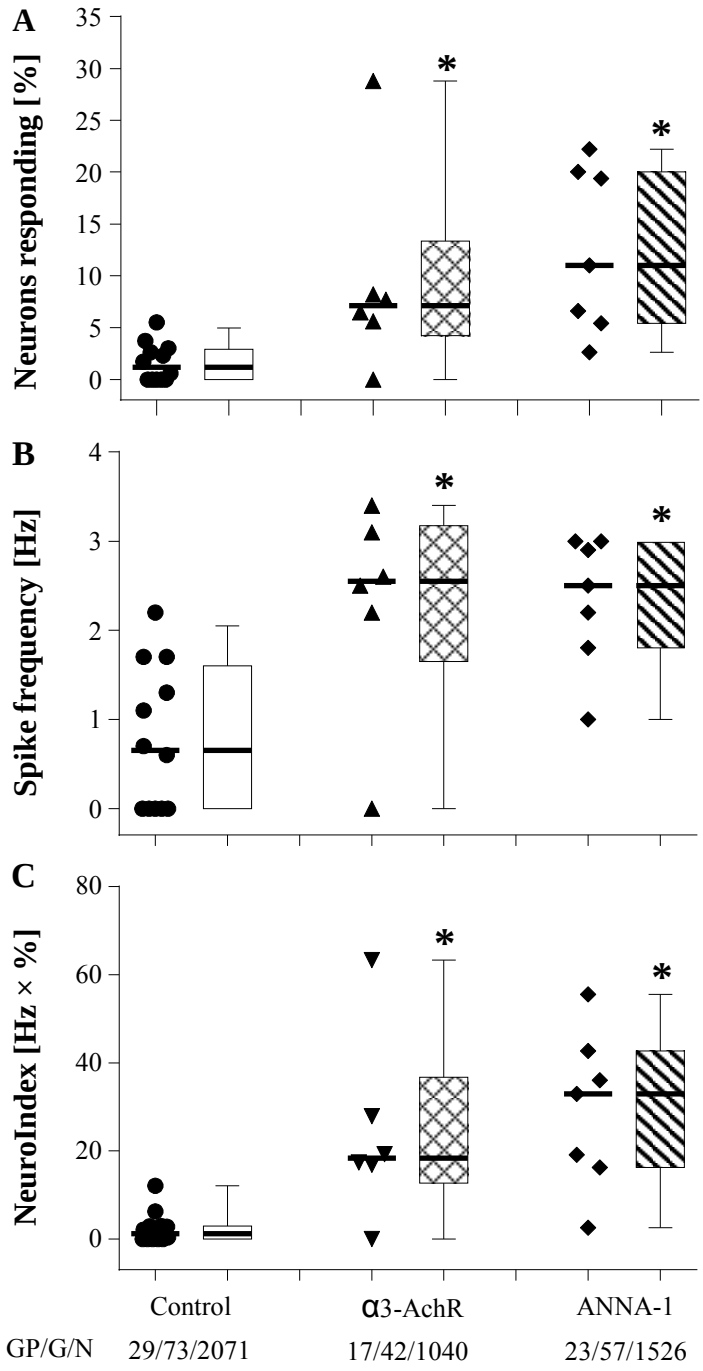

Figure 10: Effect of sera α3-AchR and ANNA-1 IgG samples on myenteric neurons of guinea pig. The graph shows for each sample the scatter plot and the box plot. The data for each samples of control (PC and HC), α3-AchR and ANNA-1 are pooled. Data of the samples α3-AchR and ANNA-1 were compared to control. Pooled data are shown for (A) the percentage of responding neurons per ganglion, (B) the action potential frequency as well as (C) the neuroindex which is the product of action potential frequency and proportion of responding neurons. Comparisons against control were performed with ANOVA followed by Dunn's method and Student-Newman-Keuls method. Significancy was reached when $P < 0.05$. GP/G/N: guinea pig/ganglia/neurons.

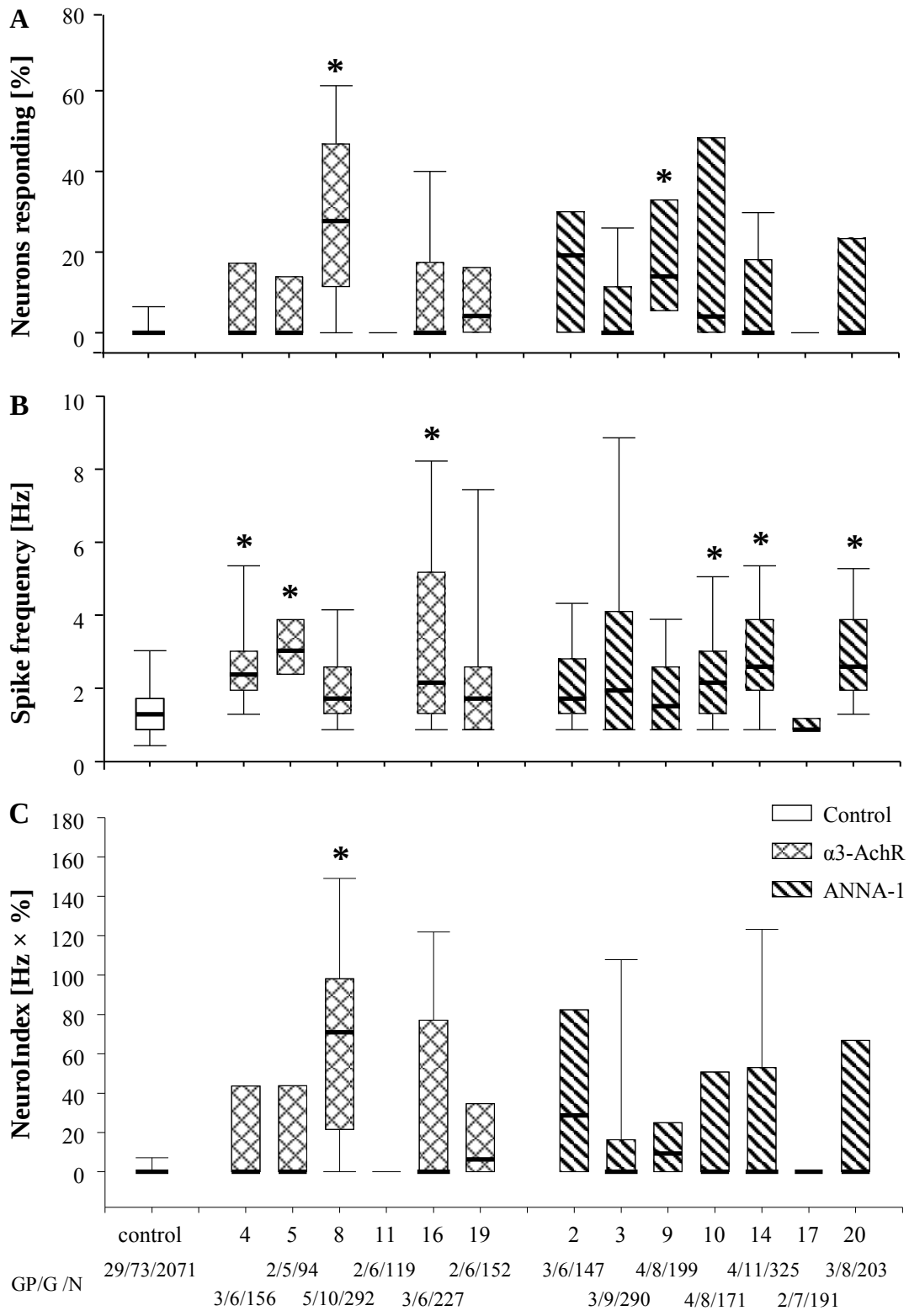

Figure 11: The box plot illustrates the effect of the individual sera α3-AchR and ANNA-1 IgG samples on guinea pig myenteric neurons. Nearly all α3-AchR samples (5 out of 6, except sample 11) and all ANNA-1 samples had excitatory effects on myenteric neurons compared to control. The control samples (PC and HC pooled) cause a weak activation in a low proportion of neurons. (A) the percentage of responding neurons per ganglion (B) the action potential frequency as well as the (C)

neuroindex. All sample data were compared to control with ANOVA followed by Dunn's Method. Differences were considered as significanct when $P < 0.05$. GP/G/N: guinea pigs/ganglia/neurons.

Table 4: There was no significant difference between the effect of PC and HC or α3-AchR and ANNA-1 samples (non-paired t test).

Guinea pig					
PC and HC			α3-AchR and ANNA-1		
Neurons responding [%]	Spike frequency [Hz]	Neuroindex [Hz × %]	Neurons responding [%]	Spike frequency [Hz]	Neuroindex [Hz × %]
$P = 0.088$	$P = 0.324$	$P = 0.268$	$P = 0.559$	$P = 0.939$	$P = 0.642$
Human					
PC and HC			α3-AchR and ANNA-1		
Neurons responding [%]	Spike frequency [Hz]	Neuroindex [Hz × %]	Neurons responding [%]	Spike frequency [Hz]	Neuroindex [Hz × %]
$P = 0.413$	$P = 0.684$	$P = 0.272$	$P = 0.616$	$P = 0.284$	$P = 0.916$

3.2.1.2 Human submucous neurons responded to IgG serum

We further studied the effect of the α3-AchR, ANNA-1, PC and HC serum IgG samples on human submucous neurons. Experiments were performed using 45 tissues from 23 female patients and 22 male patients. A total of 79 submucous ganglia containing 614 neurons were analyzed. The mean number of neurons per ganglion was 8.0±3.1 neurons (range, 3-15).

All α3-AchR and ANNA-1 samples evoked a neural activation (**Figure 12**, **Figure 13, Figure 14** and **Table 13**). Samples from PC and HC did not yield a significant activation of submucous neurons and were pooled (**Table 4**).

If analysed as a group the α3-AchR and the ANNA-1 samples evoked an excitatory response in a significantly larger population of neurons compared to control samples (39.7[17.7/70.9]% and 60.6[19.6/68.6]%) versus 11.7[0.9/15.4]%, $P < 0.05$, **Figure 13**A). Those neurons that responded to α3-AchR and ANNA-1 samples fired at a significantly higher discharge rate

than those that were activated by the control samples (3.9±1.1 Hz and 3.2±1.2 Hz versus 1.1±0.8 Hz, P <0.05, **Figure 13**B). The neuroindex of α3-AchR and ANNA-1 samples were significantly higher than of control samples (169.9[47.9/317.9]% × Hz and 260.7[50.9/266.4]% × Hz versus 17.6[0.5/28.5]% × Hz, P <0.05, **Figure 13**C).

Similar to the effects in the guinea pig myenteric plexus all α3-AchR and ANNA-1 samples evoked a neural activation (**Figure 14**). Samples from PC and HC did not yield a significant activation of submucous neurons (**Table 4**) and were pooled. In contrast, more of the α3-AchR samples (samples 8, 19) and ANNA-1 samples (2, 3, 14, 20) activated a significantly larger number of responding (71.4[56.3/90.0]%, 85.7[50.0/87.5]%, 75.0[63.6/83.3]%, 69.7[59.5/76.5]%, 66.1[51.5/85.7]%, 51.2[38.3/100.0]%) compared to control samples (0.0[0.0/23.6]%, P <0.05, **Figure 14A**). The α3-AchR sample 4, 5, 8, 19 and the ANNA-1 samples 2, 3, 14, 20 significantly increased the rate of action potential discharge (3.2.3[1.8/5.6] Hz, 4.5[2.4/7.2] Hz, 5.4[2.3/7.4] Hz, 4.2[1.8/5.9] Hz and 3.6[1.8/4.7] Hz, 2.9[2.4/5.3] Hz, 4.2[2.4/7.1] Hz, 4.2[2.8/6.1] Hz) compared to control samples (1.2[1.2/1.8] Hz, P <0.05, **Figure 14B**). The neuroindex of α3-AchR sample 8, 19 (534.1[145.9/584.9]% × Hz and 351.8[118.7/385.8]% × Hz) and ANNA-1 samples 2, 3, 14, 20 (167.3[163.2/420.4]% × Hz, 245.2[206.1/407.2]% × Hz, 292.3[153.8/484.1]% × Hz, 150.6[94.9/524.2% × Hz) were significantly higher than of control samples (0.0[0.0/30.3]% × Hz, P <0.05, **Figure 14C**). Most of the α3-AchR samples and the ANNA-1 samples had similar effects on spike frequency and on the proportion of neurons activated, but some sample evoked a significantly increased action potential frequency but the percentage of responding neurons did not differ.

There was no significant correlation or difference between the proportions of neuron activated by the α3-AchR and the ANNA-1 samples and the following parameters related to the patients or the regions from which the surgical specimens were resected (**Table 5**). The excitatory action of the α3-AchR samples was not related to patients age or gender (56.3[0.0/69.7]% in male versus 57.8[0.0-84.5]% in female). Likewise, there was no relation to the diagnosis that led to surgery (57.1[0.0/80.0]% from patients with cancer versus 57.7[0.0/85.7]% in non-cancer patients). Similarily, the number of neurons responding to ANNA-1 samples were not related to the age of the patient and gender (55.2±27.6% in male versus 44.3±31.1% in female) or the diagnosis that led to surgery (50.9±30.5% from patients with cancer versus 40.8±31.3% in non-cancer patients) (**Table 5**). Differences between the number of neurons activated by the α3-AchR samples or the ANNA-1 samples were only analyzed in the colon and the sigma because we had more samples from these two regions. The percentage of neurons responding to the α3-AchR samples was 38.6±32.3% in the colon and 66.2±26. 8% in

the sigma (P =0.056, unpaired t-test). Corresponding values for the ANNA-1 samples were 69.2±19.0% in the colon and 46.4±29.6% in the sigma (P =0.062, unpaired t-test).

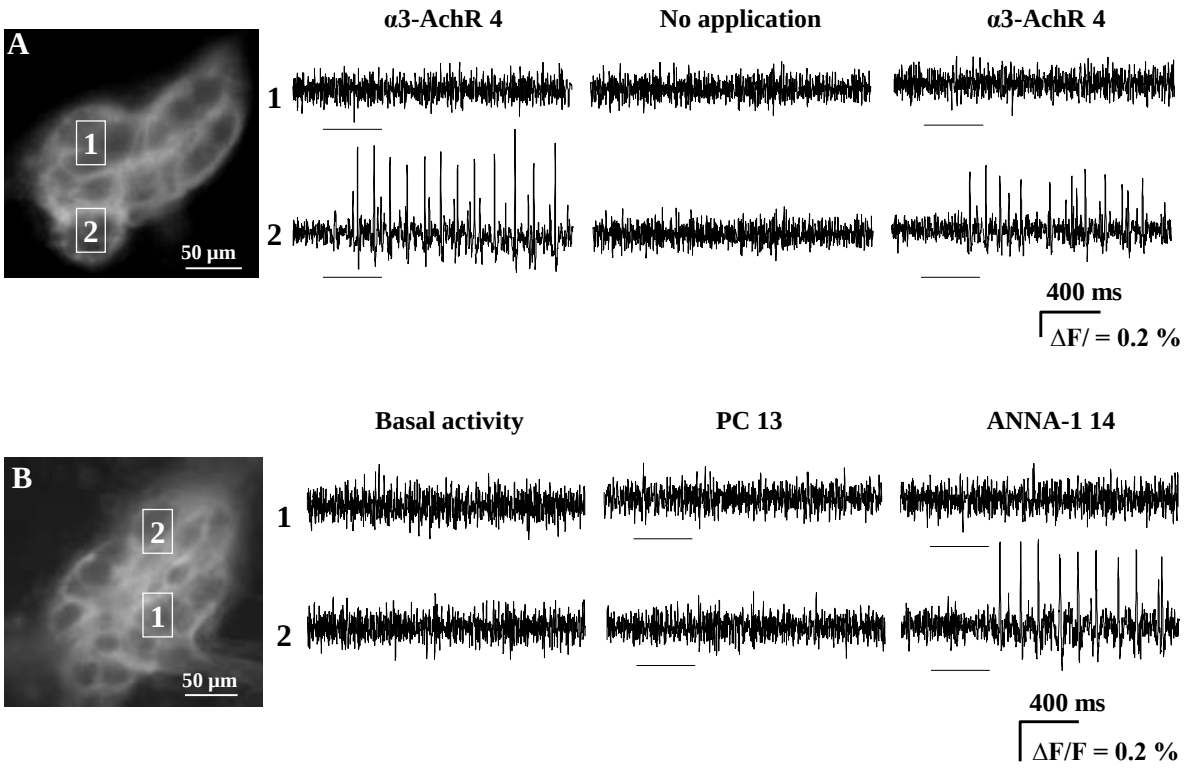

Figure 12: Neural activation of serum IgG samples α3-AchR and ANNA-1 in human submucosal plexus. The left images show outline of Di-8-ANEPPS stained neurons in human submucosal ganglia. The traces to the right are from two corresponding neurons (marked by white rectangles and numbers) in the (A) and (B) images, respectively. (A) Neuron 1 did not respond to application of α3-AchR, whereas α3-AchR application evoked a strong reproducible spike discharge and obtained reproducible results in neuron 2. (B) ANNA-1 14 application evoked a strong spike discharge in neuron 2, whereas neuron 1 and 2 did not respond to the application of the PC 13. The bars below the traces indicate the 400 ms application.

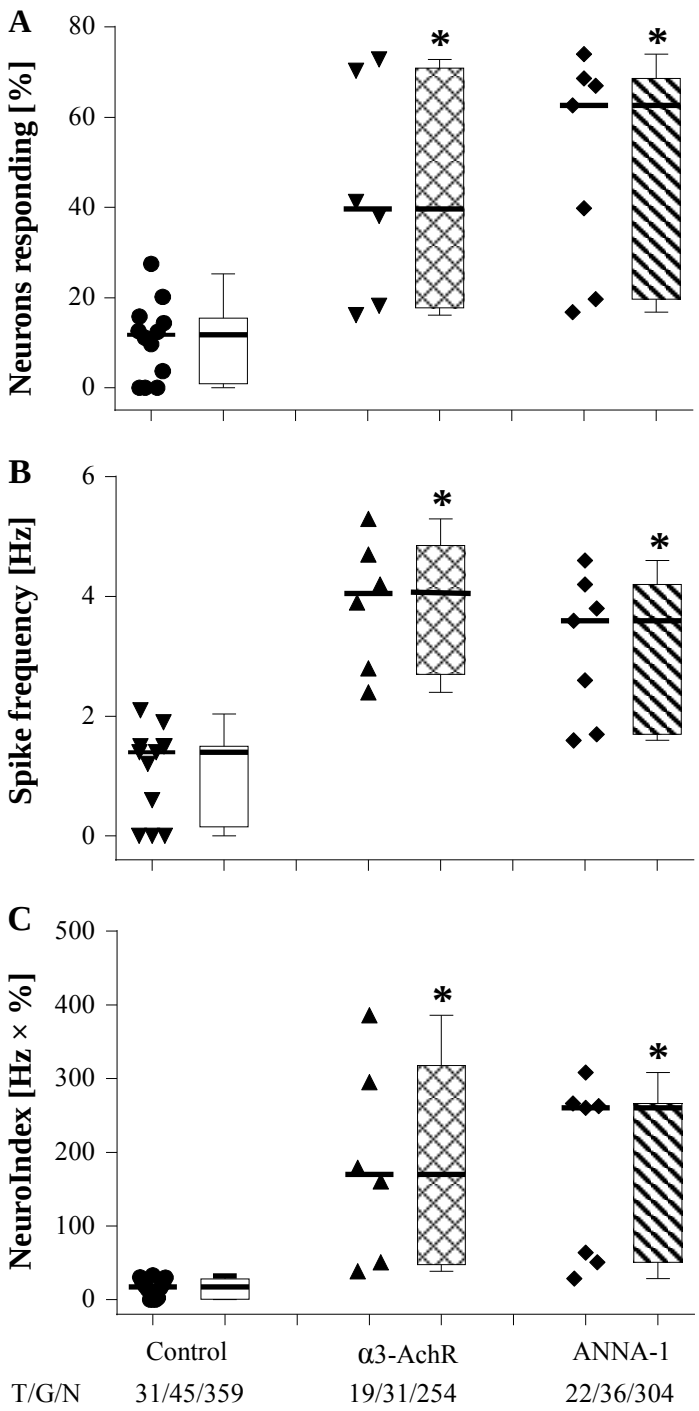

Figure 13: Pooled data of α3-AchR and ANNA-1 IgG samples had excitatory effects on human submucosal neurons. The scatter plot and box plot show pooled data for each samples of control (PC and HC), α3-AchR and ANNA-1 for (A) the percentage of responding neurons per ganglion, (B) the action potential frequency (C) as well as the neuroindex. Comparisons to the control were performed with ANOVA followed by Dunn's Method and and Student-Newman-Keuls method. Differences were considered as significant with $P < 0.05$, T/G/N: tissue/ganglia/neurons.

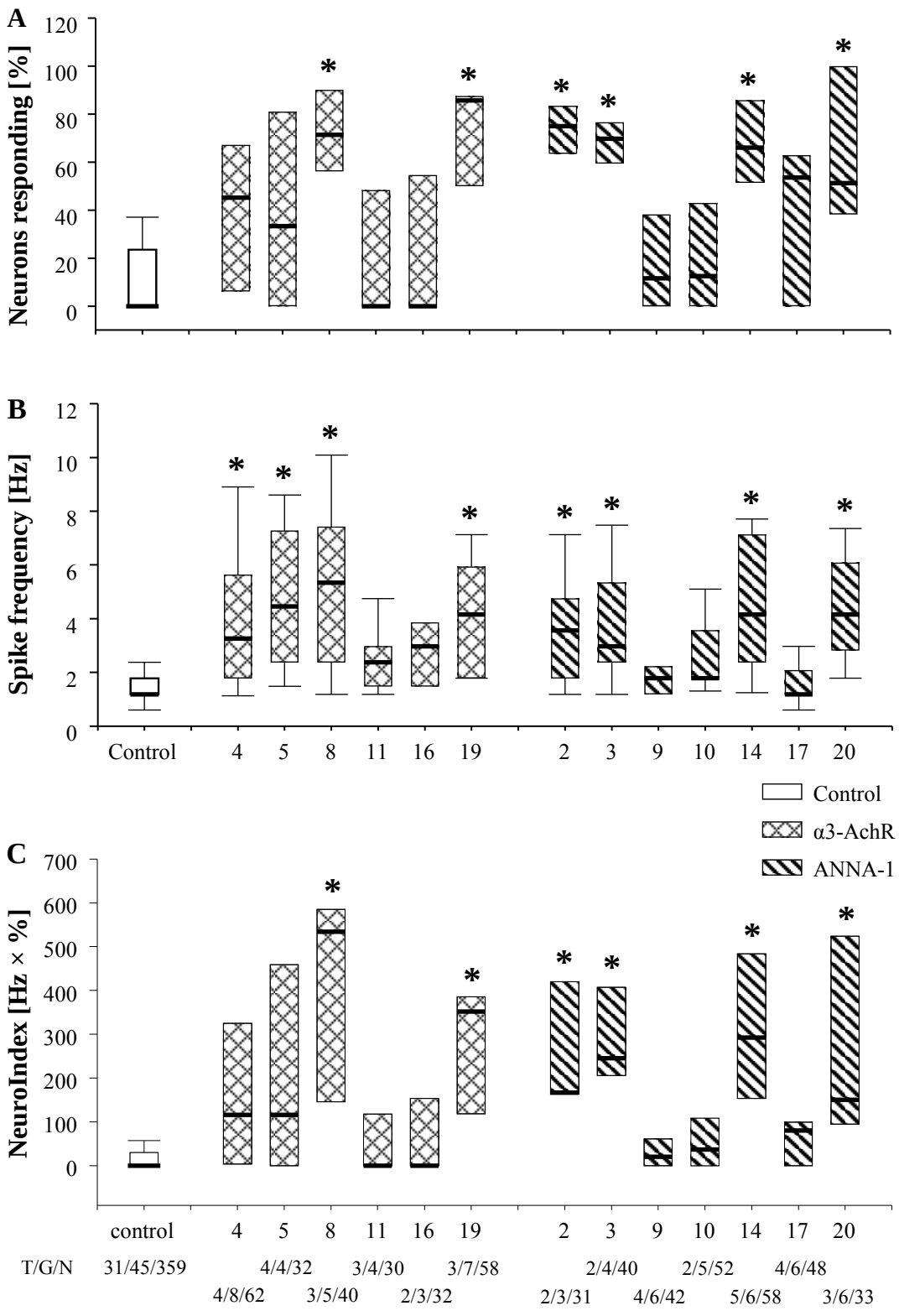

Figure 14: Effect of sera α3-AchR and ANNA-1 IgG samples on human submucosal neurons. All α3-AchR samples and ANNA-1 samples had excitatory effects on human submucosal neurons. The control samples (pooled HC and PC) cause weak activation in a low proportion of neurons. The box plot show for all α3-AchR and ANNA-1 samples as well as the control sample (A) the percentage of responding neurons per ganglion, (B) the action potential frequency (C) as well as the neuroindex.

Comparisons to the control samples were performed with ANOVA followed by Dunn's Method. Differences were considered as significant if $P < 0.05$, T/G/N: tissue/ganglia/neurons.

Table 5: There is no correlation between the number of neurons activated by the IgG samples and the patient or tissue characteristics.

	Age	Gender	Diagnosis	Region of gut
α3-AchR	$P = 0.225$	$P = 0.777$	$P = 0.924$	$P = 0.056$
ANNA-1	$P = 0.248$	$P = 0.266$	$P = 0.361$	$P = 0.062$

There was no correlation between concentration of the α3-AchR or ANNA-1 antibodies in individual samples and the percentage of responding neurons or action potential frequency (**Table 6**).

Table 6: Association of neuronal activity evoked by the IgG samples and the antibody concentrations.

Samples	Guinea pig			Human		
	Neurons responding [%]	Spike frequency [Hz]	neuroindex [%×Hz]	Neurons responding [%]	Spike frequency [Hz]	neuroindex [%×Hz]
α3-AchR	$P = 0.398$	$P = 0.603$	$P = 0.220$	$P = 0.379$	$P = 0.236$	$P = 0.289$
ANNA-1	$P = 0.287$	$P = 0.082$	$P = 0.912$	$P = 0.686$	$P = 0.289$	$P = 0.280$

Data were analyzed by using the Pearson Product Moment Correlation.

3.2.2 Which antibody is responsible for the excitatory effect on myenteric neurons?

The sera of patients with the ANNA-1 (anti-Hu) antibodies usually contain a mixture of the anti-Hu subtypes (anti-HuA, B, C and D). In cooperation with Euroimmun (Euroimmun Medizinische Labordiagnostika AG, Lübeck, Germany) we were able to obtain fractions of two patient sera containing either the purified anti-HuD antibodies or the remaining anti-Hu antibodies (not tested for other antibodies). The immunohistochemistry experiments already had shown differences in the staining (binding) pattern for the different fractions. Therefore

we also used both fractions in neuroimaging experiments to examine if the purified antibodies had effects on neurons and possible differences in the effects of the different antibodies on neurons. Those experiments were performed in guinea pig preparations which were more readily available than human tissues. We tested the two fractions in 93 myenteric ganglia from 19 guinea pig ileum myenteric plexus preparations containing 3,428 neurons.

3.2.2.1 Response to anti-HuD and comparison with anti-HuA/B/C in the guinea pig myenteric neurons

These experiments were performed with 16 guinea pig ileum myenteric plexus preparations. A total of 76 myenteric ganglia containing 2785 neurons were analyzed.

The anti-HuD as well as the anti-HuA/B/C fractions (from patients 26_EI and 27_PR) were applied (**Figure 15**A). Based on the response pattern, four groups of neurons were identified: The first group of neurons responded to anti-HuD. A second much smaller group of neurons responded to anti-HuA/B/C. The third group of neurons responded to anti-HuD as well as to anti-HuA/B/C (for the action potential frequency the neruons responding to anti-HuD were named both_anti-HuD; neurons responding to anti-HuABC named both_anti-HuABC). The fourth group of neurons did not respond to either of the fractions.

Analysis of the pooled data for the fractions of the two patients 26_EI and 27_PR showed that significantly more neurons responded to anti-HuD (45.3±11.1%) than to anti-HuABC and both (22.8±11.2% and 14.3±8.9%, **Figure 16A**). The mean frequency of action potentials was not significantly different between anti-HuD (3.0±0.9 Hz), anti-HuABC (1.7±0.7 Hz), both_anti-HuABC (1.7±1.0 Hz) and both_anti-HuD (2.9±2.0 Hz, P =0.06, **Figure 16B)**. The neuroindex for anti-HuD (148.8±71.5% × Hz) was significantly different from the value for anti-HuABC (48.2±34.5% × Hz), both_anti-HuABC (34.2±30.5% × Hz) and both_anti-HuD (56.8±45.8% × Hz, **Figure 16C**).

Similar results for the four groups of neurons were found for the application of the fractions of patient 26_EI (**Figure 15**A). The first group of neurons responded to anti-HuD (49.7[28.2/69.9]%, **Figure 17A** and **Table 7**) with a significantly higher neuroindex (51.7[27.4/134.8]% × Hz, **Figure 17C** and **Table 7**) than the response to anti-HuABC and both. Spike frequencies for the responses to anti-HuD and also both_anti-HuD (2.1[1.3/5.2] Hz and 3.4[1.6/6.6] Hz) were significantly higher than the values for anti-HuABC and both_anti-HuABC (P <0.05, **Figure 17B** and **Table 7**)

A second, much smaller group of neurons responded to anti-HuA/B/C (21.2[10.9/37.2]%, **Figure 17A** and **Table 7**) with a lower firing frequency (1.7[0.9/3.0] Hz) and neuroindex value (40.7[24.5/112.4]% × Hz, **Figure 17B, Figure 17C** and **Table 7**).

The third group of neurons responded to anti-HuD as well as to anti-HuA/B/C (**Figure 17** and **Table 7**).

The fourth group of neurons showed no response to either of the antibody fractions.

Pressure application of anti-HuD and anti-HuA/B/C from 27_PR evoked similar responses like the fractions from patient 26_EI. There was a significantly larger proportion of neurons which responded to the application of anti-HuD compared to the neurons that responded to anti-HuA/B/C and both (46.4[22.9/59.5]% versus 26.8[3.9/33.8]% versus 14.3[0.0/28.6]%, **Figure 17A** and **Table 7**). In comparison to anti-HuA/B/C and both_anti-HuABC, the application of anti-HuD evoked a significantly higher spike discharge (1.3[0.9/2.2] Hz and 1.2[0.9/2.2] Hz versus 1.7[1.3/3.5] Hz, **Figure 17B** and **Table 7**). The neurons that responded to both_anti-HuD antibodies had significantly different spike frequencies compared to both_anti-HuABC (2.6[1.3/4.9] Hz versus 1.7[1.3/3.5] Hz), but there was no significant difference between the spike frequency of neurons responding to both_anti-HuD and anti-HuD antibodies (**Figure 17B** and **Table 7**). The neuroindex for anti-HuD (96.3[50.8/145.7]% × Hz) was significantly different from the anti-HuABC (33.5[4.7/70.3]% × Hz), both_anti-HuABC (22.2[0.0/38.6]% × Hz and both_anti-HuD (22.8[0.0/81.1]% × Hz, **Figure 17**C and **Table 7**).

3.2.2.2 Responses to anti-HuD in comparison with blood donor serum in guinea pig myenteric neurons

We compared the effect of the application of the anti-HuD (from 27_PR) with the application of serum from a blood donor on the guinea pig ileum myenteric neurons (**Figure 15**B). We applied the two substances onto the same ganglia to compare the responses in a paired manner.

A small subset of neurons was activated by the blood donor serum (15.3[7.8/35.4]%). This was much lower than the population that responded to anti-HuD (48.2[30.0/67.2]%, $P < 0.05$, **Figure 17**A and Error! Reference source not found.). The action potential frequency of the neurons which responded to the blood donor serum (0.9[0.4/1.7] Hz) was also significant lower than that evoked by anti-HuD (2.2[1.3/3.9] Hz, **Figure 17B** and Error! Reference source not found.). The neuroindex of anti-HuD (139.3[60.7/186.9]% × Hz) was significantly different from the blood donor (20.8[9.2/41.6]% × Hz), both_blood donor (11.4[1.4/30.0]% × Hz) and both_anti-HuD (16.8[4.2/67.2]% × Hz, **Figure 17**C and **Table 7**).

3.2.2.3 Responses to anti-HuD compared with HuD antigen in the guinea pig myenteric neurons

We studied the responses to application of anti-HuD antibody (from 27_PR) and HuD antigen onto the same myenteric ganglia of the guinea pig ileum (**Figure 15C**). The anti-HuD application resulted in a significantly larger proportion of excited neurons (41.3[23.4/63.9]%) whereas the application of the HuD antigen had almost no effect (0.0[0.0/5.0]%, P <0.05, **Figure 17A** and **Table 7**). While anti-HuD evoked a spike discharge of 2.1[1.3/3.5] Hz, firing rate after application of HuD antigen was significantly lower (1.1[0.4/2.1] Hz, **Figure 17B** and **Table 7**). The neuroindex of anti-HuD (101.7[47.7/108.4]% × Hz) was significantly different from the antigen (0.0[0.0/4.8]% × Hz), **Figure 17**C and **Table 7**).

Table 7: The table shows response to the various agents applied to the ileum myenteric plexus neurons in guinea pig.

RN [%]	SF [Hz]	NI [Hz×%]	RN [%]	SF [Hz]	NI [Hz × %]	RN [%]	SF [Hz]	NI [Hz × %]	RN [%]	SF [Hz]	NI [Hz × %]	GP/G/N
26-EI AntiHuABC			**Both_anti-HuABC**			**Both_26_EI anti-HuD**			**26-EI Anti-HuD**			
21.2 [10.9/37.2]	1.7 [0.9/3.0]	40.7 [24.5/112.4]	12.7 [8.5/27.5]	1.7 [0.8/3.0]	32.4 [18.0/49.2]	12.7 [8.5/27.5]	3.4 [1.6/6.6]	51.7 [27.4/134.8]	49.7 [28.2/69.9]	2.1 [1.3/5.2]	179.5 [80.9/330.8]	**3/18/655**
27-PR AntiHuABC			**Both_anti-HuABC**			**Both_27_PR anti-HuD**			**27-PR Anti-HuD**			
26.8 [3.9/33.8]	1.3 [0.9/2.2]	33.5 [4.7/70.3]	14.3 [0.0/28.6]	1.2 [0.9/2.2]	22.2 [0.0/38.6]	14.3 [0.0/28.6]	2.6 [1.3/3.9]	22.8 [0.0/81.1]	46.4 [22.9/59.5]	1.7 [1.3/3.5]	96.3 [50.8/145.7]	**3/18/533**
Blood donor serum			**Both_Blood donor serum**			**Both_27_PR anti-HuD**			**27-PR Anti-HuD**			
15.3 [7.8/35.4]	0.9 [0.4/1.7]	20.8 [9.2/41.6]	9.3 [1.7/17.6]	1.3 [0.9/2.2]	11.4 [1.4/30.0]	9.3 [1.7/17.6]	2.2 [1.3/4.8]	16.8 [4.2/43.8]	48.2 [30.0/67.2]	2.2 [1.3/3.9]	139.3 [60.7/186.9]	**5/22/863**
HuD antigen			**Both_antigen**			**Both_27_PR anti-HuD**			**27-PR Anti-HuD**			
0.0 [0.0/5.0]	1.1 [0.4/2.1]	0.0 [0.0/4.8]	0.0 [0.0/0.5	0.6 [0.4/1.8]	0.0 [0.0/0.3]	0.0 [0.0/0.5]	1.1 [0.9/3.7]	0.0 [0.0/0.6]	41.3 [25.4/63.9]	2.1 [1.3/3.5]	101.7 [47.7/108.4]	**5/18/734**
									27-PR serum			
									30.8 [23.8/44.4]	2.2 [1.3/3.5]	75.7 [42.7/118.0]	**3/17/634**

Note: Each row shows a separate set of experiments with samples from patient 26_EI and 27_PR. RN [%]: percent of neurons responding; M ± SD: mean value ± standard deviation; SF [Hz]: spike frequency; NI: neuroindex; GP/G/D: numbers of guinea pig/ganglia/neurons; Median, 25th-75th: median values with the 25% and 75% quartiles. Data were analyzed by using the One Way ANOVA on rank combined with multiple comparison procedures of Dunn's Method and paired t-test.

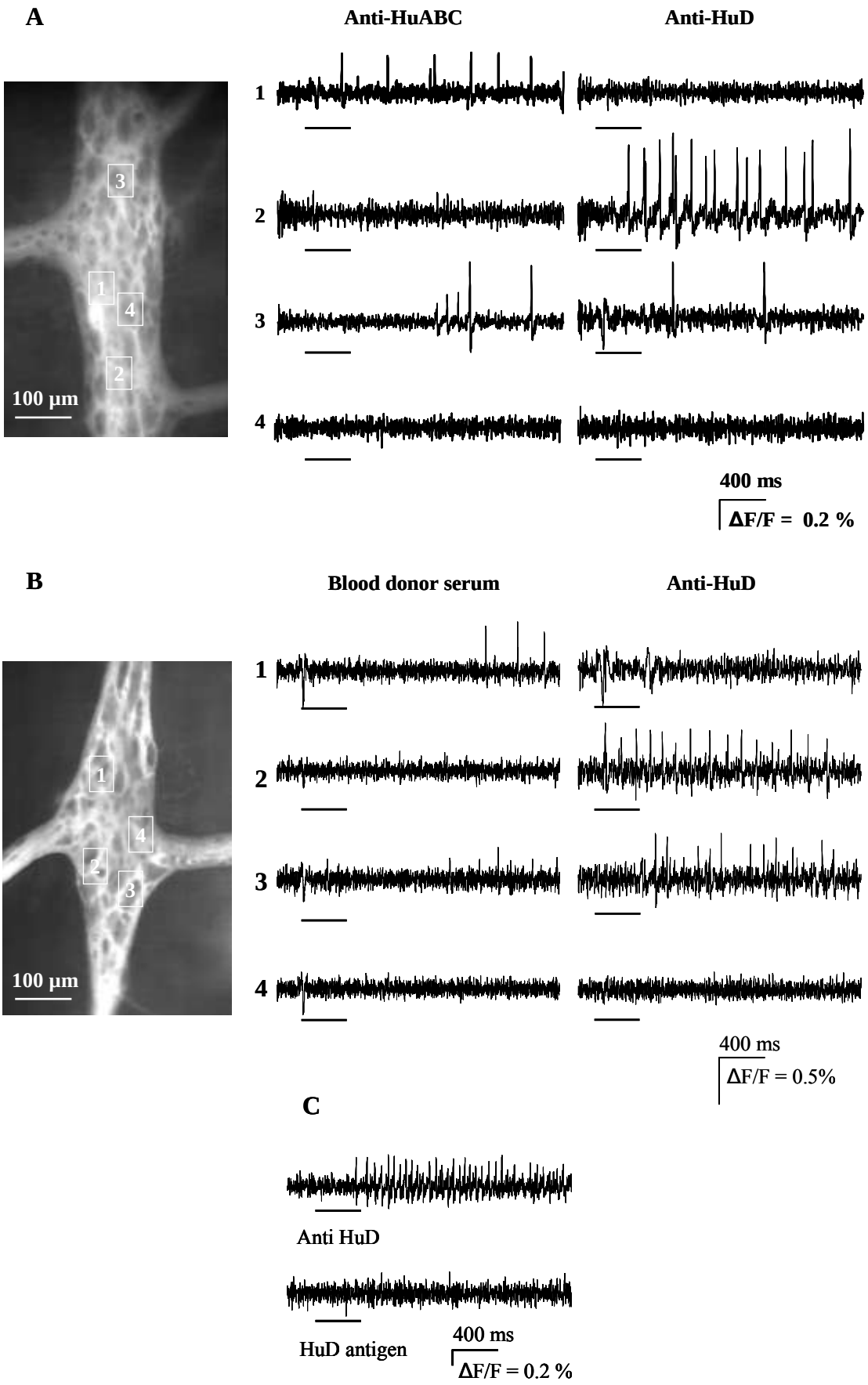

Figure 15: Comparison of the neuronal response to anti-HuD with (A) anti- HuA/B/C antibodies , with (B) blood donor serum, and with (C) HuD antigen in guinea pig ileum myenteric plexus. The

images on the left show Di-8-ANEPPS labeled myenteric ganglia. As representative examples the signals from four neurons (marked with white rectangles and numbered 1–4) in response to substances applied are shown in the right part of the figure. (A) Application of anti- HuA/B/C (from 26_EI) evoked a response inneurons 1 and 3 whereas neurons 2 and 4 remained quiet. Application of anti-HuD (from 26_EI) evoked action potential discharge in the neurons 2 and 3, neurons 1 and 4 showed no effect. (B) Blood donor serum caused a weaker activation in a lower proportion of neurons. The neuron 1 responded to blood donor serum exclusively, the neuron 2 responded to anti-HuD (from 27_PR) exclusively, the neuron 3 responded to anti-HuD as well as blood donor serum, while neuron 4 did not respond to any of the substances. (C) Two representative traces illustrating the comparison of the responses to the application of the anti-HuD antibodies (from 27_PR) with the application of the HuD antigen in the same myenteric neuron. The first one evoked a strong response but the second did not evoke any response.

The substance application (400 ms) is shown by the bars below the traces. The recording period was 2.5 s.

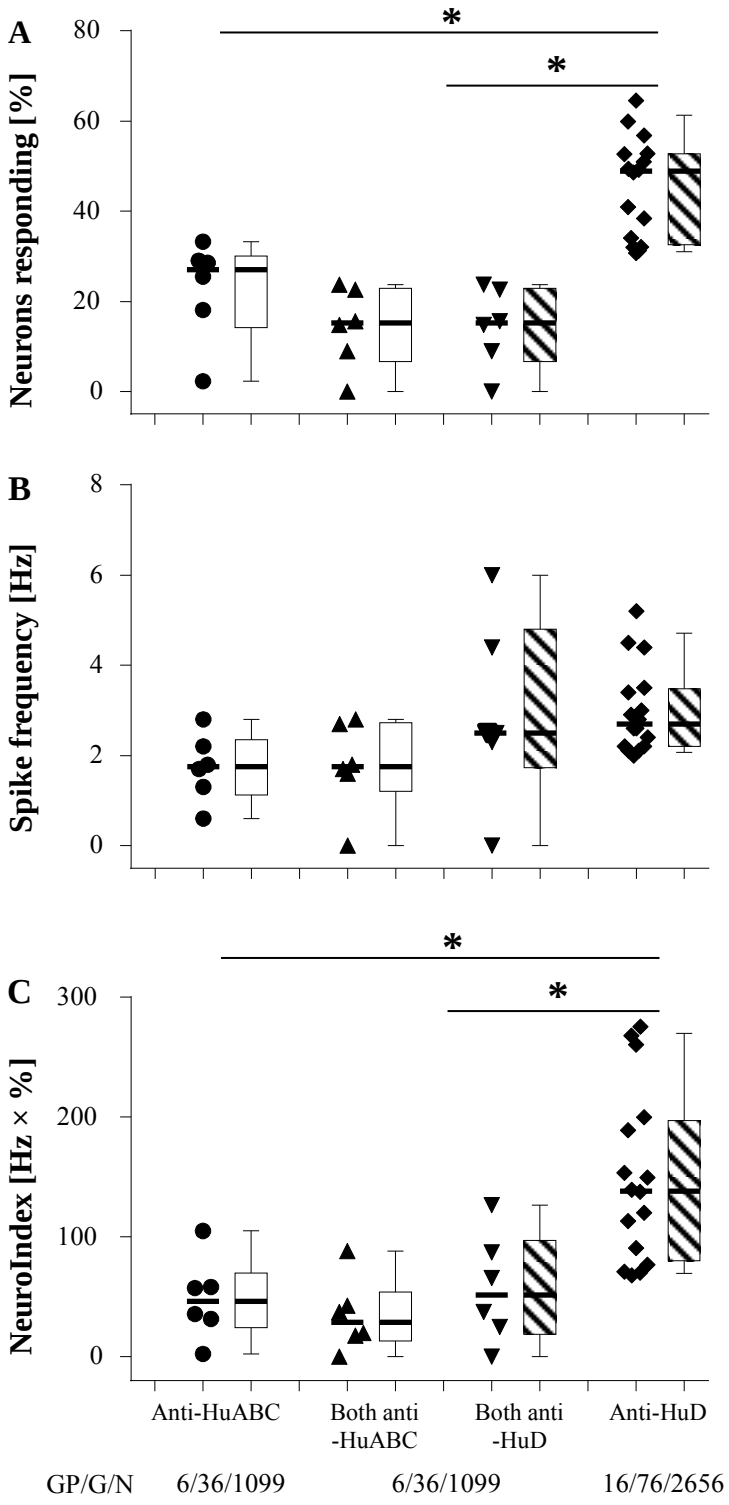

Figure 16: Effect of anti-HuD and anti-HuA/B/C antibodies from 26_EI and 27_PR on myenteric neurons of guinea pig. The scatter plot and box plot show the pooled data for each expriment with the antibodies (A) for the percentage of responding neurons per ganglion, (B) the action potential frequency as well as (C) the neuroindex which is the product of action potential frequency and proportion of responding neurons. Comparisons were performed with ANOVA followed by Dunn's method and Student-Newman-Keuls method. Results were considered as significanct when $P < 0.05$. GP/G/N: guinea pig/ganglia/neurons.

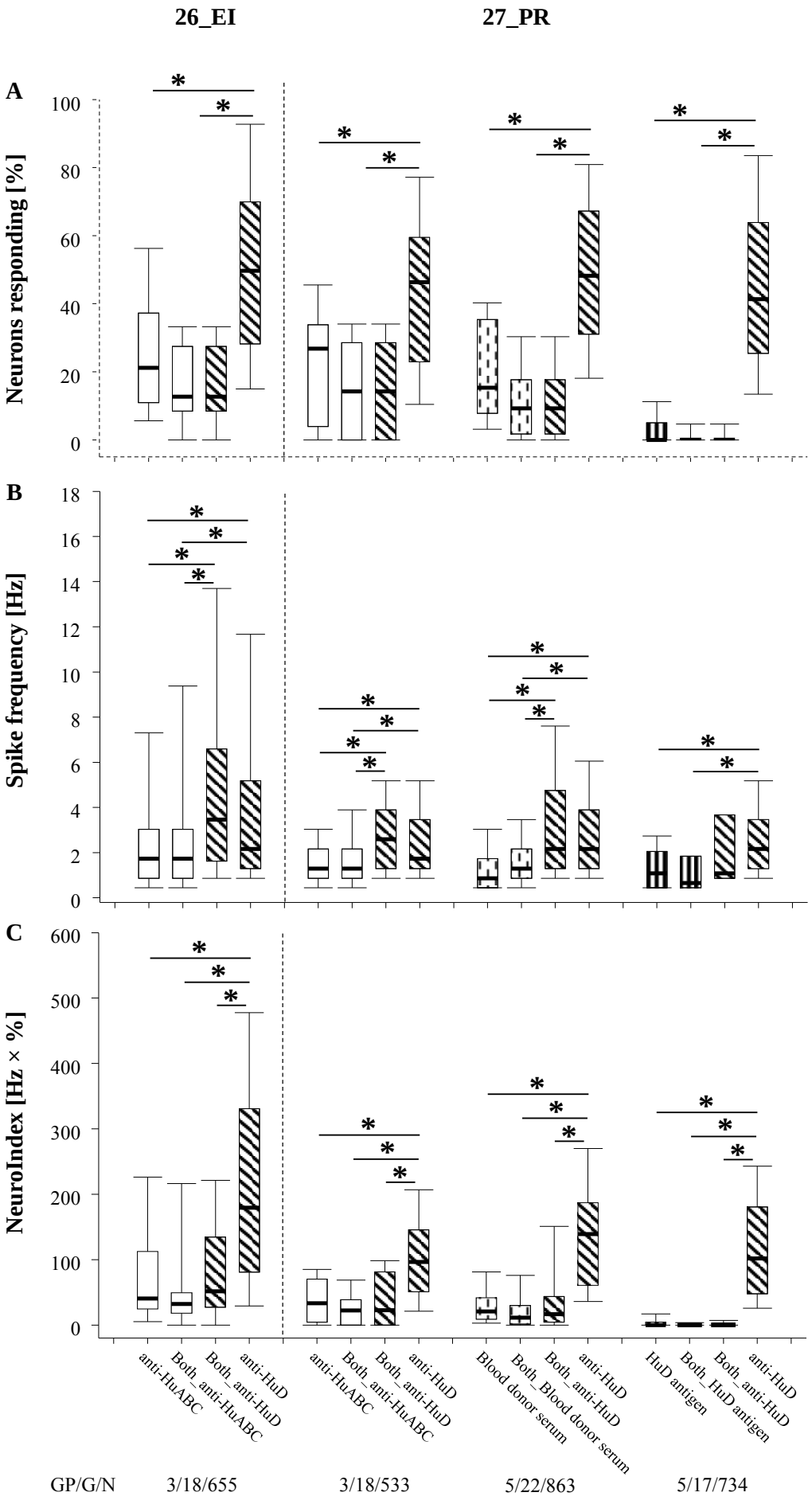
26_EI
27_PR
A
Neurons responding [%]
B
Spike frequency [Hz]
C
NeuroIndex [Hz × %]
anti-HuABC
Both_anti-HuABC
Both_anti-HuD
anti-HuD
Blood donor serum
Both_Blood donor serum
HuD antigen
Both_HuD antigen
GP/G/N
3/18/655
3/18/533
5/22/863
5/17/734

Figure 17: The neuronal response of the guinea pig ileum myenteric plexus to the various applied agents. The box plot show that pooled data of (A) the percentage of responding neurons per ganglion, (B) the action potential frequency as well as (C) the neuroindex. Comparisons were performed with ANOVA followed by Dunn's Method. Results were considered as significant if P <0.05. GP/G/D: guinea pigs/ganglia/neurons.

3.2.2.4 Responses to patient serum was similar to responses to anti-HuD antibody in the guinea pig myenteric neurons

In a set of experiments we used the complete serum from patient 27_PR (27_PR serum) and compared its effects to the anti-HuD fraction (27_PR anti-HuD) from the same patient to test the excitatory effects on neurons. The experiments were performed in 3 guinea pig ileum myenteric plexus preparations. A total of 17 myenteric ganglia containing 643 neurons were analyzed. There was no significant difference in the number of neurons showing a response to the application of the 27_PR serum (30.8[23.8/44.4]%) and to 27_PR anti-HuD antibody (46.4[25.8/61.5]%, unpaired *t*-test, P =0.07, **Figure 18**A). The frequency of action potential discharge and neuroindex between the two groups were also not significantly different (2.2[1.3/3.5] Hz versus 2.2[1.3/3.9] Hz, unpaired *t*-test, P =0.29; 75.7[42.7/117.9]% × Hz versus 117.1[55.3/172.4]% × Hz, unpaired *t*-test, P =0.14, **Figure 18B** and **Figure 18C**).

3.2.2.5 Responses to patient serum compared to blood donor serum and HC

We also analyzed the effect of the complete serum (27_PR serum) and compared it to the effect of blood donor serum and HC (purified IgG serum) on myenteric ganglia of the guinea pig ileum. There were significant differences in the number of neurons showing a response to the application of the 27_PR serum (30.8[23.8/44.4]%) and blood donor (15.3[7.8/35.4]%) versus HC (0.0[0.0/5.8]%, **Figure 19**A). The 27_PR serum evoked spike discharge (2.2[1.3/3.5] Hz) with a frequency that was significantly different to both blood donor (0.9[0.4/1.7] Hz) and HC (1.3[0.9/2.2] Hz, **Figure 19B).** The neuroindex for the effect of 27_PR serum (75.7[42.7/117.9]% × Hz), blood donor (20.8[9.2/41.6]% × Hz) and HC (0.0[0.0/3.9]) were significantly different when compared to each other (**Figure 19C)**.

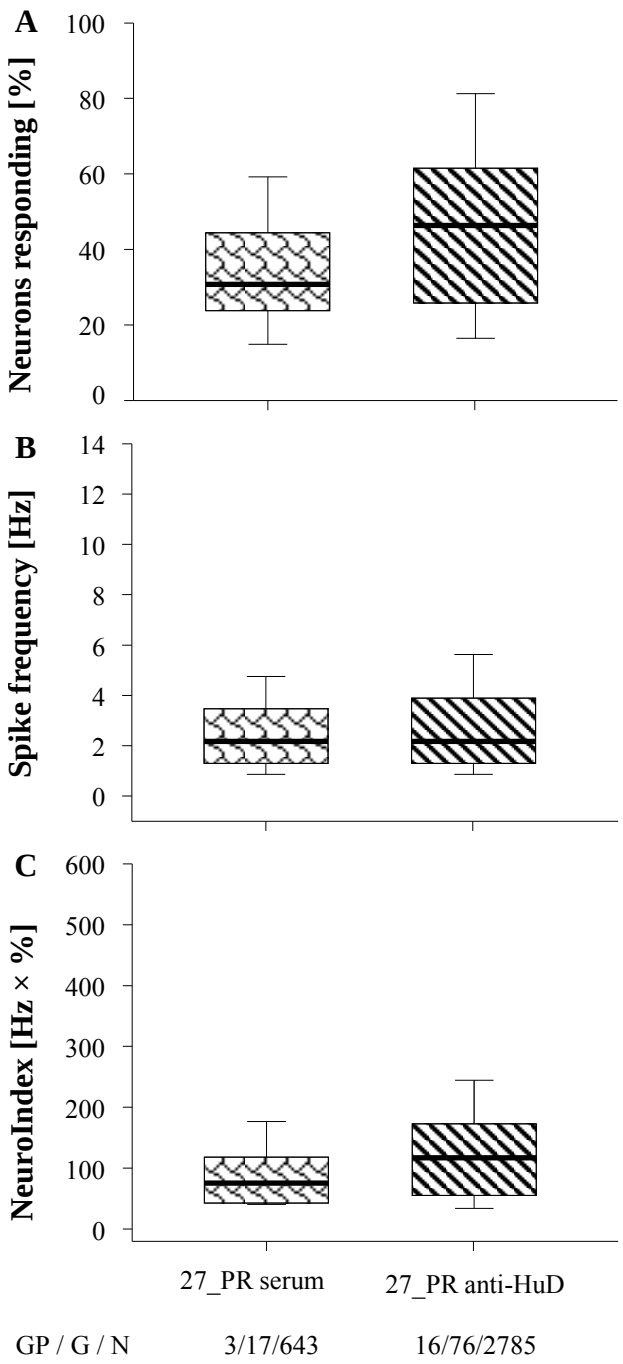

Figure 18: The patient serum and anti-HuD antibodies (from patient 27_PR) had similar effects in the guinea pig myenteric neurons. (A) Box plot showing percentage of neurons responding to patient serum and anti-HuD antibodies. (B) The frequency of action potentials in response to the application of patient serum and anti-HuD antibodies. (C) The neuroindex graph indicates a product from mean frequency of action potential discharge per ganglion and proportion of responding neurons. The differences in the median values among the two groups were not statistically significant different. Data were analyzed by using the unpaired *t*-test. GP/G/D: guinea pigs/ganglia/neurons.

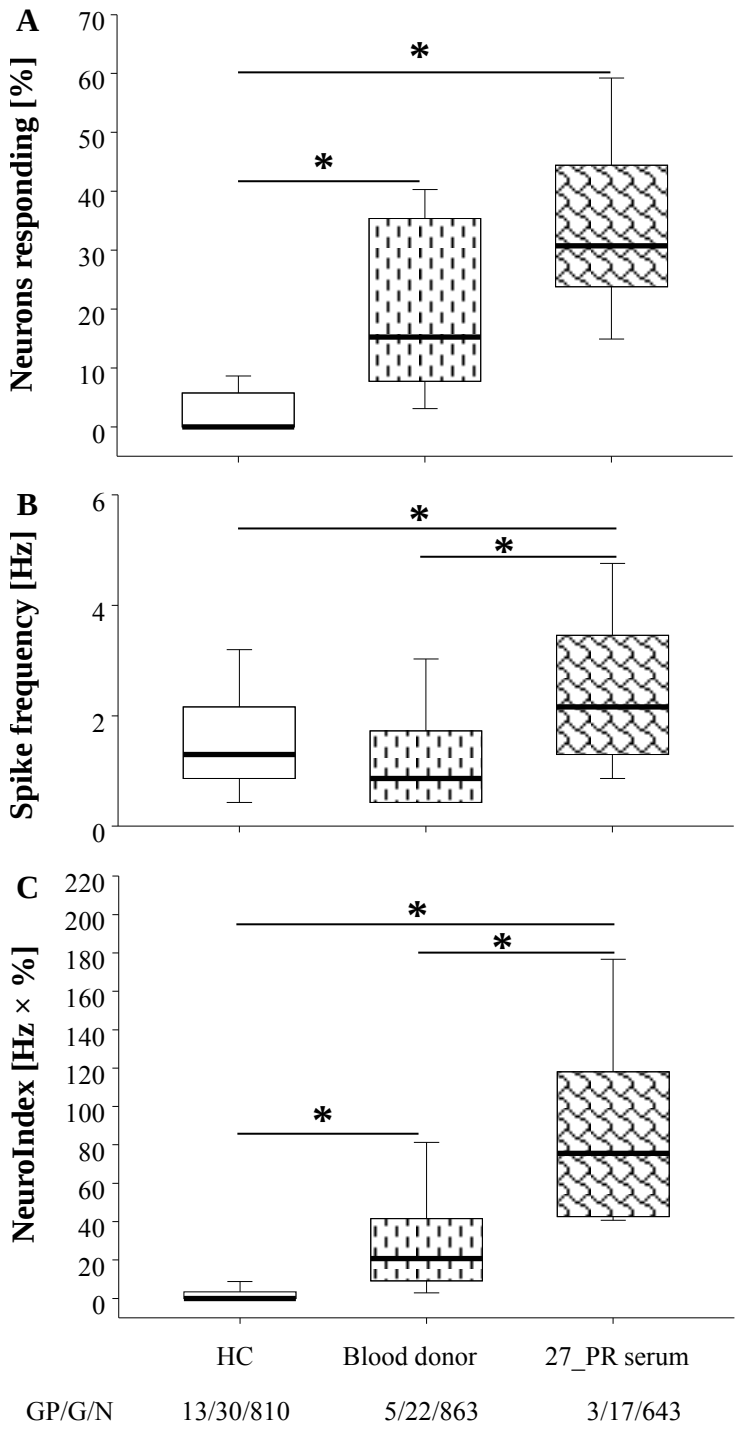

Figure 19: Responses to patient serum compared to blood donor serum and HC in the guinea pig myenteric neurons. (A) Box plot showing percentage of neurons responding. (B) The frequency of action potentials. (C) The neuroindex. * $P < 0.05$, data was analyzed by using the ANOVA followed by Dunn's method. GP/G/D: guinea pigs/ganglia/neurons.

3.2.3 The nicotinic acetylcholine receptor blocker hexamethonium reduces ANNA-1 induced neuronal reseponses in guinea pig myenteric neurons

In a preliminary set of experiments, we used a pharmacological approach to check whether the response to ANNA-1 was via the nicotinic acetylcholine receptors. We reapplied the ANNA-1 after a 20 min perfusion with the nicotinic acetylcholine receptor antagonist hexamethonium (200 μM). Hexamethonium significantly reduced the spike discharge evoked by ANNA-1 **(Figure 20**). In 74.9% of the guinea pig myenteric neurons the spike discharge was reduced and did not completely recover after a 40 min washout period.

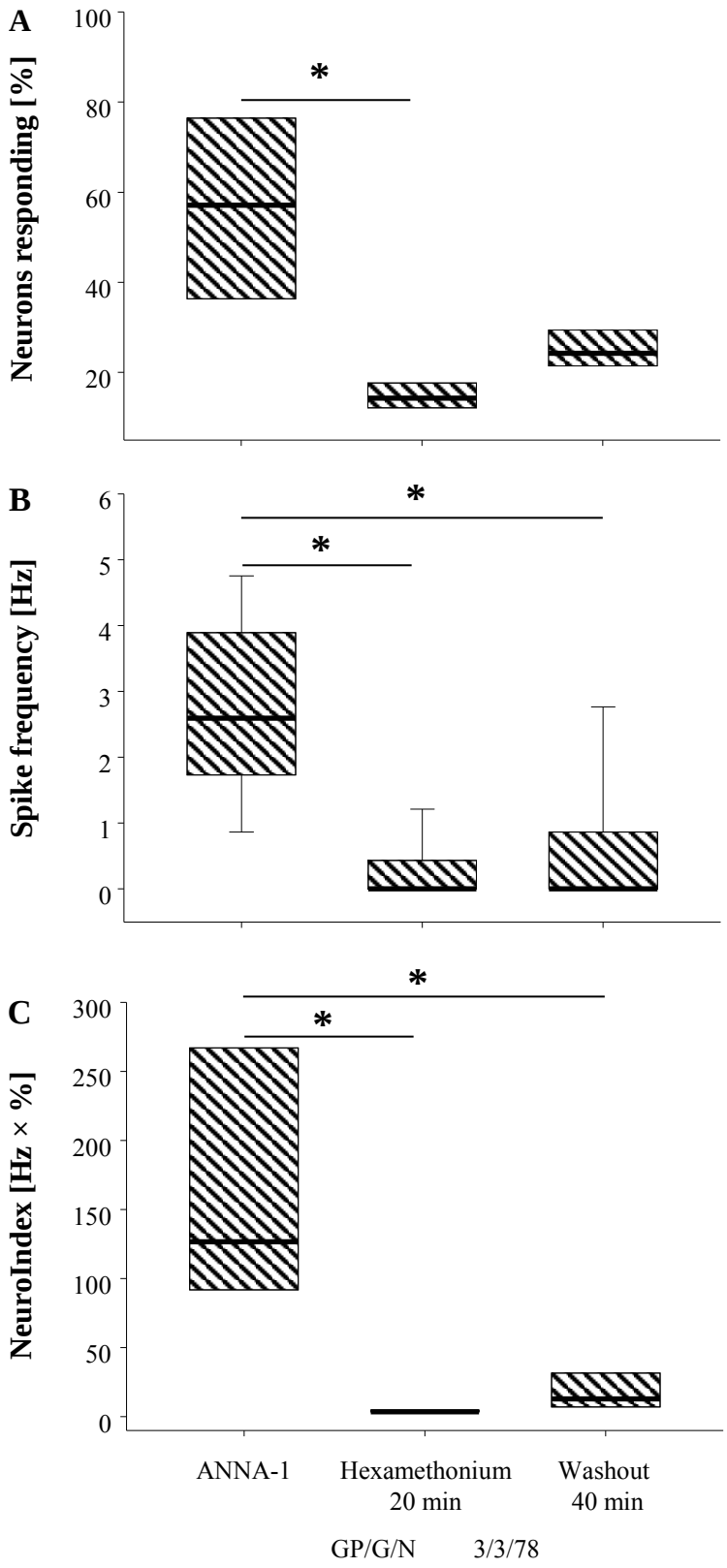

Figure 20: Hexamethonium (200 µM), an antagonist for nicotinic acetylcholine receptors reduced the ANNA-1 induced neuronal reseponse in the guinea pig myenteric neurons. (A) The box plot shows that hexamethonium significantly reduced the percentage of neurons responding. (B) Hexamethonium significantly reduced the action potential frequency. (C) Hexamethonium significantly reduced the neuroindex. Data were considered as significant if * P <0.05. Comparisons were performed with

ANOVA followed by Dunn's and Student-Newman-Keuls post hoc test. GP/G/D: guinea pigs/ganglia/neurons

3.2.4 Estimation of the concentration of the antibodies at the level of the ganglion

The sera IgG samples excited enteric neurons. The neuronal spike discharge occurred at concentrations of IgG that were equivalent to that found in human blood. The α3-AchR and ANNA-antibodies were in concentration range of between 0.7 - 5.4 nmol/L in 6 patients and 7,600 - 123,000 titer in 7 patients, respectively. Considering the antineuronal antibody levels in sera of patients with a large concentration range, we estimate that the antibody concentration in the vicinity of neurons is close to that occuring in vivo in the tissue. This is achieved by dilution of IgG samples when administered onto the ganglia. The spritz pipette contained sera IgG samples diluted 1:1 with Krebs buffer and were applied onto single ganglia by pressure ejection from micropipettes (1-2psi, 200-400 ms duration, ejection speed 55±27 nL/s, 100-200 μm distance from the ganglion). According to previously published calibration curves, we estimate that any substance applied via pressure ejection pulses will be diluted by about 1:10 once it reaches the ganglion (Breunig et al., 2007).

3.2.5 Possible inhibitory effects of antibodies and reproducibility of the antibody induced effect

Although the effect of the antibody preparations was excitatory, we observed sometimes a decrease in the frequency of action potential discharge in spontaneously active neurons after the application of the antibody preparation. To further characterize this phenomenon, we analysed separately the antibody mediated effects in all neurons that were found to be spontaneously active before the first application of the substances. Data for guinea pig and human preparations is summarized in **Table 8** and **Table 9**. As expected, spike discharge increased significantly in a large group of neurons while it decreased significantly in a smaller group of neurons. A third group of neurons showed no change of spike frequency compared to spontaneous activity (data see **Table 8**). These effects could also be due to naturally occurring variations in spontaneous spike discharge. Therefore spontaneous activity during blank recordings between applications of antibody preparations was analysed (**Table 9)**. The spike frequency of spontaneous fired action potentials increased significantly in a small group

of neurons. This group was much smaller than the group of neurons that showed an increase in firing rate after the application of antibody preparations. On the other hand, there was a much larger group of neurons in which the frequency of spontaneous fired action potentials decreased significantly (data see **Table 9**). Both results indicate that the antibody preparations do not have an inhibitory effect on enteric neurons.

The reproducibility of the response to antibody preparations was tested by applying sera IgG samples (α3-AchR and ANNA-1) at least twice within a 20 min time period. These experiments showed a clear reproducibility of the effects as none of the analysed parameters changed significantly (data see **Table 10**).

Table 8: Application of sera IgG samples and antibodies on spontaneously active neurons.

	Samples	Spontaneous (+)				Spontaneous (-)				Same (0)		T/G/N
		Spontaneous SF	Samples SF	P value	% (+)	Spontaneous SF	Samples SF	P value	% (-)	SF	% (0)	
Guinea-pig	α3-AchR	1.3 [0.4/3.0]	2.6 [1.3/6.8]	< 0.001	53	2.6 [1.5/2.6]	1.5 [0.4/2.2]	= 0.008	23	0.9 [0.4/1.7]	23	2/4/94
	ANNA-1	0.4 [0.4/0.9]	2.2 [1.0/4.3]	< 0.001	80	1.3 [0.5/1.7]	0.2 [0.0/0.8]	= 0.016	13	0.6 [0.4/0.9]	**7**	4/5/127
	Anti-HuD	0.9 [0.4/2.6]	9.1 [2.2/14.7]	< 0.001	82	0.4 [0.4/2.4]	0.0 [0.0/0.0]	= 0.125	14	-	4	3//253
	Anti-HuABC	1.5 ± 1.3	2.0 ± 1.2	= 0.276	78	0.4 [0.4/4.3]	0.0 [0.0/0.0]	= 0.250	17	-	6	3/6/225
Human	AchRR	1.2 [0.6/1.3]	4.7 [3.5/8.0]	< 0.001	95	-	-		0	-	4	4/6/57
	ANNA-1	1.8 [0.9/3.0]	4.2 [3.0/6.5]	< 0.001	76	1.1 ±1.0	1.3 ±1.8	= 0.862	18	0.6 [0.6/0.6]	6	10/12/123

Note: Spontaneous (+): increase in spike discharge in spontaneously active neurons; Spontaneous (-): decrease in spike discharge in spontaneously active neurons; Same (0): no chang of spike frequency compared to spontaneous activity; SF [*Hz*]: spike frequency; T/G/N: numbers of tissues/ganglia/neurons; Normally distributed data presented as their mean value±standard deviation. Non-normally distributed data were expressed as their median together with the 25th and 75th percentiles. Data were analyzed by using the paired t-test.

Table 9: The spike frequency of spontaneously active neurons (1st) decreased after application of the IgG samples (2nd).

	Spontaneous (+)				Spontaneous (-)				Same (0)		T/G/N
Guinea-pig myenteric plexus	Spontaneous 1st SF	Spontaneous 2nd SF	P value	% (+)	Spontaneous 1st SF	Spontaneous 2nd SF	P value	% (-)	SF	% (0)	
	0.9 [0.6/1.9]	3.0 [1.5/3.2]	= 0.046	14	2.6 [1.5/3.2]	0.4 [0.0/1.1]	< 0.001	68	0.9 [0.4/1.3]	19	3/4/144
Human submucosal plexus	0.6 [0.6/1.8]	1.2 [1.2/2.4]	= 0.250	8	2.1 [1.2/3.0]	0.6 [0.0/1.6]	< 0.001	74	0.6 [0.6/1.2]	18	3/6/64

Note: Spontaneous (+): increase in spike discharge in spontaneously active neurons; Spontaneous (-): decrease in spike discharge in spontaneously active neurons; Same (0): no change of the spike frequency of 1st compared to 2nd; SF [*Hz*]: spike frequency; T/G/N: numbers of tissues/ganglia/neurons; Non-normally distributed data were expressed as their median together with the 25th and 75th percentiles. Data were analyzed by using the paired t-test.

Table 10: Reproducibility of the evoked spike frequency and the proportions of responding neurons.

	Samples	RN [%]			SF [*Hz*]			NI [Hz x %]			T/G/N
		1st	2nd	P value	1st	2nd	P value	1st	2nd	P value	
Guinea-pig myenteric plexus	α3-AchR (8,16)	33.2 ± 18.4	35.2 ± 30.8	0.902	1.3 [0.9/3.0]	1.3 [0.9/2.2]	0.415	56.9 ± 60.8	37.7 ± 46.1	0.742	2/3/81
	ANNA-1 (9,10,20)	38.8 ± 20.9	36.6 ± 16.5	0.865	1.3 [0.9/2.6]	1.3 [0.9/2.2]	0.642	49.4 ± 24.7	53.3 ± 65.0	0.934	3/3/62
Human submucosal plexus	α3-AchR (5,8,16,19)	68.7 ± 21.3	67.2 ± 12.7	0.782	2.4 [1.8/4.2]	2.9 [2.1/5.9]	0.075	214.2 ± 184.9	268.3 ± 195.4	0.389	7/8/70
	ANNA-1 (2,3,9,14,17,20)	57.5 ± 20.1	57.5 ± 14,8	0.989	2.4 [1.2/3.6]	3.1 [1.2/4.9]	0.207	138.3 ± 110.7	157.1 ± 144.4	0.432	7/10/101

Note: RN [%]: percent of neurons responding; SF [*Hz*]: spike frequency; NI: neuroindex [Hz x %]; T/G/N: numbers of tissues/ganglia/ neurons. Normally distributed data are presented as their mean value±standard deviation. Non-normally distributed data were expressed as their median together with the 25th and 75th percentiles. RN [%] and NI were analyzed by using the paired t-test and SF [*Hz*] was analyzed by using the unpaired t-test

3.3 Extracellular recordings from vagal afferents

The following experiments were performed in the laboratory of Professor Grundy (Department of Biomedical Science, University of Sheffield, UK).

Spontaneous nerve activity

Recordings were made from 14 mice. In the experimental conditions of the present study, the vagal afferents of gastric fundus exhibited irregular spontaneous activity which did not change after perfusion of oxygenated Krebs buffer.

3.3.1 Effect of ATP and DMPP on vagal afferents of the murine gastric fundus

To get control values we applied drugs with already known effects on a small number of mechanosensitive receptive fields (3 C57Bl6 mice; 4„hot spots'). 3 out of 5 units (60%, **Table 11**, Mice/hot spots/units: 3/4/5) responded to the application of ATP (1 mmol/L) with a rapid increase in firing rate (peak increase by 7.8[5.37/18.1] spikes/s (**Figure 21**, **Figure 22)**, median latency 15.7[6.4/16.7] s, peak after 19.2[8.5/21.5] s **(Figure 23, Table 12)).**

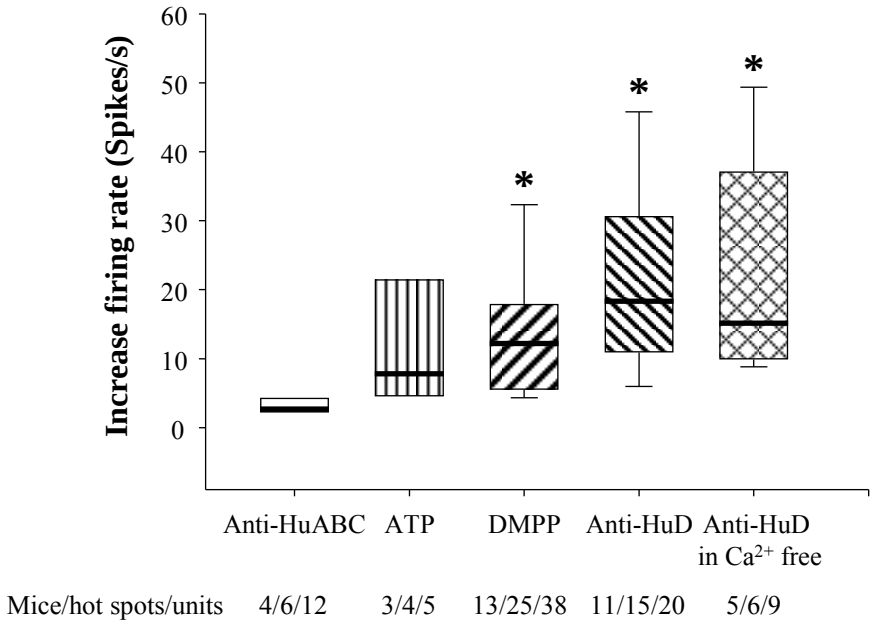

Figure 21: The box plot shows the peak increase in gastric vagal afferent discharge in response to anti-HuA/B/C, ATP, DMPP, anti-HuD and anti-HuD in Ca^{2+} free Krebs buffer. Comparisons were performed with ANOVA followed by Dunn's Method. The analyzed Data were considered as significant if $*P < 0.05$.

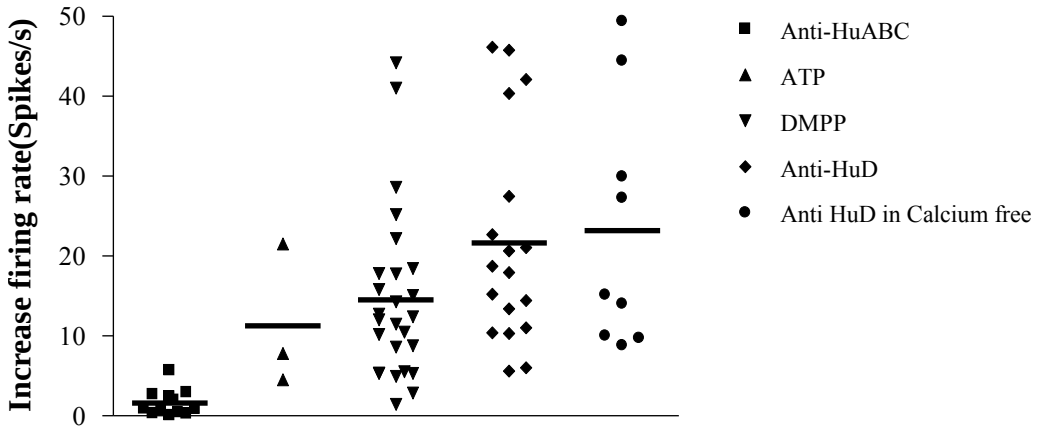

Figure 22: The scatter plot shows the peak increases in vagal afferents of gastric fundus discharge in individual units for anti-HuA/B/C, ATP, DMPP, anti-HuD and anti-HuD in Ca^{2+} free Krebs buffer. The administration of anti-HuA/B/C did not result in a significant increase in vagal afferents of gastric fundus discharge.

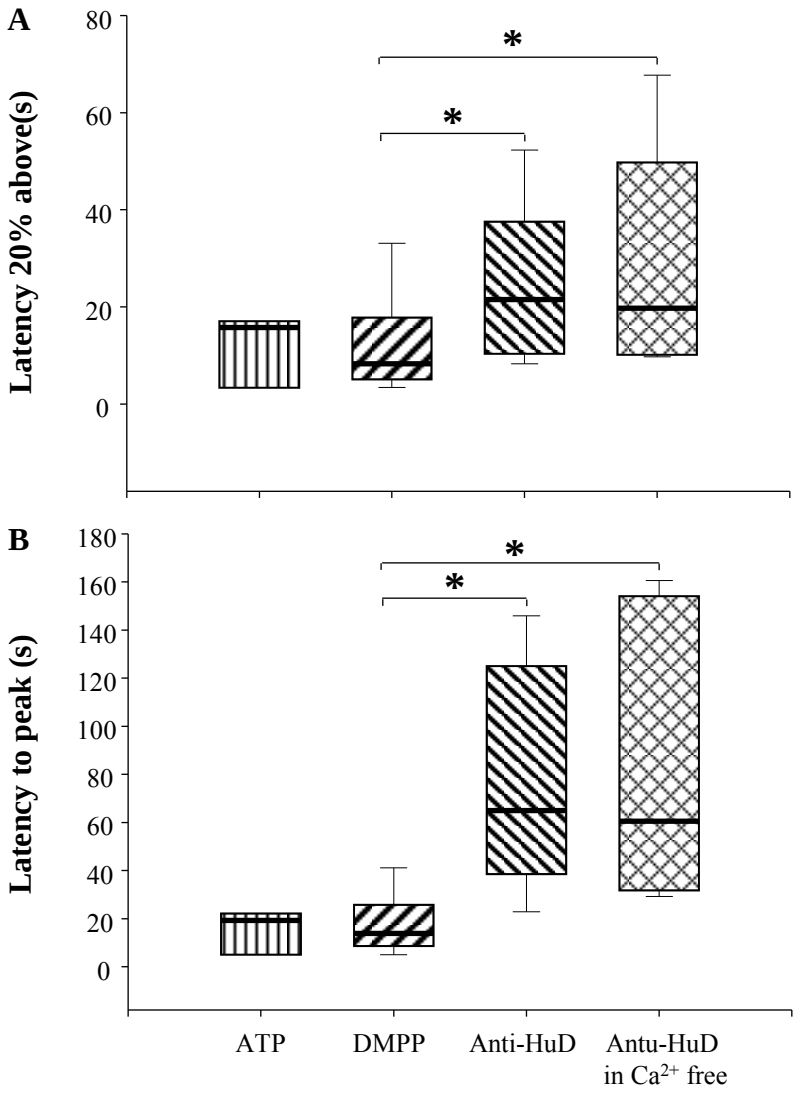

Mice/hot spots/units	3/4/5	13/25/38	11/15/20	5/6/9

Figure 23: Latency of units that are responsive to the various agents applied to the mechanosensitive "hot spots". (A) Latency from application of the drugs to firing rate increase by 20% above baseline (s). (B) Latency from application of the drugs to peak firing rate (s). Comparisons were performed with ANOVA followed by Dunn's Method. Data were considered as signifanct if $*P < 0.05$.

In 13 C57Bl6 mice and 25 mechanosensitive receptive fields, the effect of DMPP (1 mmol/L) was investigated. 26 out of 38 units (68.4%, **Table 11,** 13/25/38) responded with a rapid increase in firing rate (peak increase by 12.2[5.5/17.8] spikes/s (**Figure 21**, **Figure 22**), median latency 8.2[5.1/17.7] s, peak after 13.8[8.6/23.2] s see **Figure 23** and **Table 12**). Consistent with previous experiments in the same laboratory, DMPP excited a majority of hot spots.

3.3.2 Effect of anti-HuD and anti-HuA/B/C on vagal afferents supplying the gastric fundus

Purified anti-HuD antibody (1:10 dilution, from 26_EI) was applied to 15 mechanosensitive "hot spots" from 10 C57Bl6 mice and a total of 20 units were analysed. 18 out of 20 units (90%; **Table 11**; 10/15/20) responded with a marked increase in firing rate (peak increase by 18.3[11.0/27.5] spikes/s; (**Figure 21, Figure 22** and **Figure 24)** compared to anti-HuA/B/C (*P* <0.05), median latency 21.5[10.4/37.4]s, peak after 65.0[40.6/123.0] s; (**Figure 23, Table 12**)). In 2 experiments for 3 „hotspots' the effect was reproducible for several consecutive applications (2-5). Both DMPP and ATP sensitive or insensitive hotspots showed responses to anti-HuD antibody.

In contrast, anti-HuA/B/C had no significant effect on firing rate (2.7[2.3/3.6] spikes/s; **Figure 21**, **Figure 22** and **Figure 24**) although in individual units there was a modest increase in vagal afferents discharge.

The latency of the response to anti-HuD was significantly longer than the latency to the response to DMPP (21.5[10.4/37.4] s vs 8.2[5.1/17.7] s; *P* <0.05; see **Figure 23** and **Table 12**) although the peak increase was not different (18.3[11.0/27.5] spikes/s vs 12.2[5.5/17.8] spikes/s; *P* >0.05; **Figure 21**, **Figure 22** and **Table 11**).

3.3.3 Effect of anti-HuD on gastric vagal afferents in calcium-free Krebs buffer.

To study if the anti-HuD evoked increase in spike discharge is mediated by direct activation of the vagal terminals, we examined the role of extracellular calcium in the response to anti-HuD (from 26_EI). In Ca^{2+} free high magnesium Krebs buffer (0 mM $CaCl_2$, 3.6 mM $MGCl_2$), the response to anti-HuD was not significantly different from that in standard Krebs solution (18.3[11.0/27.5] spikes/s vs 15.2[9.9/33.6] spikes/s in calcium free, *P* >0.05; **Figure 21 Figure 22, Figure 25A, Figure 25B** and **Table 11**; 5/6/9**)**, indicating a direct effect on the afferent terminals. Likewise, the latency of the response and the time to reach the peak response were not different (21.5[10.4/37.4] s vs. 19[10.2/48.4] s, *P* >0.05; 65.0[40.6/123.0s vs. 60.6[32.7/151.5] s, *P* >0.5, see **Figure 23, Table 12**). To assess possible differences in the desensitization of the effect the afferent activity was measured in three second periods during

the late phase of the response. The time course of the response did not differ significantly in Ca^{2+} free Krebs buffer (P =0.99, **Figure 25C**).

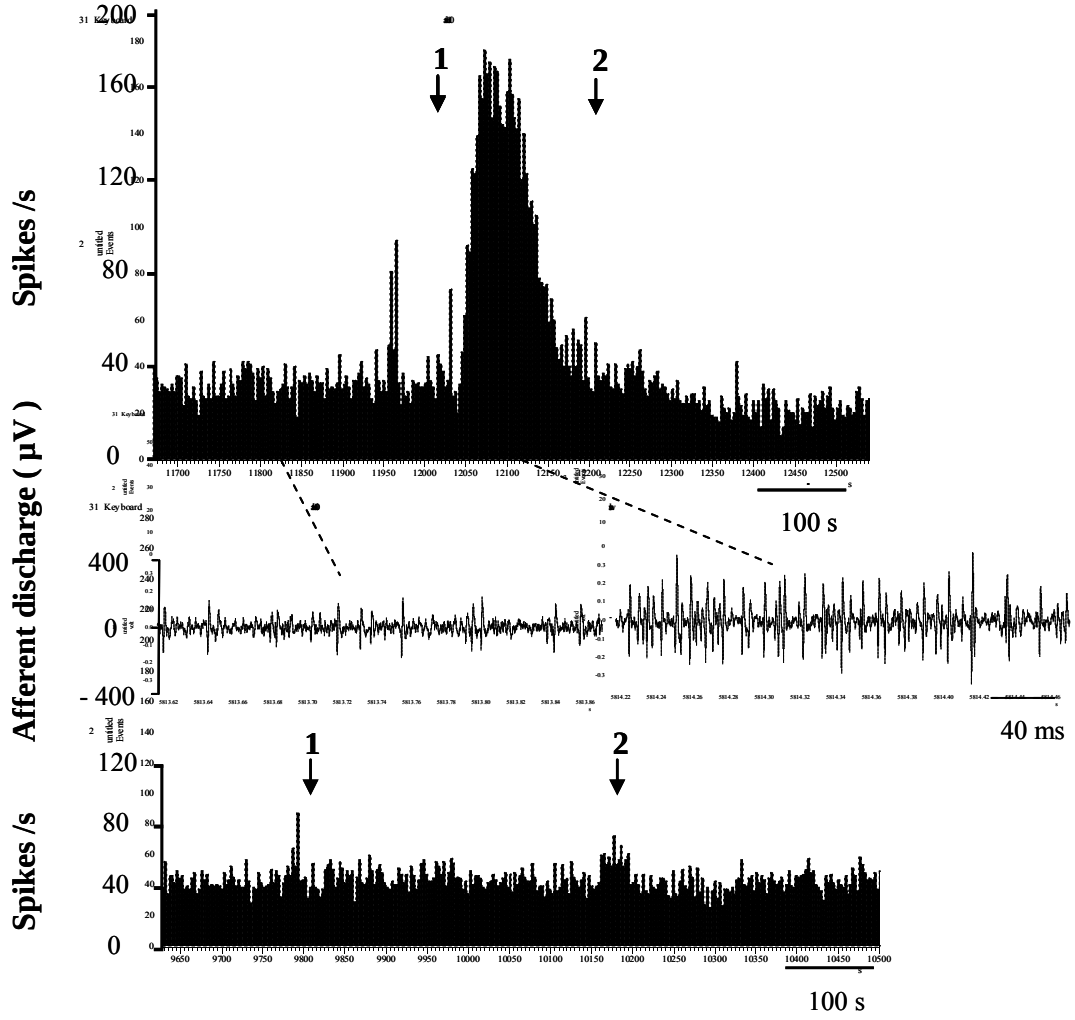

Figure 24: Effect of anti-HuD and anti-HuA/B/C (26_EI) on mechanosensitive vagal afferents of gastric fundus in mouse in vitro. The *upper trace* is a representative example of sequential rate histogram of vagal afferent discharge showing a rapid increase in discharge frequency activity to local application of anti-HuD (arrow 1) and reversed after washout (arrow 2). The *middle trace* shows "snapshots" of raw afferent fibre recording taken during baseline and during the response peak to anti-HuD at the times indicated by the dashed lines. Note the recruitment of large amplitude spikes following anti-HuD application. The *bottom trace* shows that the application of anti-HuA/B/C (arrow 1) had no effect on spike discharge in this afferent (wash out: arrow 2).

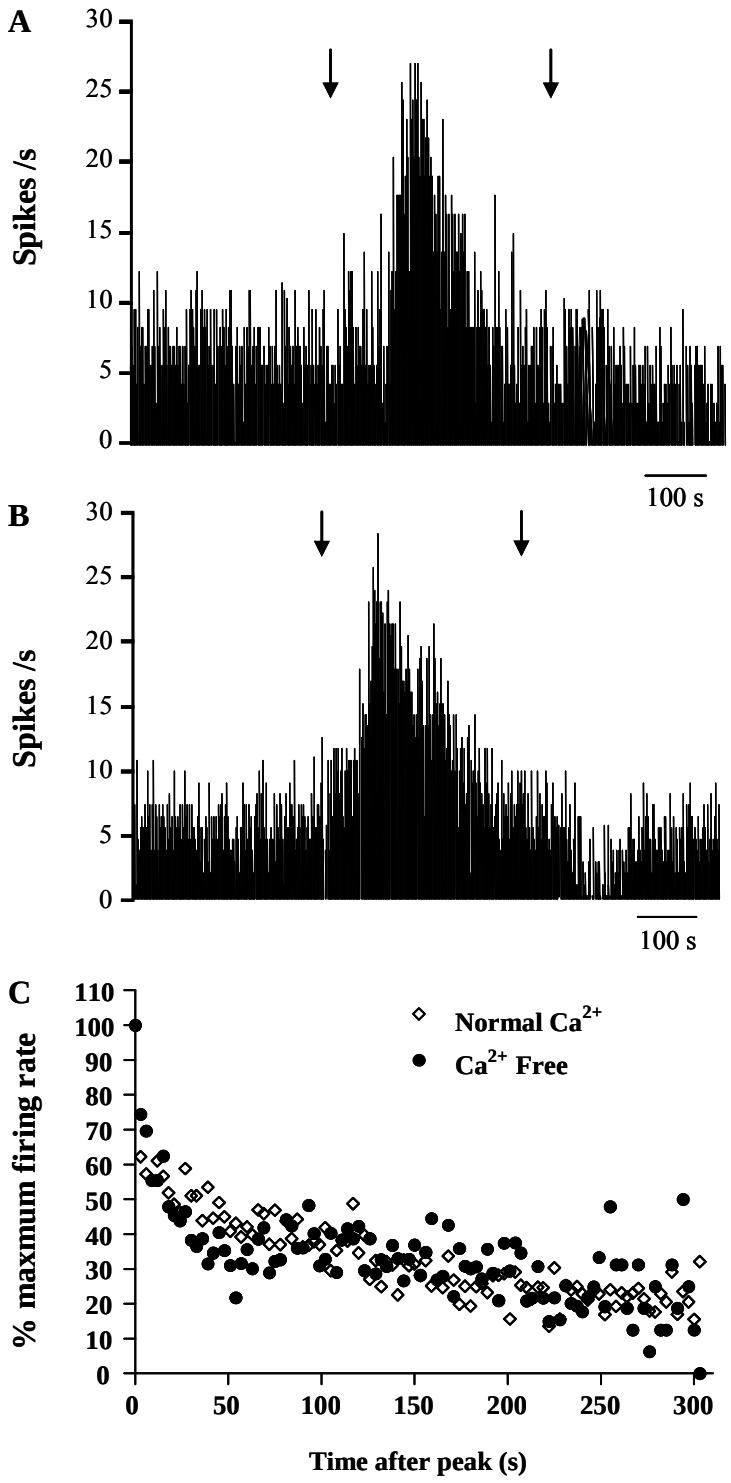

Figure 25: The vagal afferents of gastric fundus respond to anti-HuD and anti-HuD in Ca^{2+} -free Krebs buffer. (A) The trace shows an example of the vagal afferents responding to local application of anti-HuD. (B) The trace shows an example of the vagal afferents responding to local application of anti-HuD in Ca^{2+} -free Krebs buffer. (C) Time after peak course of the vagal afferent response to anti-HuD and anti-HuD in Ca^{2+} -free Krebs buffer. Data as % increase above baseline was shown every three second period during the late phase of desensitizing response. The time course of desensitizing response phase did not differ significantly in calcium free Krebs buffer (unpaired Student's *t-test, P* =0.99).

Table 11: The percentage of units responding that are responsive to the various agents applied to the mechanosensitive "hot spots".

	Units responding	peak increase (Spikes/s) median[25th/75th]	% units responding	Mice/hot spots/units
anti-HuABC	5	2.7[2.3/3.6]	41.0%	4/6/12
ATP	3	7.8[5.3/18.1]	60.0%	3/4/5
DMPP	26	12.2[5.5/17.8]	68.4%	13/25/38
anti-HuD	18	18.3[11.0/27.5]	90.0%	11/15/20
anti-HuD in Ca^{2+} freee	9	15.2[9.9/33.6]	100.0%	5/6/9

Table 12: Latency of units responding that are responsive to the various agents applied to the mechanosensitive "hot spots".

Latency	**From deliver drugs to firing rate increase by 20% above baseline (s)**	**From delivery of drugs to peak (s)**
ATP	15.7[6.4/16.7] (n=3)	19.2[8,5/21.5] (n=3)
DMPP	8.2[5.1/17.7] (n=26)	13.8[8.6/23.2] (n=26)
anti-HuD	21.5[10.4/37.4] (n=18)*	65.0[40.6-123.0] (n=18)*
anti-HuD in Ca^{2+} Free	19.7[10.2/48.4] (n=9)*	60.6[32.7/151.5] (n=9)*

Kruskal–Wallis one-way analysis of variance on ranks follow by the Dunn's method, *significantly different from DMPP, $P < 0.0$

Table 13: Characteristics of the study participants.

	Sample	Guinea pig myenteric neurons				Human submucous neurons			
		RN[%]	**SF[*Hz*]**	**NI[%×*Hz*]**	**T/G/N**	**RN[%]**	**SF[*Hz*]**	**NI[%×*Hz*]**	**T/G/N**
α3-AchR	4	0.0[0.0/17.3]	2.4[1.9/3.0]	0.0[0.0/43.6]	3/6/156	45.2[6.3/67.1]	3.2.3[1.8/5.6]	115.9[3.7/325.1]	4/8/62
	5	0.0[0.0/13.9]	3.0[2.4/3.9]	0.0[0.0/43.8]	2/5/94	33.3[0.0/80.9]	4.5[2.4/7.2]	116.2[0.0/458.7]	4/4/32
	8	27.7[11.4/46.9]	1.7[1.3/2.6]	70.9[21.6/98.2]	5/10/292	71.4[56.3/90.0]	5.4[2.3/7.4]	534.1[145.9/584.9]	3/5/40
	11	0.0[0.0/0.0]	0.0[0.0/0.0]	0.0[0.0/0.0]	2/5/119	0.0[0.0/48.2]	2.4[1.5/2.9]	0.0[0.0/117.6]	3/4/30
	16	0.0[0.0/17.5]	2.2[1.3/5.2]	0.0[0.0/77.1]	3/10/227	0.0[0.0/54.5]	2.9[1.5/3.9]	0.0[0.0/153.8]	2/3/32
	19	4.2[0.0/16.2]	1.7[1.0/2.6]	6.3[0.0/34.6]	2/6/152	85.7[50.0/87.5]	4.2[1.8/5.9]	351.8[118.7/385.8]	3/7/58
	Σ=6	**7.1[4.2/13.6]**	**2.3 ± 1.2**	**18.3[12.7/36.8]**	**17/42/1040**	**39.7[17.7/70.9]**	**3.9 ± 1.1**	**169.9[47.9/317.9]**	**19/31/254**
ANNA-1	2	19.1[0.0/30.1]	1.7[1.3/2.8]	28.7[0.0/82.4]	3/6/147	75.0[63.6/83.3]	3.6[1.8/4.7]	167.3[163.2/420.4]	2/3/31
	3	0.0[0.0/11.4]	1.9[0.9/4.1]	0.0[0.0/16.3]	3/9/290	69.7[59.5/76.5]	2.9[2.4/5.3]	245.2[206.1/407.2]	2/4/40
	9	14.0[5.4/32.9]	1.5[0.9/2.6]	9.3[0.0/24.9]	4/8/199	11.5[0.0/38.1]	1.8[1.2/2.2]	20.5[0.0/61.2]	4/6/42
	10	4.0[0.0/48.4]	2.2[1.3/3.0]	0.0[0.0/50.7]	4/8/171	12.5[0.0/42.9]	1.8[1.8/3.6]	37.1[0.0/108.5]	2/5/52
	14	0.0[0.0/18.2]	2.6[1.9/3.9]	0.0[0.0/53.0]	4/11/325	66.1[51.5/85.7]	4.2[2.4/7.1]	292.3[153.8/484.1]	5/6/58
	17	0.0[0.0/0.0]	0.9[0.9/1.2]	0.0[0.0/0.0]	2/7/191	53.6**[**0.0/62.9]	1.2[1.2/2.1]	80.5[0.0/99.4]	4/6/48
	20	0.0[0.0/23.4]	2.6[1.9/3.9]	0.0[0.0/66.9]	3/8/203	51.2[38.3/100.0]	4.2[2.8/6.1]	292.3[153.8/484.1]	3/6/33
	Σ=7	**11.0[5.4/20.0]**	**2.3 ± 0.7**	**33.0[16.2/42.7]**	**23/57/1526**	**60.6[19.6/68.6]**	**3.2 ± 1.2**	**260.7[50.9/266.4]**	**22/36/304**
PC	1	0.0[0.0/1.3]	0.6 ± **0.3**	0.0[0.0/0.5]	3/8/311	0.0[0.0/0.0]	0.0	0.0[0.0/0.0]	3/4/24
	6	0.0[0.0/8.8]	1.7 ± **0.4**	0.0[0.0/15.5]	2/6/147	25.0[0.0/39.3]	1.5 ± 1.1	37.1[4.9/48.6]	2/3/31
	7	0.0[0.0/0.0]	0.0	0.0[0.0/0.0]	2/4/100	3.6[0.0/0.0]	2.1 ± 0.3	8.5[0.0/79.9]	3/4/43

	12	0.0[0.0/0.0]	0.0	0.0[0.0/0.0]	2/7/189	0.0[0.0/0.0]	0.0	0.0[0.0/0.0]	2/3/24
	13	0.0[0.0/4.2]	1.7 ± 0.0	0.0[0.0/7.2]	2/5/160	0.0[0.0/37.5]	1.9 ± 0.8	0.0[0.0/72.3]	3/4/42
	15	0.0[0.0/0.0]	0.0	0.0[0.0/0.0]	2/7/191	0.0[0.0/30.9]	1.5 ± 0.9	0.0[0.0/44.7]	3/5/29
	18	0.0[0.0/0.0]	0.0	0.0[0.0/0.0]	3/6/163	24.3[12.5/46.2]	1.2 ± 0.3	30.5[14.8/55.1]	5/6/39
	Σ=7	**0.0[0.0/0.0]**	**1.7[0.9/1.7]**	**0.0[0.0/0.0]**	**16/43/1261**	**0.0[0.0/27.9]**	**1.2[1.2/2.4]**	**0.0[0.0/36.4]**	**21/29/232**
HC	21	0.0[0.0/6.9]	1.3[1.3/1.3]	0.0[0.0/8.9]	2/3/71	0.0[0.0/0.0]	0.0	0.0[0.0/0.0]	2/4/27
	22	0.0[0.0/7.4]	0.4[0.4/1.1]	0.0[0.0/5.2]	2/5/143	0.0[0.0/11.1]	0.6 ± 0.0	0.0[0.0/6.6]	2/3/21
	23	0.0[0.0/0.0]	0.0	0.0[0.0/0.0]	2/5/111	9.1[0.0/20.0]	1.4 ± 0.3	10.8[0.0/27.7]	2/3/30
	24	0.0[0.0/5.9]	2.2[0.9/3.0]	0.0[0.0/3.6]	3/8/216	11.1[0.0/22.2]	1.5 ± 1.3	16.5[0.0/32.9]	2/2/15
	25	0.0[0.0/2.9]	0.9[0.9/1.3]	0.0[0.0/3.8]	4/9/269	15.0[0.0/32.5]	1.4 ± 0.6	20.8[0.0/45.0]	2/4/34
	Σ=5	**0.0[0.0/5.8]**	**1.3[0.9/2.2]**	**0.0[0.0/3.5]**	**13/30/810**	**0.0[0.0/17.8]**	**1.5[0.6/1.8]**	**0.0[0.0/23.5]**	**10/16/127**
PC&HC	Σ=12	**0.0[0.0/0.0]**	**1.3[0.9/1.7]**	**0.0[0.0/0.0]**	**29/73/2071**	**0.0[0.0/23.6]**	**1.2[1.2/1.8]**	**0.0[0.0/30.3]**	**31/45/359**
Σ PC&HC	Σ=12	**1.2[0.0/2.9]**	**0.7 ± 0.8**	**1.2[0.0/2.9]**	**29/73/2071**	**11.7[0.9/15.4]**	**1.1 ± 0.8**	**17.6[0.5/28.5]**	**31/45/359**

NOTE. RN[%]: percent of neurons responding; SF (*Hz*): spike frequency; NI[%×Hz]: the neuroindex which is the product of action potential frequency and proportion of responding neurons M±SD: mean value ± standard deviation; Median, 25th-75th, median values with the 25% and 75% quartiles; PC: patient control; HC: healthy control. T/G/N: numbers of tissues, ganglia, neurons. Comparisons were performed with ANOVA followed by Dunn's Method and Student-Newman-Keuls Method.

4. Discussion

This is the first study describing that IgG samples from sera of patients with autoimmune GI disorder elicit activation of enteric neurons and vagal afferents. This study revealed four major findings. Firstly, sera from patients with paraneoplastic GI syndromes containing α3-AchR or ANNA-1 antibodies but not sera from healthy controls evoke a fast onset spike discharge in a substantial proportion of guinea pig and human enteric neurons. Secondly, the excitatory action of anti-ANNA-1 containing sera in enteric neurons is mainly caused by anti-HuD and to a lesser extent by anti-HuA/B/C antibodies. However, only anti-HuD exerted an excitatory action in vagal afferents. The effect of the antibodies was reproducible and could not be explained by natural variations of spontaneous activity of the neurons. Thirdly, both HuD as well as HuA/B/C antibodies label neuronal somata in the ENS. Fourthly, there was no correlation between the concentration of the α3-AchR or ANNA-1 antibodies and the level of activation in the ENS.

The concept that autoimmune mechanisms contribute to the clinical manifestations of autoimmune GI disorder is supported by the detection of circulating antibodies that target enteric neurons in patients with these disorders (Kashyap and Farrugia, 2008; DiBaise, 2011). This theory is supported in autoimmune GI disorder by the findings that antineuronal antibodies exist in sera from autoimmune GI disorder patients. We used sera IgG samples from patients with autoimmune GI disorder in immunohistochemistry to label whole mount preparations of ileum of the guinea pig for testing circulating antineuronal antibodies.

ANNA-1 recognizes the nuclear and cytoplasmatic binding protein Hu. Except for HuA which is ubiquitously expressed in extraneuronal tissues, the Hu proteins are specifically detected in the neurons of the central, peripheral and enteric nervous system but not in other cell types (with the possible exception of the testes) (Dalmau and Posner, 1999). The Hu proteins have been implicated in multiple aspects of neuronal function, including the commitment and differentiation of neuronal precursors, as well as synaptic remodeling in mature neurons (Posner and Dalmau, 1997). In our study, the immunoreactivity results show that many neurons were labeled by human ANNA-1 autoantibody in all seven IgG samples and by the α3-AchR in two out of six samples while the control samples stained virtually no structures in the guinea pig myenteric plexus.

Our immunohistochemistry study in guinea pig myenteric neurons showed that immunostaining of the enteric neurons by HuD antibody was different from HuA/B/C antibodies. The results indicate that all neurons in the myenteric plexus of guinea pig were

specifically labeled by the anti-HuD antibody. In contrast with the finding of the anti-HuD antibody, the anti-HuA/B/C antibodies labeled neurons and nerve fibres. These experimental data may indicate that the expression pattern of HuD is different to HuB or HuC in the enteric neurons. The data reported here support the observation that ANNA-1 antineuronal antibodies that target enteric neurons are present in the sera of paraneoplastic GI dysmotility patients.

We mainly focused on the actions of antineuronal antibodies, specifically α3-AchR, ANNA-1 of sera IgG samples and purified anti-HuD and anti-HuA/B/C antibodies from patients with autoimmune GI disorders.

Pathologically, paraneoplastic enteric neuropathy has been associated with inflammatory destructive processes affecting myenteric ganglia of the gut. In postmortem or surgical samples of the gut, the enteric plexus shows reduction in neurons and axons, and lymphocytic infiltration (Chinn et al., 1988). For example, in ANNA-1 associated pseudo obstruction, abnormalities are generally confined at the myenteric plexus. Smooth muscle and the submucosal plexus are often normal (Jun et al., 2005).

In this study the α3-AchR IgG sera samples isolated from patients consistently had an immediate excitatory effect on guinea pig myenteric neurons and human submucosal neurons. These results were reproducible in the α3-AchR IgG samples from six different patients but they did not show a concentration correlation with excitatory action on the neurons. Importantly, under identical conditions, IgG from control patients caused a significantly weaker activation in a lower proportion of neurons. Our observations demonstrated that human sera α3-AchR samples from patients have direct excitatory effects on enteric neurons in vitro.

The α3-type ganglionic AChR mediates fast synaptic transmission in the whole peripheral autonomic nervous system and it is homologous but immunologically distinct from the AChR at the neuromuscular junction (Vernino, 2008). The AchR antibody is one of the membrane receptor antibodies that can be found in patients with both paraneoplastic and non-paraneoplastic disorders. The ganglionic AchR antibody targeting this protein can disrupt cholinergic synaptic transmission leading to autonomic failure (Vernino et al., 1998). Unlike the other paraneoplastic antibodies, these membrane receptor antibodies are each associated with a particular neurological disorder. It has been shown that AchR antibodies can reach their targets on intact neurons, so they have a great potential to directly affect neuronal function (Vernino, 2009). For some disorders, there is convincing evidence of an antibody-mediated pathophysiology. The reduction of the AchR antibody level is going along with clinical improvement, as symptoms improve after plasma exchange or other immunotherapies

(Vernino et al., 2000; Klein et al., 2003, Schroeder C et al., 2005). Symptoms of autonomic failure can also be induced experimentally by passive transfer of antibodies. Mice that were injected with rabbit IgG containing neuronal nicotinic AChR antibodies develop gastrointestinal dysmotility and autonomic dysfunction. Similar results are obtained by injecting mice with sera from patients with ganglionic α3-AchR antibody. The pathogenicity of α3-AChR antibody was also demonstrated in rabbits immunized with a recombinant extracellular fragment of the α3-AChR subunit (Vernino, 2004).

Other evidence indicate that antibodies (IgG) isolated from sera of patients with autoimmune autonomic ganglionopathy directly affect ganglionic AChR in vitro. When cultured IMR-32 human neuroblastoma cells are exposed to ganglionic AChR IgG up to 80 minutes, the amplitude of neuronal AChR membrane currents was progressively reduced. The characteristics and time course of this AChR inhibition suggest that these AChR antibodies act by binding and cross-linking the receptors leading to active internalization (Wang et al., 2007). Wang Z et al. found in a recent study after passive transfer of serum AChR IgG to mice a decrease of EPSP amplitude or even a total block in isolated mouse superior cervical ganglia (Wang et al., 2010). This would suggest that the AChR antibodies strongly inhibit neurons. In contrast, we found that sera AChR IgG samples evoked an immediate excitatory effect on a subpopulation of neurons. There is, however, an important difference in the experimental design between the two studies. While Wang et al. used a long term exposure of the antibodies and reported only late onset changes; we applied the antibodies for 400 ms and recorded the immediate response. Studies with autoantibodies directed against glutamate receptors have shown an excitotoxic effect of these autoantibodies. These effects were either mediated by a facilitation of the normal excitatory action of glutamate or a direct excitatory effect of the autoantibodies (Faust et al., 2010, Levite et al., 1999). It can be concluded that the effect (excitatory, inhibitory, toxic) of neuronal autoantibodies is not only determined by the type of autoantibody and the localization of the antigene (intracellular or on the cell surface) but also by the duration of the exposition of the target cells to the antibody (Lancaster et al., 2011).

Intriguingly, our results revealed that ANNA-1 IgG samples isolated from patients with paraneoplastic GI dysmotility, which is associated with SCLC, had similar direct excitatory effects on guinea pig myenteric neurons and human submucosal neurons. All ANNA-1 IgG samples had similar effects on spike frequency and the proportion of activated neurons, whereas PC and HC samples had negligible effects. The pathogenesis of paraneoplastic neurological syndromes is thought to be related to autoimmune processes. In patients with

SCLC and dysmotility of the bowel increased levels of circulating antineuronal autoantibodies are found, supporting this theory. SCLC is the most common cancer associated GI dysmotility (Kiers et al., 1991). The tumor that prevalently expresses ANNA-1 is SCLC. It is reported that more than 80% of adult patients with ANNA-1 antibodies will have cancer, usually SCLC (Pittock et al., 2004). Other tumors that may express ANNA-1 include breast, prostate, ovarian carcinomas, and lymphomas (Lucchinetti et al., 1998). Consequential ANNA-1 is the most identified antineuronal autoantibody in patients with SCLC associated paraneoplastic GI dysmotility (Kashyap and Farrugia, 2008; DiBaise, 2011). Although the neurologic syndromes may develop at any time during the course of the disease the symptoms are often evident up to one year prior to diagnosis of lung cancer (Pittock et al., 2004). This finding gives a new possibility for early diagnosis of cancer, because the presence of ANNA-1 antibodies gives a hint to the development of lung cancer.

Although there is a strong association between the presence of an occult or manifest tumor and antineuronal antibodies in the setting of gastrointestinal dysmotility disorders, the exact mechanism by which these ANNA-1 antibodies are generated remains unclear (Kashyap and Farrugia, 2008). It is postulated that aberrant expression of neuronal antigens by tumor cells is leading to an autoimmune response against the myenteric and submucous plexus (Dropcho, 2002; De Giorgio et al., 2004). However, the precise mechanism by which ANNA-1 antibodies cause enteric neuronal dysfunction is not known. We found that ANNA-1 IgG samples from patients with paraneoplastic GI dysmotility evoked a significantly higher rate of action potential discharge and activated higher percentage of neurons compared with control sera samples. The results suggest that serum ANNA-1 antibodies can be directly excitatory to enteric neurons and may play a pathogenic role in paraneoplastic GI dysmotility. It has been shown previously that ANNA-1 antibodies alter ascending reflex pathway of peristalsis in isolated guinea pig ileum in vitro preparations (Caras et al., 1995). These evidences have indicated that antibodies may exert a direct functional effect and impair enteric neuronal circuitries. On the other hand, previous reports concerning direct pathogenic role of ANNA-1 antineuronal antibodies were inconsistent. For example, passive transfer of these antibodies or immunization has failed to reproduce the disease in animals (Sillevis Smitt et al., 1995) and in vitro studies have found toxic effects as well as no effects on primary cultures from the guinea pig myenteric plexus and mouse brain, respectively (de Giorgio et al., 2003, Tanaka et al., 2004). There is also a report that found a toxic effect of anti-Hu serum but attributes this effect rather to an unknown soluble factor different from the antibodies as it was still present in IgG depleted serum (Verschuuren et al., 1997). These discrepancies may be due to

differences in study design but underline also the importance of the present study with human neurons. However, we are not able to conclude if the excitatory effect that we found is related to toxicity or if both effects are unrelated.

In order to further test whether the IgG fractions of patients with paraneoplastic GI dysmotility and high ANNA-1 titers have an excitatory effect on enteric neurons, we used myenteric plexus preparations of the guinea pig, which are a suitable source for the investigation of effects on enteric neurons. We found that the affinity purified fraction of anti-HuD antibodies and the rest fraction of anti-HuA/B/C antibodies IgG produced a marked neuronal activation, demonstrating an ANNA-1 antibody effect on enteric neurons mediated by anti-HuD and anti-HuA/B/C antibodies. Anti-HuD antibodies evoked a stronger response in a higher percent of neurons with a high action potential frequency compared to anti-HuA/B/C antibodies. It is noteworthy that we found four types of neurons responding to these autoantibodies: a high proportion of neuron responded to anti-HuD; a smaller group of neurons responded to anti-HuA/B/C; neurons that responded to both; and neurons that did not respond to any of the substances. Neuronal excitation was further confirmed by blood donor sera and HuD protein application as controls. Control applications excited only very few neurons with a low action potential discharge. These findings would imply that the anti-HuD antibodies act on different targets than the anti-HuA/B/C antibodies.

As described above, the most striking result was that anti-HuD antibody evoked a prominent response characterized by marked hyperexcitability in a large proportion of myenteric neurons. Importantly, other studies have shown that anti-HuD antibodies can alter neuronal function. Anti-HuD positive sera from patients with a paraneoplastic GI dysmotility disorder as well as commercial anti-HuD antibodies induced apoptosis through caspase-3 activation both in a human neuroblastoma cell line (SH-Sy5Y) and in guinea pig cultured myenteric neurons, suggesting that anti-HuD antibodies may contribute to ENS impairment and related gut motor disorders (De Giorgio et al., 2003). In other studies anti-Hu sera react with HuD, HuC and HuB, however from the three antigens only HuD is expressed in SCLC. Thus, HuD plays the main role in triggering the immune response (Senties-Madrid and Vega-Boada, 2001). All of these findings taken together indicate that anti-HuD antibodies play a major role in evoking neuronal damage underlying severe paraneoplastic GI dysmotility.

Our data showed that binding of sera IgG antibodies or purified anti-HuD and anti-HuA/B/C antibodies alone, in the absence of the complement, exert a direct functional effect and impair enteric neuronal circuitries. Exactly how these antibodies bind to enteric neurons is unclear, because the epitopes against which the antibody is directed are believed to be not expressed in

the cell membrane. It is therefore unknown whether an extracellular epitope may react with the antibody. The fast onset of the the response to the antibodies within ms would support the idea that the antibodies bind to an extracellular epitope. It cannot be totally excluded that the antibodies bind directly to ion channels and thereby activate neurons. Likely candidates would be sodium, calcium or potassium channels. In this case however, one would expect that the excitatory effect would be more general and not confined to a limited percentage of neurons as in our experiments.

Further possible sites of interaction that would explain our results are neurotransmitter receptors. In preliminary experiments from our laboratory we found evidence that the sera IgG and anti-HuD evoked response of enteric neurons was blocked by hexamethonium and may therefore be mediated by nicotinic acetylcholine receptors. The results in vagal afferents, where fibers with as well as without nicotinic receptors responded to anti-HuD would then suggest a different mode of action in enteric neurons and vagal afferents. These results have to be verified in further experiments.

Finally, it could be also possible that the antibodies interact with Fcγ receptors on the surface of enteric neurons. Although these receptors have so far not been demonstrated on enteric neurons, a recent report found functional Fcε receptors on mouse myenteric neurons. Additionally it has been found that the high affinity IgG receptor FcγRI was expressed on mouse primary sensory neurons and that it was activated by IgG-antigen complex. (Andoh and Kuraishi, 2004; van der Kleij et al., 2010; Qu et al., 2011). We were not able to test the presence of IgG-antigen complexes in our samples

It is generally assumed that enteric ganglia are protected by a blood-ganglion barrier that resembles the blood-brain barrier, and one may wonder how circulating antibodies and antibody-antigen complex get access to the neurons. One possibility is that activation of the immune system may result in a break down of the blood-ganglion barrier followed by antibody and antibody-antigen complex deposition within the ganglion. The alteration of the blood-ganglion barrier makes it plausible that neuronal autoantibodies may reach their target and deposits of autoantibodies in the neruons (Senties et al., 2001; De Giorgio et al., 2003).

There exists a correlation between the anti-HuD antibody level and the clinical course of paraneoplastic neurological symptoms (Rauer et al., 2002). Neuronal nicotinic acetylcholine receptor antibodies levels correspond to the severity of autonomic dysfunction, and a decrease in their level is accompanied by clinical improvement (Vernino et al., 2000). However, the present study showed no correlation between the concentration of the α3-AchR or ANNA-1

samples and the percentage of responding neurons or action potential frequency. This may be due to the relatively low number of samples used in our study.

We furthermore showed in our study that the excitatory effects of patient´s sera and blood donor sera were stronger than HC in guinea myenteric neurons. A likely reason may be that patients and blood donor sera containing more mediators than HC. Beause the IgG samples HC belong to affinity-purified IgG that was isolated from healthy serum by adsorption to protein, whereas the patients and blood donor sera induced activation of enteric neurons involved multiple mediators with interactions among these mediators.

To summarize our data above and current knowledges, we speculate there is a blood-ganglion barrier breakdown and antibody deposition in neurons that play a role in the pathogenesis of paraneoplastic GI dysmotility patients (De Giorgio et al., 2003). First of all, the enteric neurons are excited but not inhibited by these antibodies. The data that showed an immediate response to the antibodies within millisecnds support the idea of selectively binding to specific receptors or channels. The antibodies elicit hyperexcitability and impair enteric neuronal circuitries. Furthermore the ENS is exposed to elevated levels of the antibodies, it is possiple that antibodies enter neurons and bind to antigens, thereby further altering neuronal function and result in clinical symptoms. This is also supported by the experimental data that after long term exposure to anti-Hu antibodies sera from patients with a paraneoplastic GI dysmotility disorder induced apoptosis through caspase-3 activation both in a human neuroblastoma cell line (SH-Sy5Y) and in guinea pig cultured myenteric neurons (De Giorgio et al., 2003). In addition, the neurotoxicity in enteric neurons can be caused by excessive exposure to glutamate, or related agonists (Kirchgessner et al., 1997). We speculate that prolonged stimulation with antibodies induces overactivation and increases the intracellular concentration of Ca^{2+} ions that causes necrosis and apoptosis in enteric neurons. These findings supported the idea that activation of the apoptotic cascade was responsible for enteric neurodegeneration and for damaged areas of the ENS and in turn contribute to the neurologic dysfunction in paraneoplastic GI dysmotility.

Vagal mechanosensitive receptive fields, so called hot spots, can be located by probing with calibrated von Frey hairs. Most units were tested for sensitivity to DMPP (nicotinic receptor agonist) and/or ATP. Consistent with previous experiments, ATP excited vagal endings innervating the stomach and esophagus through action on P2X receptors (Page et al., 2000; Page et al., 2002). DMPP excited the majority of hot spots (Jiang et al., 2002; Beyak and Grundy, 2004). Functional studies indicate the presence of these channels on IGLE mechanosensitive endings (Beyak and Grundy, 2004). Our results show for the first time that

the purified anti-HuD, but not anti-HuA/B/C antibodies caused an increase in firing rate of mechanosensitive vagal fibers. Anti-HuD had a significantly stronger excitatory action than DMPP and ATP and in addition activated more hot spots than DMPP and ATP. These results suggest that the anti-HuD in these receptive fields effect is independent of nicotinic or purinergic receptor activation.

The FcγRI is expressed on primary sensory neurons and nerves and it was shown that the FcγRI is able to directly respond to stimulation with antibody-antigen complex (van der Kleij et al., 2010; Qu et al., 2011). An intradermal injection of the antigen formed IgG-antigen-complex on nerve fibers and caused itch-associated responses (Andoh and Kuraishi, 2004). Thus, it is possible that the formation of Anti-HuD-HuD protein complex activates vagal afferents through FcγRI in mice of gastric fundus.

The finding that the response to anti-HuD remained in depleted calcium buffer argues for a direct effect of anti-HuD on vagal afferents and at the same time suggests that extracellular calcium influx is not crucial for activation of vagal afferents by anti-HuD.

Surprisingly, anti-HuA/B/C did not activate vagal afferents, whereas it excites enteric neurons although to a lesser degree than anti-HuD. We have no final explanation for this difference but species differences, different concentrations of the antibody-antigen complexes or lack of binding sites at vagal afferent terminals may be considered.

All in all the results showed that sera IgG isolated from patients with severe paraneoplastic GI dysmotility causes activation of both enteric neurons and vagal afferents. This effect likely involves the nicotinic acetylcholine receptors and FcγRI activation. These results show that humoral autoimmunity may generate immuno-neural signaling in enteric and vagal mechanosensory neurons which may contribute to the pathophysiology of gastrointestinal motility disorders.

References

Albert ML, Austin LM, Darnell RB: Detection and treatment of activated T cells in the cerebrospinal fluid of patients with paraneoplastic cerebellar degeneration. *Ann Neurol* 2000; 47: 9-17.

Albert ML, Darnell JC, Bender A, Francisco LM, Bhardwaj N, Darnell RB: Tumor-specific killer cells in paraneoplastic cerebellar degeneration. *Nat Med* 1998, 4:1321-1324.

Andoh T, Kuraishi Y. Direct action of immunoglobulin G on primary sensory neurons through Fc gamma receptor I. *FASEB J* 2004 Jan; 18(1): 182-4. Epub 2003 Nov 20.

Andrews PL, Grundy D, Scratcherd T. Vagal afferent discharge from mechanoreceptors in different regions of the ferret stomach. *J Physiol* 1980; 298: 513-24.

Andrews PLR. Vagal afferent innervation of the gastrointestinal tract. *Progress in Brain Research* 1986; 67: 65-86.

Bayliss, WM; Starling, EH. The movements and innervation of the large intestine. *The Journal of Physiology* 1900; 26: 107-118.

Bayliss, WM; Starling, EH. The movements and innervation of the small intestine. *The Journal of Physiology* 1899; 24: 99-143.

Beckstead RM and Norgren R. An autoradiographic examination of the central distribution of the trigeminal, facial, glossopharyngeal, and vagal nerves in the monkey. *J Comp Neurol* 1979; 1; 184(3): 455-72.

Berthoud HR, Blackshaw LA, Brookes SJ, Grundy D. Neuroanatomy of extrinsic afferents supplying the gastrointestinal tract. *Neurogastroenterol Motil* 2004; (16 Supp 1): 28-33.

Berthoud HR, Carlson NR, Powley TL. Topography of efferent vagal innervation of the rat gastrointestinal tract. *Am J Physiol* 1991; 260: R200-R207.

Berthoud HR, Neuhuber WL. Functional and chemical anatomy of the afferent vagal system. *Auton Neurosci* 2000; 20; 85(1-3): 1-17.

Berthoud HR, Patterson LM, Neumann F, Neuhuber WL. Distribution and structure of vagal afferent intraganglionic laminar endings (IGLEs) in the rat gastrointestinal tract. *Anat Embryol (Berl)* 1997;195: 183-191.

Berthoud HR, Powley TL. Vagal afferent innervation of the rat fundic stomach: morphological characterization of the gastric tension receptor. *J Comp Neurol* 1992; 319: 261-276.

Beyak MJ and Grundy D. Nicotinic Agonists Activate Mouse Gastric Vagal Afferents *in vitro*. *Gastroenterology* 2004; 126: 838(A).

Blackshaw LA, Brookes SJ, Grundy D, Schemann M. Sensory transmission in the gastrointestinal tract. *Neurogastroenterol Moti.* 2007; 19 (1 Suppl): 1-19.

Bornstein JC, Costa M, Grider JR. Enteric motor and interneuronal circuits controlling motility. *Neurogastroenterol Moti.* 2004;16 Suppl 1: 34-8.

Breunig E, Michel K, Zeller F, Seidl S, Weyhern CW, Schemann M. Histamine excites neurones in the human submucous plexus through activation of H1, H2, H3 and H4 receptors. *J Physiol* 2007; 1; 583(Pt 2): 731-42.

Brookes SJ., Meedeniya AC, Jobling P and Costa M. Orally projecting interneurones in the guinea-pig small intestine. *J Physiol (London)* 1997; 505: 473-491.

Bruley des Varannes S, Chevalier J, Pimont S, Le Neel J-C, Klotz M, Schafer K-H et al. Serum from achalasia patients alters neurochemical coding in the myenteric plexus and nitric oxide mediated motor response in normal human fundus. *Gut* 2006; 55 (3): 319-326.

Buhner S, Li Q, Vignali S, Barbara G, De Giorgio R, Stanghellini V, Cremon C, Zeller F, Langer R, Daniel H, Michel K, Schemann M Activation of human enteric neurons by supernatants of colonic biopsy specimens from patients with irritable bowel syndrome. *Gastroenterology* 2009; 137(4): 1425-34

Campos AR, Grossman D, White K. Mutant alleles at the locus elav in Drosophila melanogaster lead to nervous system defects. A developmental-genetic analysis. *J Neurogenet* 1985; 2: 197- 218

Caras SD, McCallum RW, Brashear HR, et al. The effect of human antineuronal antibodies on the ascending excitatory reflex and peristalsis in isolated guinea pig ileum. *American Journal of Gastroenterology* 1995; 110: A643.

Castelucci P, Robbins HL, Furness JB. P2X(2) purine receptor immunoreactivity of intraganglionic laminar endings in the mouse gastrointestinal tract. Cell Tissue *Res* 2003; 312: 167-174.

Cervero F and Sharkey KA. An electrophysiological and anatomical study of intestinal afferent fibers in the rat. *J Physiol (London)* 1988; 401: 381-397.

Chinn JS, Schuffler MD. Paraneoplastic visceral neuropathy as a cause of severe gastrointestinal motor dysfunction. *Gastroenterology* 1988; 95: 1279-1286

Chung S, Jiang L, Cheng S, Furneaux H. Purification and properties of HuD, a neuronal RNA-binding protein. *J Biol Chem* 1996; 271:11518-11524.

Clerc N, Furness JB, Bornstein JC and Kunze WAA. Correlation of electrophysiological and morphological characteristics of myenteric neurons of the duodenum in the guinea-pig. *Neuroscience.* 1997; 82: 899-914.

Collins SM. The immunomodulation of enteric neuromuscular function: implications for motility and inflammatory disorders. *Gastroenterology* 1996; 111: 1683-1689.

Condom E, Vidal A, Rota R, et al. Paraneoplastic intestinal pseudo-obstruction associated with high titer of Hu autoantibodies. *Virchows Arch Pathol Anat* 1993; 423: 507-11.

Corey DP and Hudspeth AJ. Kinetics of the receptor current in bullfrog saccular hair cells. *J Neurosci* 1983; 3(5): 962-76.

Costa M, Brookes SJH, Hennig GW. Anatomy and physiology of the enteric nervous system. *Gut* 2000; 47(Suppl. 4): 15-9.

Crowe R, Kamm MA, Burnstock G, Lennard-Jones JE. Peptide-containing neurons in different regions of the submucous plexus of human sigmoid colon. *Gastroenterology* 1992 102(2): 461-7.

Dalmau J, Furneaux HM, Gralla RJ, Kris MG, Posner JB.Detection of the anti-Hu antibody in the serum of patients with small cell lung cancer--a quantitative western blot analysis. *Ann Neurol* 1990; 27: 544-552.

Dalmau J, Graus F, Rosenblum MK, Posner JB. Anti-Hu--associated paraneoplastic encephalomyelitis/sensory neuronopathy. A clinical study of 71 patients. *Medicine (Baltimore)* 1992; 71: 59-72

Dalmau J, Gultekin HS, Posner JB. Paraneoplastic neurologic syndromes: pathogenesis and physiopathology. *Brain Pathol* 1999; 9(2): 275-84

Dalmau JO, Posner JB. Paraneoplastic syndromes. *Arch Neurol* 1999; 56(4): 405-8.

Darnell RB, Posner JB. Paraneoplastic syndromes affecting the nervous system. *Semin Oncol* 2006; 33 (3): 270-98.

Darnell RB, Posner JB. Paraneoplastic syndromes involving the nervous system. *N Engl J Med* 2003; 349: 1543-1554.

De Giorgio R, Barbara G, Stanghellini V, et al. Idiopathic myenteric ganglionitis underlying intractable vomiting in a young adult. *Eur J Gastroenterol Hepatol* 2000; 12(6): 613-6.

De Giorgio R, Bovara M, Barbara G, Canossa M, Sarnelli G, De Ponti F, Stanghellini V, Tonini M, Cappello S, Pagnotta E, Nobile-Orazio E, Corinaldesi R. Anti-HuD-induced neuronal apoptosis underlying paraneoplastic gut dysmotility. *Gastroenterology* 2003; 125 (1): 70-79.

De Giorgio R, Guerrini S, Barbara G, et al. Inflammatory neuropathies of the enteric nervous system. *Gastroenterology* 2004; 126: 872-83.

De Giorgio R, Stanghellini V, Barbara G, et al. Primary enteric neuropathies underlying gastrointestinal motor dysfunction. *Scand J Gastroenterol* 2000; 35(2): 114-22.

DeLellis RA, Xia L. Paraneoplastic endocrine syndromes: a review. *Endocr Pathol* 2003; 14(4): 303-17.

Dhamija R, Meng Tan K, Pittock SJ, et al. Serologic profiles aiding the diagnosis of autoimmune gastrointestinal dysmotility. *Clin Gastroenterol Hepatol* 2008; 6: 988-92.

DiBaise JK. Paraneoplastic gastrointestinal dysmotility: when to consider and how to diagnose. *Gastroenterol Clin North Am* 2011; 40(4): 777-86.

Dogiel AS. Uber den bau der ganglien in den geflechten des darmes und der gallenblase des menschen und der säugetiere. *Arch Anat Physiol (Leipzig Anat Abt Jg)* 1899; 130-158.

Dropcho EJ. Remote neurologic manifestations of cancer. *Neurol Clin* 2002; 20(1): 85-122.

Evans DH, Murray JG. Histological and functional studies on the fibre composition of the vagus nerve of the rabbit. *J Anat* 1954; 88(3): 320-37.

Faust TW, Chang EH, Kowal C, Berlin R, Gazaryan IG, Bertini E, Zhang J, Sanchez-Guerrero J, Fragoso-Loyo HE, Volpe BT, Diamond B, Huerta PT. Neurotoxic lupus autoantibodies alter brain function through two distinct mechanisms. *Proc Natl Acad Sci U S A* 2010; 107(43):18569-18574.

Freeman R., Autonomic peripheral neuropathy, *Lancet* 2005; 365: 1259-1270.

Furness JB, Costa M, Keast JR. Choline acetyltransferase- and peptide immunoreactivity of submucous neurons in the small intestine of the guinea-pig. *Cell Tissue Res* 1984; 237:329-336.

Furness JB, Costa M. Types of nerves in the enteric nervous system. *Neuroscience* 1980; 5(1): 1-20.

Furness JB, Jones C, Nurgali K, and Clerc N. Intrinsic primary afferent neurons and nerve circuits within the intestine. *Prog Neurobiol* 2004; 72:143-164.

Furness JB, Kunze WA, Bertrand PP, Clerc N, Bornstein JC. Intrinsic primary afferent neurons of the intestine. *Prog Neurobiol* 1998; 54: 1-18..

Furness JB, Kunze WA, Clerc N. Nutrient Tasting and Signaling Mechanisms in the Gut II. The intestine as a sensory organ:neural, endocrine, and immune responses. *Am J Physiol* 1999; 277(5 Pt 1): G922-8.

Furness JB, Trussell DC, Pompolo S, Bornstein JC, Smith TK. Calbindin neurons of the guinea-pig small intestine: quantitative analysis of their numbers and projections. *Cell Tissue Res* 1990; 260 (2): 261-72.

Furness JB. The Enteric Nervous System. *Oxford: Blackwell Publishing Ltd* 2006.

Furness JB. Types of neurons in the enteric nervous system. *J Auton Nerv Syst* 2000; 81: 87-96.

Galligan JJ, North RA. Pharmacology and function of nicotinic acetylcholine and P2X receptors in the enteric nervous system. *Neurogastroenterol Motil* 2004; 16 (suppl 1): 64-70.

Galligan JJ. Ligand-gated ion channels in the enteric nervous system. *Neurogastroenterol Motil* 2002; 14: 611-623.

Gibbons CH, Vernino SA, Freeman R. Combined immunomodulatory therapy in autoimmune autonomic ganglionopathy. *Arch Neurol* 2008; 65: 213-217.

Glazebrook PA, Ramirez AN, Schild JH, Shieh CC, Doan T, Wible BA and Kunze DL. Potassium channels Kv1.1, Kv1.2 and Kv1.6 influence excitability of rat visceral sensory neurons. *J Physiol* 2002; 1: 467-482.

Graus F, Cordon-Cardo C, Posner JB. Neuronal antinuclear antibody in sensory neuronopathy from lung cancer. *Neurology* 1985; 35: 538-43.

Graus F, Elkon KB, Cordon-Cardo C, Posner JB. Sensory neuronopathy and small cell lung cancer. Antineuronal antibody that also reacts with the tumor. *Am J Med* 1986; 80: 45-82.

Graus F, Keime-Guibert F, Rene R et al. Anti-Hu-associated paraneoplastic encephalomyelitis: analysis of 200 patients. *Brain* 2001; 124: 1138-1148.

Griesmann GE, Lennon VA. Detection of autoantibodies in myasthenia gravis and Lambert-Eaton myasthenic syndrome. Manual of clinical laboratory immunology. *5th edition. Washington DC*1997; ASM Press.

Grundy D. Vagal control of gastrointestinal function. *Baillieres Clin Gastroenterol.* 1988; 2(1): 23-43.

Grundy D, Schemann M. Enteric nervous system. *Curr Opin Gastroenterol* 2007; 23(2): 121-126.

Grundy D, Schemann M. Enteric nervous system. *Curr Opin Gastroenterol* 2006; 22(2): 102-110.

Grundy D, Schemann M. Enteric nervous system. *Curr Opin Gastroenterol* 2005; 21(2): 176-182

Grundy D, Scratcherd T. Sensory afferents from the gastrointestinal tract. In: Rauner, B.B. (Ed.), Motility and Circulation. Handbook Physiology, Vol. I. *The American Physiological Society, Oxford.University Press, New York* 1989; 593-620, Section 6: the gastrointestinal system.

Hendriks R., Bornstein JC, and Furness JB. An electrophysiological study of the projections of putative sensory neurons within the myenteric plexus of the guinea pig ileum. *Neurosci Lett.* 1990; 110: 286-290.

Hirst GD and McKirdy HC. Synaptic potentials recorded from neurones of the submucous plexus of guinea-pig small intestine. *J Physiol (London)* 1975; 249: 369-385.

Hirst GD, Holman ME, Spence I. Two types of neurones in the myenteric plexus of duodenum in the guinea-pig. *J Physiol* 1974; 236: 303-326.

Honnorat J, Antoine JC. Paraneoplastic neurological syndromes. *Orphanet J Rare Dis* 2007; 2: 22

Hoyle CH, Burnstock G. Neuronal populations in the submucous plexus of thehuman colon. *J Anat* 1989; 166: 7-22.

Ibba-Manneschi L, Martini M, Zecchi-Orlandini S, Faussone-Pellegrini MS. Structural organization of enteric nervous system in human colon. *Histol. Histopathol* 1995; 10(1): 17-25

Jiang W, Kirkup AJ, Berthoud H, Kreis ME, and Grundy D. Effects of neuronal nicotinic acetylcholine receptor antagonists on jejunal mesenteric afferent firing evoked by nicotinic agonist DMPP. *Gastroenterology* 2002; 122(4(2): 159.

Jun S, Dimyan M, Jones KD, Ladabaum U. Obstipation as a paraneoplastic presentation of small cell lung cancer: case report and literature review. *Neurogastroenterol Motil* 2005; 17: 16-22

Kalia M, Sullivan JM. Brainstem projections of sensory and motor components of the vagus nerve in the rat. *J Comp Neurol* 1982; 211(3): 248-65

Kashyap P, Farrugia G. Enteric autoantibodies and gut motility disorders. *Gastroenterol Clin North Am* 2008; 37 (2): 397-410.

Kashyap V, Panganamamula H, Parkman P. Chronic intestinal pseudo-obstruction. *Curr Treat Options Gastroenterol* 2005; 8: 3-11.

Kiers L, Altermatt HJ, Lennon VA. Paraneoplastic anti-neuronal nuclear IgG autoantibodies (type I) localize antigen in small cell lung carcinoma. *Mayo Clin Proc* 1991; 66: 1209-1216.

KirkupAJ, BrunsdenAM, GrundyD. Receptors and transmission in the brain–gut axis: potential for novel therapies. I. Receptors on visceral afferents. *Am J Physiol Gastrointest Liver Physiol* 2001; 280: G787-94

Kirchgessner AL, Liu MT, Alcantara F. Excitotoxicity in the enteric nervous system. *J Neurosci.* 1997, 15; 17(22): 8804-16.

Klein CM, Vernino S, Lennon VA, Sandroni P, Fealey RD, Benrud-Larson L, Sletten D, Low PA. The spectrum of autoimmune autonomic neuropathies. *Ann. Neurol.* 2003; 53: 752-758.

Krishnamurthy S, Schuffler M. Pathology of neuromuscular disorders of the small intestine and colon. *Gastroenterology* 1987; 93: 610-39.

Lancaster E, Martinez-Hernandez E, Dalmau J. Encephalitis and antibodies to synaptic and neuronal cell surface proteins. *Neurology* 2011; 77(2):179-189.

Langley, JN. The autonomic nervous system. *Heffner. London* 1921.

Lawrentjew BJ. Experimentell-morphologische studien über den aufbau des ganglien des spieserohre nebst einigen bemerkungen über das vorkommen und die verteilung zweier arten von nervenzellen im autonomen nervensystem. *Z Zellforsch Mikrosk Anat Forsch* 1929; 18: 233-62.

Lee HR, Lennon VA, Camilleri M, et al. Paraneoplastic gastrointestinal motor dysfunction: clinical and laboratory characteristics. *Am J Gastroenterol* 2001; 96: 373-9.

Lee HR, Lennon VA, Camilleri M, Prather CM. Paraneoplastic gastrointestinal motor dysfunction: clinical and laboratory characteristics. *Am J Gastroenterol* 2001; 96: 373-379.

Lennon VA, Sas DF, Busk MF, et al. Enteric neuronal antibodies in pseudoobstruction with small-cell lung cancer. *Gastroenterology* 1991; 100: 137-42.

Leonard R. Johnson. Physiology of the Gastrointestinal tract. Fourth Edition, *Academic Press* 2006; 1: 585-726.

Leonard R. Johnson. Physiology of the Gastrointestinal tract. *Fourth Edition, Academic Press* 2006; 1: 577-602

Levite M, Fleidervish IA, Schwarz A, Pelled D, Futerman AH. Autoantibodies to the glutamate receptor kill neurons via activation of the receptor ion channel. *J Autoimmun.* 1999;13(1): 61-72.

Lomax AE, Furness JB. Neurochemical classification of enteric neurons in the guinea-pig distal colon. *Cell Tissue Res* 2000; 302: 59-72.

Lorusso L, Hart IK, Ferrari D, Ngonga GK, Gasparetto C, Ricevuti G. Autonomic paraneoplastic neurological syndromes. *Autoimmun Rev* 2007; 6(3): 162-8.

Lucchinetti CF, KimmelDW, Lennon VA. Paraneoplastic and oncologic profiles of patients seropositive for type 1 antineuronal nuclear autoantibodies. *Neurology* 1998; 50(3): 652-657.

Lynn PA, Olsson C, Zagorodnyuk V, Costa M, Brookes SJ. Rectal intraganglionic laminar endings are transduction sites of extrinsic mechanoreceptors in the guinea pig rectum. *Gastroenterology* 2003; 125: 786-794.

Maverakis E, Goodarzi H, Wehrli LN, Ono Y, Garcia MS. The etiology of paraneoplastic autoimmunity. *Clin Rev Allergy Immunol* 2012; (2): 135-44.

Mazzuoli G, Schemann M. Multifunctional rapidly adapting mechanosensitive enteric neurons (RAMEN) in the myenteric plexus of the guinea pig ileum. *J Physiol* 2009; 587.19: 4681-4693.

McMahon SB. Sensitisation of gastrointestinal tract afferents. *Gut* 2004; 53 Suppl 2: ii13-ii15.

Michel K, Zeller F, Langer R, Nekarda H, Kruger D, Dover TJ, Brady CA., Barnes NM, Schemann M. Serotonin excites neurons in the human submucous plexus via 5-HT3 receptors. *Gastroenterology* 2005; 128: 1317-1326.

Moll JWB, Vecht CJ. Immune diagnosis of paraneoplastic neurological disease. *Clin Neurol Neurosurg* 1995; 97: 71-81.

Mueller K, Michel K, Krueger D, Demir IE, Ceyhan GO, Zeller F, Kreis ME, Schemann M. Activity of protease-activated receptors in the human submucous plexus. *Gastroenterology* 2011; 141(6): 2088-2097.

Neuhuber WL, Kressel M, Stark A and Berthoud HR. Vagal efferent and afferent innervation of the rat esophagus as demonstrated by anterograde DiI and DiA tracing: focus on myenteric ganglia. *J Auton Nerv Syst* 1998; 70: 92-102.

Neuhuber WL, Sandoz PA, Fryscak T. The central projections of primary afferent neurons of greater splanchnic and intercostal nerves in the rat. A horseradish peroxidase study. *Anat Embryol (Berl)* 1986; 174(1): 123-44.

NeuhuberWL. Sensory vagal innervation of the rat esophagus and cardia. a light and electron microscopic anterograde tracing study. *J Auton Nerv Syst* 1987; 20: 243-55.

Neunlist M, Peters S, Schemann M. Multisite optical recording of excitability in the enteric nervous system. *Neurogastroenterol Motil* 1999; 11: 393-402.

Page AJ, Martin CM and Blackshaw LA. Vagal mechanoreceptors and chemoreceptors in mouse stomach and esophagus. *J Neurophysiol* 2002; 87: 2095-2103.

Page AJ, O'Donnell TA and Blackshaw LA. P2X purinoceptor-induced sensitization of ferret vagal mechanoreceptors in oesophageal inflammation. *J Physiol* 2000 ; 2: 403-411.

Pardi DS, Miller SM, Miller DL, et al. Paraneoplastic dysmotility: loss of interstitial cells of Cajal. *Am J Gastroenterol* 2002; 97:1828-33.

Phillips RJ, Baronowsky EA, Powley TL. Afferent innervation of gastrointestinal tract smooth muscle by the hepatic branch of the vagus. *J Comp Neurol* 1997; 384: 248-270.

Phillips RJ, Powley TL. Gastric volume detection after selective vagotomies in rats. *Am J Physiol* 1998; 274: R1626-R1638.

Phillips RJ, Powley TL. Tension and stretch receptors in gastrointestinal smooth muscle: re-evaluating vagal mechanoreceptor electrophysiology. *Brain Res Brain Res Rev* 2000; 34(1-2): 1-26.

Pittock SJ, Kryzer TJ, Lonnon VA. Paraneoplastic antibodies coexist and predict cancer, not neurological syndrome. *Ann Neurol* 2004; 56: 715-719.

Plonquet A, Garcia-Pons F, Fernandez E, Philippe C, Marquet J, Rouard H, Delfau-Larue MH, Kosmatopoulos K, Lemonnier F, Farcet JP, Gherardi RK, Langlade-Demoyen P: Peptides derived from the onconeural HuD protein can elicit cytotoxic responses in HHD mouse and human. *J Neuroimmunol* 2003; 142: 93-100.

Posner JB, Dalmau J. Paraneoplastic syndromes. *Curr Opin Immunol* 1997; 9(5): 723-9.

Posner JB, Dalmau JO. Paraneoplastic syndromes affecting the central nervous system. *Annu Rev Med* 1997; 48: 157-166.

Powley TL, Phillips RJ. Musings on the wanderer: what's new in our understanding of vago-vagal reflexes? I. Morphology and topography of vagal afferents innervating the GI tract. *Am J Physiol Gastrointest Liver Physiol* 2002; 283(6): G1217-25.

Powley TL, Prechtl JC, Fox EA, Berthoud HR. Anatomical considerations for surgery of the rat abdominal vagus: distribution, paraganglia and regeneration. *J Auton Nerv Syst* 1983; 9: 79-97.

Prechtl JC and powley TL. The fiber composition of the abdominal vagus of the rat. *Anat Embryol (Berl)* 1990; 181(2): 101-15

Prechtl JC, Powley TL. Organization and distribution of the rat subdiaphragmatic vagus and associated paraganglia. *J Comp Neurol* 1985; 235: 182-195

Qu L, Zhang P, LaMotte RH, Ma C. Neuronal Fc-gamma receptor I mediated excitatory effects of IgG immune complex on rat dorsal root ganglion neurons. *Brain Behav Immun* 2011: 25: 1399-1407.

Rauer S, Czygan M, Kaiser R. Quantification of circulating anti-Hu antibody in serial samples from patients with paraneoplastic neurological syndromes: possible correlation of antibody concentration and course of neurological symptoms. *J Neurol* 2002; 249(3): 285-9.

Roberts WK, Darnell RB. Neuroimmunology of the paraneoplastic neurological degenerations. *Curr Opin Immunol* 2004; 16: 616-622.

Rodrigo J, Hernandez J, Vidal MA, Pedrosa JA. Vegetative innervation of the esophagus. II. Intraganglionic laminar endings. *Acta Anat (Basel)* 1975; 92: 79-100.

Rong W, Hillsley K, Davis JB, Hicks G, Winchester WJ, Grundy D. Jejunal afferent nerve sensitivity in wild-type and TRPV1 knockout mice. *J Physiol* 2004; 560: 867-881.

Rong W, Spyer KM, Burnstock G. Activation and sensitisation of low and high threshold afferent fibres mediated by P2X receptors in the mouse urinary bladder. *J Physiol* 2002; 541: 591-600.

Sachs F. Biophysics of mechanoreception. *Membr Biochem* 1986; 6(2): 173-95.

Schäfer KH, Klotz M, Mergner D, Mestres P, Schimrigk K, Blaes F. IgG-mediated cytotoxicity to myenteric plexus cultures in patients with paraneoplastic neurological syndromes. *J Autoimmun* 2000; 15(4): 479-484.

Schemann M, Hafsi N, Michel K, Kober OI, Wollmann J, Li Q, Zeller F, Langer R, Lee K, Cellek S. The beta3-adrenoceptor agonist GW427353 (Solabegron) decreases excitability of human enteric neurons via release of somatostatin. *Gastroenterology* 2010; 138(1): 266-74.

Schemann M, Mazzuoli G. Multifunctional mechanosensitive neurons in the enteric nervous system. *Auton Neurosci* 2010; 16: 153(1-2): 21-5.

Schemann M, Michel K, Ceregrzyn M, Zeller F, Seidl S, Bischoff SC. Human mast cell mediator cocktail excites neurons in human and guinea-pig enteric nervous system. *Neurogastroenterol Motil* 2005; 17: 281-289.

Schemann M, Michel K, Peters S, Bischoff SC, Neunlist M. Cutting-edge technology. III. Imaging and the gastrointestinal tract: mapping the human enteric nervous system. *Am J Physiol Gastrointest Liver Physiol* 2002; 282: G919-G925.

Schicho R, Krueger D, Zeller F, Von Weyhern CW, Frieling T, Kimura H, Ishii I, De Giorgio R, Campi B, Schemann M. Hydrogen sulfide is a novel prosecretory neuromodulator in the Guinea-pig and human colon. *Gastroenterology* 2006; 131: 1542-1552.

Schroeder C, Vernino S, Birkenfeld AL, Tank J, Heusser K, Lipp A, Benter T, Lindschau C, Kettritz R, Luft FC, Jordan J. Plasma exchange for primary autoimmune autonomic failure. *N Engl J Med* 2005; 353: 1585-1590.

Sengupta JN, Gebhart GF. Gastrointestinal afferent fibers and sensation. In: Physiology of the Gastrointestinal Tract, edited by Johnson LR. *Raven Press* 1994; 483-520.

Senties-Madrid H, Vega-Boada F. Paraneoplastic syndromes associated with anti-Hu antibodies. *Isr Med Assoc J* 2001; 3: 94-103.

Sillevis Smitt P, Grefkens J, de Leeuw B et al. Survival and outcome in 73 anti-Hu positive patients with paraneoplastic encephalomyelitis/sensory neuronopathy. *J Neurol* 2002; 249:

Sillevis Smitt PA, Manley GT, Posner JB. Immunization with the paraneoplastic encephalomyelitis antigen HuD does not cause neurologic disease in mice. *Neurology* 1995; 45: 1873-1878.

Skok MV, Voitenko LP, Voitenko SV, Lykhmus EY, Kalashnik EN, Litvin TI, Tzartos SJ, Skok VI. Alpha subunit composition of nicotinic acetylcholine receptors in the rat autonomic ganglia neurons as determined with subunit-specific anti-alpha (181-192) peptide antibodies. *Neuroscience* 1999; 93: 1427-1436.

Smith TK, Hennig GW, Spencer NJ. Sensory transduction in the ENS. *Physiol News* 2005; 58: 1-3.

Smith VV, Gregson N, Foggensteiner L, et al. Acquired intestinal aganglionosis and circulating autoantibodies without neoplasia or other neural involvement. *Gastroenterology* 1997; 112(4): 1366-71.

Staszewski H Hematological paraneoplastic syndromes. Semin Oncol. 1997 Jun;24(3):329-33.

Steele HA, George BJ. Mucocutaneous paraneoplastic syndromes associated with hematologic malignancies. *Oncology (Williston Park)* 2011; 25(11): 1076-83.

Sutton IJ, Steele J, Savage CO, Winer JB, Young LS: An interferongamma ELISPOT and immunohistochemical investigation of cytotoxic T lymphocyte-mediated tumour immunity in patients with paraneoplastic cerebellar degeneration and anti-Yo antibodies. *J Neuroimmunol* 2004, 150: 98-106.

Szabo A, Dalmau J, Manley G, Rosenfeld M, Wong E, Henson J, Posner JB, Furneaux HM.. HuD, a paraneoplastic encephalomyelitis antigen, contains RNA-binding domains and is homologous to Elav and Sex-lethal. *Cell* 1991; 67: 325-333.

Talamonti L, Li Q, Beyak M, et al. Sensory motor abnormalities in severe gut dysmotility: role of anti-HuD neuronal antibodies. *Neurogastroenterol Motil* 2006; 18: 669.

Tanaka K, Ding X, Tanaka M. Effects of antineuronal antibodies from patients with paraneoplastic neurological syndrome on primary-cultured neurons. *J Neurol Sci* 2004; 217(1): 25-30.

Timmermans JP, Adriaensen D, Cornelissen W, Scheuermann DW. Structural organization and neuropeptide distribution in the mammalian enteric nervous system, with special attention to those components involved in mucosal reflexes. *Comp Biochem Physiol A Physiol* 1997; 118(2): 331-40.

Timmermans JP, Hens J, Adriaensen D. Outer submucous plexus: an intrinsic nerve network involved in both secretory and motility processes in the intestine of large mammals and humans. *Anat Rec* 2001; 262(1): 71-8.

Trousseau A. Phlegmasia alba dolens. *ClinMed Hotel Dieu de Paris.* 1865(3): 94.

Trousseau A. Phlegmasia alba dolens. *In: Cormak JRT, ed. Lectures on Clinical Medicine.* Philadelphia: Lindsay & Blakiston; 1873: 859-890.

van der Kleij H, Charles N, Karimi K, Mao YK, Foster J, Janssen L, Chang Yang P, Kunze W, Rivera J, Bienenstock J. Evidence for neuronal expression of functional Fc (epsilon and gamma) receptors. *J Allergy Clin Immunol* 2010; 125(3): 757-60.

Vernino S, Adamski J, Kryzer TJ, Fealey RD, Lennon VA. Neuronal nicotinic ACh receptor antibody in subacute autonomic neuropathy and cancer-related syndromes. *Neurology* 1998; 50: 1806-1813.

Vernino S, Ermilov LG, Sha L, et al. Passive transfer of autoimmune autonomic neuropathy to mice. *J Neurosci* 2004; 24(32): 7037-42.

Vernino S, Hopkins S, Wang Z. Autonomic ganglia, acetylcholine receptor antibodies, and autoimmune ganglionopathy. *Auton Neurosci* 2009; 146(1-2): 3-7

Vernino S, Lennon VA. Autoantibody profiles and neurological correlations of thymoma. *Clin Cancer Res* 2004; 10: 7270-7275.

Vernino S. Paraneoplastic neurologic syndromes. *Curr Neurol Neurosci Rep*. 2006 ;6(3): 193-9.

Vernino S, Low PA, Fealey RD, et al. Autoantibodies to ganglionic acetylcholine receptors in autoimmune autonomic neuropathies. *N Engl J Med* 2000; 343(12): 847-55.

Vernino S. Antibody testing as a diagnostic tool in autonomic disorders. *Clin Auton Res* 2009;19(1):13-9.

Vernino S. Neuronal acetylcholine receptor autoimmunity. *Ann N Y Acad Sci* 2008; 1132: 124-8.

Verschuuren JJ, Dalmau J, Hoard R, Posner JB. Paraneoplastic anti-Hu serum: studies on human tumor cell lines. *J Neuroimmunol* 1997; 79(2): 202-210.

Vignali S, Peter N, Ceyhan G, Demir IE, Zeller F, Senseman D, Michel K, Schemann M. J Recordings from human myenteric neurons using voltage-sensitive dyes. *Neurosci Methods* 2010;15; 192(2): 240-8.

Wakamatsu Y, Weston JA. Sequential expression and role of Hu RNA-binding proteins during neurogenesis. *Development* 1997; 124(17): 3449-60.

Wang FB, Powley TL. Topographic inventories of vagal afferents in gastrointestinal muscle. *J Comp Neurol* 2000; 421: 302-324.

Wang Z, Low PA, Jordan J, Freeman R, Gibbons CH, Schroeder C, Sandroni P, Vernino S. Autoimmune autonomic ganglionopathy: IgG effects on ganglionic acetylcholine receptor current. *Neurology* 2007; 68: 1917-1921.

Wang Z, Low PA, Vernino S. Antibody-mediated impairment and homeostatic plasticity of autonomic ganglionic synaptic transmission. *Exp Neurol* 2010; 222(1): 114-9.

Weber FP, Hill TR. Short Notes and Clinical Cases: Complete Degeneration of the Posterior Columns of the Spinal Cord with Chronic Polyneuritis in a Case of Widespread Carcinomatous Disease elsewhere. *J Neurol Psychopathol.* 1933;14(53): 57-60.

Wilkinson PC, Zeromski J. Immunofluorescent detection of antibodies against neurons in sensory carcinomatous neuropathy. *Brain* 1965; 88: 529-38.

Wilson AJ, Llewellyn-Smith IJ, Furness JB, Costa M. The source of the nerve fibres forming the deep muscular and circular muscle plexuses in the small intestine of the guinea-pig. *Cell Tissue Res* 1987; 247: 497-504.

Wood JD. Enteric neuroimmunophysiology and pathophysiology. *Gastroenterology* 2004; 127(2): 635-57.

Wood JD. Integrative functions of the enteric nervous system. In: Johnson LR ed. Physiology of the Gastrointestinal Tract, Vol. 1, 4th edn, Ch 24. Burlington, MA, USA: Elsevier *Academic Press* 2006; 665-683.

Wood JD. Intrinsic neural control of intestinal motility. *Annu Rev Physiol* 1981; 43: 33-51.

Wood JD. Neural and humoral regulation of gastrointestinal motility. In: Schuster MM, Crowell MD, Koch KL, eds. *Gastrointestinal Motility in Health and Disease*. London: BC Decker, 2002; 19-42.

Wood JD. Neuropathophysiology of functional gastrointestinal disorders. *World J Gastroenterol* 2007; 13(9): 1313-32.

Yu S, Undem BJ, Kollarik M. Vagal afferent nerves with nociceptive properties in guinea-pig oesophagus. *J Physiol* 2005; 563: 831-842.

Zagorodnyuk VP, Brookes SJ. Transduction sites of vagal mechanoreceptors in the guinea pig esophagus. *J Neurosci* 2000; 20: 6249-6255.

Zagorodnyuk VP, Chen BN, Brookes SJ. Intraganglionic laminar endings are mechano-transduction sites of vagal tension receptors in the guinea-pig stomach. *J Physiol* 2001; 534: 255-268.

Zagorodnyuk VP, Chen BN, Costa M and Brookes SJ. Mechanotransduction by intraganglionic laminar endings of vagal tension receptors in the guinea-pig oesophagus. *J Physiol* 2003; 553: 575-587.

Zagorodnyuk VP, Chen BN, Costa M, Brookes SJ. 4-aminopyridine- and dendrotoxin-sensitive potassium channels influence excitability of vagal mechano-sensitive endings in guinea-pig oesophagus. *Br J Pharmacol* 2002;137(8): 1195-206.

Zagorodnyuk VP, Chen BN, Costa M, Brookes SJ. Mechanotransduction by intraganglionic laminar endings of vagal tension receptors in the guinea-pig oesophagus. *J Physiol* 2003; 1: 553(Pt 2): 575-587.

List of tables

List of figures

Acknowledgments

I am very grateful to Prof. Dr. Schemann for giving me the chance to study in the laboratory at the Department of Humanbiology and enlightening me during my PhD degree study. Furthermore thanks for giving me the chance to work on this interesting topic and the excellent working conditions.

I would like to express my deep gratitude to Prof. Dr. Schemann for providing me the chance to be in Prof. Dr. Grundys laborotory (Department of Biomedical Science, University of Sheffield, UK) to perform some of the experiments described in the PhD thesis. Thanks also to Dr. Beyak for his help.

I am grateful to Dr. Michel for helping me throughout my time here in the lab. He was very patient with me and exchanged a lot of ideas with me. Additionally, I want to thank him for carefully reviewing my thesis.

Thanks to all laboratory members for supporting me and the nice atmosphere in the laboratory, especially to all members of the “International office”. I am also very thankful to Birgit Kuch for helping in immunohistochemistry experiments.

I would also like to express my thankfulness to my friends during the time my study in Germany, for sharing the happiness and sorrow, encouraging me.

Heartfelt thanks to my family that supported me through all the years to go my own way

Curriculum Vitae (English)

Name:	Qin Li.
Date of birth:	March 21, 1960
Place of birth:	Shandong of China

Education

1978-1982	Bachelor's degree, Bachelor of Medicine (Binzhou Medical College, China)
1995-1998	Master's degree, Master of Medicine (Shandong Medical University, China)
2004-2009	MD student in Department of Human Biology, Technische Universität München, Germany
2010-present	PhD student in Department of Human Biology, Technische Universität München, Germany

Position Held

1982-1995	Teaching Assistant, Lecturer, Department of physiology, Heze Medical College
1998-2000	Lecturer, Department of physiology, School of Medicine, Shandong Medical University, China
2000-present	Associate Professor, Department of physiology, School of Medicine, Shandong University, China

Research

Mechanism for control of the respiratory center

Physiology and pathophysiology in the enteric nervous system

Awards

The Graduate Excellent Research thesis of Shandong Degree Committee, China (1999)

Third Award for the Excellence in Research, from the National Education Committee, China (research group award, 1999)

First Award for the Excellence in Research, from National Education Committee, China (research group award, 2000)

Second Awards for Excellent Research Paper of Shandong Science Associate, China (2001)

Curriculum Vitae (German)

Name:	Qin Li.
Geburtsdatum:	21.3.1960
Geburtsort:	Shandong, China

Ausbildung

1978-1982	Studium "Bachelor of Medicine" mit Abschluss (Binzhou Medical College, China)
1995-1998	Studium "Master of Medicine" mit Abschluss (Shandong Medical University, China)
2004-2009	MD Studium, Lehrstuhl für Humanbiologie, Technische Universität München
2010-present	PhD Studium, Lehrstuhl für Humanbiologie, Technische Universität München

Berufliche Erfahrungen

1982-1995	Lehrassistentin, Dozentin, Physiologisches Institut, Medizinische Hochschule Heze, China
1998-2000	Dozentin, Physiologisches Institut, Medizinische Fakultät , Shandong-Universität für Medizin, China
2000-present	Dozentin, Physiologisches Institut, Medizinische Fakultät, Shandong-Universität, China

Forschung Mechanismen der Kontrolle des Atemzentrums
Physiologie und Pathophysiologie im Enterischen Nervensystem

Auszeichnungen The Graduate Excellent Research thesis of Shandong Degree Committee, China (1999)
Dritter Preis "Excellence in Research", vom "National Education Committee", China (Preis für die Arbeitsgruppe, 1999)
Erster Preis "Excellence in Research", vom "National Education Committee", China (Preis für die Arbeitsgruppe, 2000)
Zweiter Preis "Excellent Research Paper" of "Shandong Science Associate", China (2001)